

**GROUND RADIOMETRIC SURVEY OF KUFENA, ZARIA,
NORTHWEST NIGERIA**

By

YABUWAT, BISAN

**DEPARTMENT OF PHYSICS
FACULTY OF SCIENCE
AHMADU BELLO UNIVERSITY, ZARIA, NIGERIA**

JULY, 2011

**GROUND RADIOMETRIC SURVEY OF KUFENA, ZARIA,
NORTHWEST NIGERIA**

By

YABUWAT, BISAN, B.ENG. (ATBU, 2004)

M.Sc/SCIEN/54346/2005-2006

**A THESIS SUBMITTED TO THE POSTGRADUATE SCHOOL, AHMADU
BELLO UNIVERSITY, ZARIA, IN PARTIAL FULFILMENT OF THE
REQUIREMENTS FOR THE AWARD OF THE DEGREE OF MASTERS OF
SCIENCE IN APPLIED GEOPHYSICS**

DEPARTMENT OF PHYSICS

FACULTY OF SCIENCE

AHMADU BELLO UNIVERSITY, ZARIA, NIGERIA

JULY, 2011

DECLARATION

I declare that the work in the thesis titled "Ground radiometric survey of Kufena, Zaria, northwest Nigeria" has been carried out by me in the Department of Physics under the supervisions of Dr. K. M. Lawal and Dr. A .L Ahmed.

The information derived from literature has been duly acknowledged in the text and a list of references provided. No part of this thesis was previously presented for another degree or diploma at any university.

YABUWAT, BISAN

Name of student

Signature

Date

CERTIFICATION

This thesis titled "GROUND RADIOMETRIC SURVEY OF KUFENA, ZARIA, NORTHWEST NIGERIA" by Yabuwat, Bisan meets the regulations governing the award of the degree of Master of Science in Applied Geophysics of Ahmadu Bello University, Zaria, Nigeria, and is approved for its contribution to knowledge and literary presentation.

Dr. K. M Lawal
Chairman, Supervisory Committee

Date_____

Dr. A. L Ahmed
Member, Supervisory Committee

Date_____

Dr. R. Nasiru
Head of Department

Date_____

Prof. A. A. Joshua
Dean, Postgraduate School

Date_____

DEDICATION

To The King of Glory:

And who is the King of Glory? He is God Almighty

ACKNOWLEDGEMENT

There are a number of people without whose guidance, support and encouragement this research could not have been undertaken. To all of them, I am deeply grateful.

I thank my supervisor, Dr. K. M. Lawal not only for sharing with me his time and knowledge, but also for teaching me to aim high, work hard and be modest about my achievements. I consider myself extremely fortunate for having had the opportunity to conduct this research under the supervision of scientist of Dr. Lawal's competence.

My second supervisor Dr. A. L. M. Ahmed provided more than just a 'guiding light' in this research. Although his time is such a precious commodity, he always found time for me and generously gave me access to his facilities including books and journals. His involvement in this project has been inspirational.

The department of Physics Ahmadu Bello University Zaria provided an excellent learning atmosphere. I thank the various lecturers who patiently guided me over the years, in my study of Geophysics. I am most thankful to my entire family, especially my parents for their untiring support, faith and investments in my life. Love, support and prayers from my brothers and sister Victor, Ehud, and Swatkassa were fundamental to the success of my studies and research. To Richard, Algaita, Kerian, Adasa, Emily, Cyril, Lydia, Nathan, thanks for your prayers and support.

Special thanks to Engr. Segun Awoneye, your concern, prayers and support, are remarkable. My heart filled gratitude to my friend Mr. Felix Afalalu who is resting with the LORD, for your constructive criticism, motivations, care and affection.

I am immensely grateful to Mr. Obed Bassa and Mr. Emmanuel Idibia for guidance and tutelage in the use of different computer packages; and for his support and contributions to the success of this research.

To all my friends; including Mr. Justus Usman, Mr. Joses Usman, Mr. Sylvester Mathias, Mr. Alhamdu Domi, Miss Doris Kaura and Mr. Sunday Ishaya, thanks for all your support and encouragement.

Beloved, Rev. Nathan Waziri, Mr. Collins Chiemekwe, Mr. J. Osumeje, Mr. Joel Usman, Mr. Hosea Abrak, Miss. Jummai Kure, my uncles, aunties, brothers, sisters and cousins, thanks for your assistance to the success of my studies.

A warm thank you to all my colleagues Elijah, Hilary, Inalegwu, Mu'azu, and Najoji, for their support and understanding.

ABSTRACT

A ground survey was conducted for the investigation of the amount of radioactivity in Kufena, Zaria, northwest Nigeria. The technique of gamma ray spectrometry was applied using Scintillometer and gamma ray spectrometer (DISA-300). Activity concentration levels due to K, U, and Th were measured in the area along profiles spaced at 50 metres. Activity concentration ranges of the concerned radioelements were as follows: K was 0.03 – 6.5 %, U was 23.4 – 64.1 ppm, and Th was 8.3 – 89.1 ppm. The study identified Uranium and thorium as the main sources of radioactivity in the rocks of the area while potassium is not a major contributor to the gamma ray activity observed in the field. The study also revealed that uranium mineralization in Kufena may be of low grade.

CONTENTS

TITLE	PAGE
Cover page - - - - -	i
Fly leaf - - - - -	ii
Title page - - - - -	iii
Declaration - - - - -	iv
Certification - - - - -	v
Dedication - - - - -	vi
Acknowledgement - - - - -	vii
Abstract - - - - -	ix
Contents - - - - -	x
List of Tables - - - - -	xiii
List of Figures - - - - -	xiv
List of Appendices - - - - -	xvi
List of Abbreviations and Symbols - - - - -	xvii

CHAPTER ONE: INTRODUCTION

1.1 General Introduction - - - - -	1
1.2 Location of survey area - - - - -	2
1.3 Uranium mineralization in the older granites - - - - -	4
1.4 Uranium minerals associated with common rocks - - - - -	5
1.5 Radiometric anomalies - - - - -	7
1.6 Geology of Kufena - - - - -	9
1.6.1 Physiography, drainage, and structures - - - - -	10

1.6.2	Rocks types in the area	-	-	-	-	-	-	12
1.6.3	Economic geology of Kufena	-	-	-	-	-	-	13
1.7	Objectives of the present study	-	-	-	-	-	-	13

CHAPTER TWO: PRINCIPLES OF GAMMA RAY SPECTROMETRY

2.1	Introduction	-	-	-	-	-	-	14
2.2	Decay Chain	-	-	-	-	-	-	15
2.3	U series disequilibrium	-	-	-	-	-	-	21
2.4	Secular equilibrium	-	-	-	-	-	-	22
2.5	Gamma ray spectrometry	-	-	-	-	-	-	26

CHAPTER THREE: SCINTILLOMETER FIELD SURVEY

3.1	Background	-	-	-	-	-	-	29
3.2	Field instrumentation/procedure	-	-	-	-	-	-	29
3.3	Data reduction	-	-	-	-	-	-	31
3.3.1	Data analysis	-	-	-	-	-	-	31

CHAPTER FOUR: GAMMA RAY SPECTROMETRY SURVEY

4.1	Background	-	-	-	-	-	-	37
4.2	Field procedure	-	-	-	-	-	-	37
4.3	Data processing	-	-	-	-	-	-	39

CHAPTER FIVE: DATA ANALYSIS AND INTERPRETATION OF SPECTROMETRY

5.1	Probable areas of radiometric mineralization	-	-	-	-	-	-	49
-----	--	---	---	---	---	---	---	----

5.2	Interpretation of results	-	-	-	-	-	-	59
5.2.1	Total count	-	-	-	-	-	-	59
5.2.2	Uranium (eU)	-	-	-	-	-	-	59
5.2.3	Thorium (eTh)	-	-	-	-	-	-	62
5.2.4	Potassium (K %)	-	-	-	-	-	-	62
5.3	Isolation of residual anomalies	-	-	-	-	-	-	66
5.3.1	Application and result	-	-	-	-	-	-	68

CHAPTER SIX: DISCUSSION, CONCLUSION AND RECOMMENDATION

6.1	Discussion of results	-	-	-	-	-	-	78
6.2	Conclusion	-	-	-	-	-	-	80
6.3	Recommendation	-	-	-	-	-	-	81
	References	-	-	-	-	-	-	82
	Appendices	-	-	-	-	-	-	86

LIST OF FIGURES

Fig.1.1 Simplified general Geology map of Nigeria	-	-	-	-	-	3
1.2 Geological map showing the survey area (Adopted from Lawal, 2000)	-	-	-	-	-	-
- - - - -	-	-	-	-	-	11
2.1 Spectrgrams obtained from K, Th, and U on a granite gneiss outcrop (After Doig, 1968)	-	-	-	-	-	20
2.2 Graph of activity versus time of radionuclide and decay product	-	-	-	-	-	-
- - - - -	-	-	-	-	-	23
3.1 Frequency distribution curve of count rates (corrected data)	-	-	-	-	-	-
- - - - -	-	-	-	-	-	32
3.2 Contour map of count rates (uncorrected data)	-	-	-	-	-	34
3.3 Contour map of count rates (corrected data)	-	-	-	-	-	35
3.4 Contour map of count rates showing areas of anomalous gamma Radiation	-	-	-	-	-	-
- - - - -	-	-	-	-	-	36
4.1 Contour map of total count (corrected data)	-	-	-	-	-	41
4.2 Contour map of eU (corrected data)	-	-	-	-	-	42
4.3 Contour map of eTh (corrected data)	-	-	-	-	-	43
4.4 Contour map of K (corrected data)	-	-	-	-	-	44
4.5 Contour map of total count (uncorrected data)	-	-	-	-	-	45
4.6 Contour map of eU (uncorrected data)	-	-	-	-	-	46
4.7 Contour map of eTh (uncorrected data)	-	-	-	-	-	47

4.8	Contour map of K (uncorrected data)	-	-	-	-	48
5.1	Frequency distribution curve of total count (corrected data)	-	-	-	-	50
5.2	Map of total count (corrected data) showing areas of sources of radiation	-	-	-	-	60
5.3	Contour map of eU showing areas of anomalies	-	-	-	-	61
5.4	Contour map of eTh showing areas of anomalies	-	-	-	-	63
5.5	Contour map of K % showing areas of anomalies	-	-	-	-	64
5.6	Map showing areas of eU, eTh, and K % anomalies	-	-	-	-	65
5.7a	Regional field map of total count anomalies	-	-	-	-	70
5.7b	Regional field map of eU (corrected data) anomalies	-	-	-	-	71
5.7c	Regional field map of eTh (corrected data) anomalies	-	-	-	-	72
5.7d	Regional field map of K (corrected data) anomalies	-	-	-	-	73
5.8a	Residual field map of total count anomalies	-	-	-	-	74
5.8b	Residual field map of eU (corrected data) anomalies	-	-	-	-	75
5.8c	Residual field map of eTh (corrected data) anomalies	-	-	-	-	76
5.8d	Residual field map of K (corrected data) anomalies	-	-	-	-	77

LIST OF APPENDICES

APPENDIX 1: Total count (TC), equivalent surface concentration of uranium (eU), thorium (eTh) and potassium (K %) (Corrected data).	
- - - - - - - - - -	86
APPENDIX 2: Total count (TC), equivalent surface concentration of uranium (eU), thorium (eTh) and potassium (K %) (Uncorrected data).	
- - - - - - - - - -	99

LIST OF ABBREVIATIONS and SYMBOLS

a	Years
d	Days
E	East
e	Exponential function
etc	and so forth
<i>et al</i>	and others
eTh	Equivalent surface concentration of thorium
eU	Equivalent surface concentration of uranium
h	Hour
km ²	Kilometre square
N-W	North-west
Fig.	Figure
GRS	Gamma ray spectrometry
m	Metre
MeV	Million electron volts

mins	Minutes
ms	Microsecond
N	North
NW-NE	Northwest-northeast
α	Gamma
β	Beta
$^{\circ}$	Degrees
'	Minutes
\hat{y}	Regional Components of the data (observation)
$\Delta T(x,y)$	Two-dimensional residual total spectrometric field data

CHAPTER ONE

INTRODUCTION

1.1 General Introduction

Geological and Geophysical surveys in search of uranium deposits could be said to have started in Nigeria in 1947 when the mineral pyrochlore, containing substantial amount of uranium was discovered by the Geological survey department in small granite bodies on the Jos Plateau. In 1949, Mackay who was in Nigeria on a thorium investigation considered that it would be worthwhile to examine some of these granitic bodies in order to see whether the pyrochlore was present in sufficient amount to provide likely source of uranium or niobium (Mackay and Beer, 1952).

In Nigeria, already, the initial stage in the large scale exploration for the radioelements was launched when high sensitivity aero-radiometric surveys were carried out in 1975. The survey covered the lower Benue area, the middle Niger and the Sokoto area conducted by Fairly surveys Ltd., and Hunting Geology and Geophysics Ltd. respectively on behalf of the Federal Ministry of Mines and Power. The little information on uranium occurrences in Nigeria are mainly from individuals who analyzed a few rock samples and uranium ores from some locations around the Nigerian younger granite province (Ahmed, 2006). However, the work of Uwah (1984), Dewu (1986) and Ahmed (1994;2006) who carried out detailed investigation of radiometric anomalies in the Sokoto Basin, Bisichi, Jingir

and Dutsen wai areas of Sokoto, Plateau and Kaduna States respectively, form, a very important step for a large scale search of uranium and allied minerals.

Gamma ray spectrometry (GRS) is a remote sensing geophysical technique that provides information about the distribution of naturally occurring radioactive elements (potassium K, uranium U and thorium Th). It is a surface technique and interpretation requires an understanding of the nature of the surface materials and their relation to bedrock geology. Although GRS measures a physical phenomenon, it is for geological and exploration purposes. It is worthy to note that most granitic rocks of similar older granite (Pan-African) age elsewhere in the mobile belt of Africa such as the Damara-Katanga in Zaria (within which the study area Kufena lies) are known to host uranium deposits (Oshin and Rahaman, 1984). Methods of investigation include in-situ scintillometer survey and in-situ spectrometric survey.

1.2 Location of Survey Area

The survey area lies between latitude $7^{\circ} 39.3'N$ and $7^{\circ} 40.4'N$ and longitude $11^{\circ} 04.5'E$ and $11^{\circ} 05.5'E$. It also lies within the basement complex of north western Nigeria (Figure 1.1.)

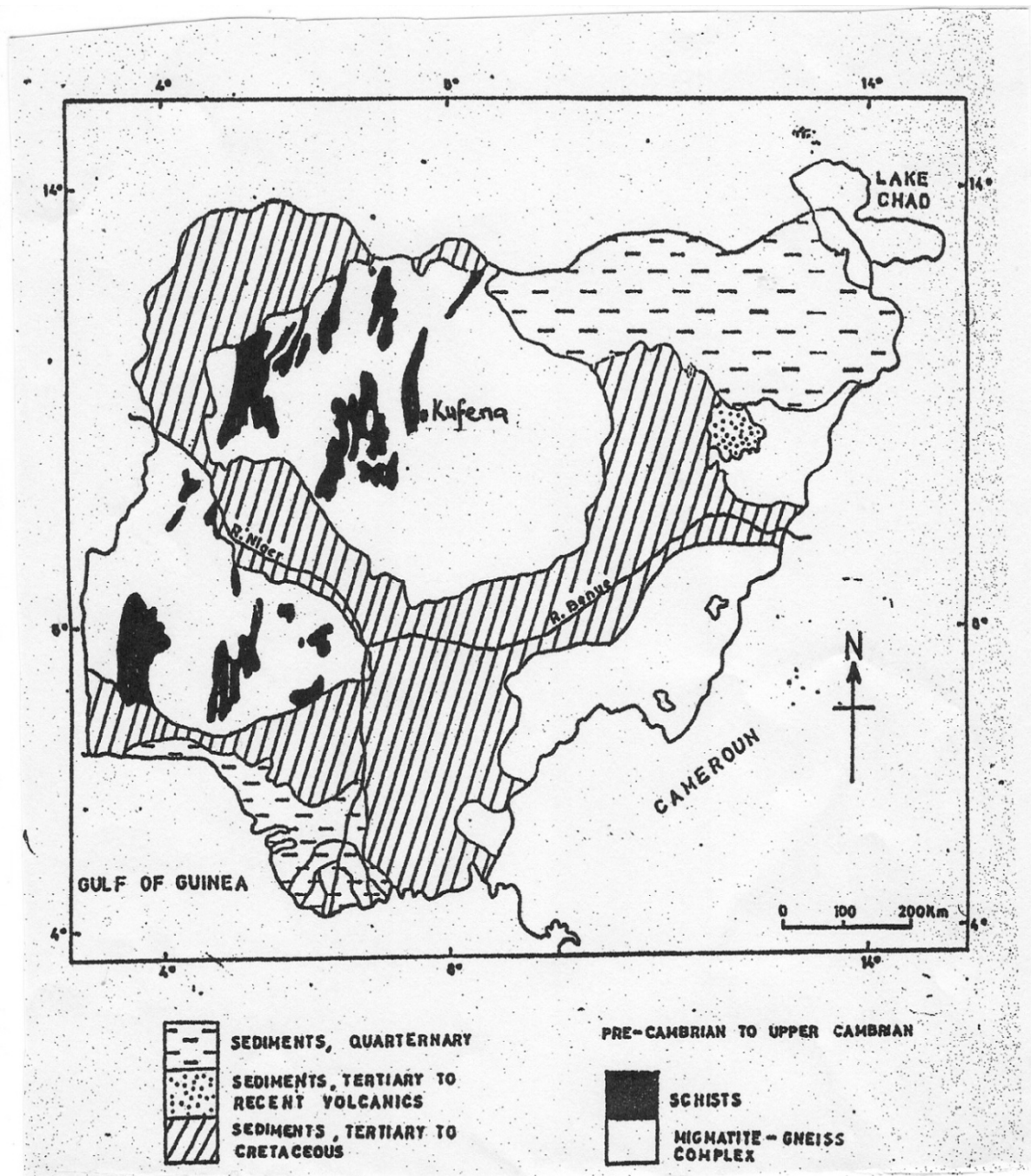


Figure 1.1 Simplified Geological map of Nigeria showing the study area (adopted from Garba, 1988)

1.3 Uranium Mineralization in the Nigerian Older Granites

The older granites emplaced during the Pan-African (600-500 Ma) orogeny was grouped into three on the basis of time of emplacement (Jones and Hockey, 1964); an early phase comprising granodiorites and quartz diorites, a main phase comprising coarse porphyritic hornblende granite and syenite and coarse porphyritic biotite granite, a late phase comprising homogeneous granites and dykes and pegmatites and aplites. Whole rock strontium isotropic isochron studies on the older Granites from central and north eastern show that these rocks are characterized by high initial $^{87}\text{Sr}/^{86}\text{Sr}$ ratio in the range 0.7070-0.7233 and reaching up to 0.7680 in Egbe pegmatites (Van Breement et al., 1977). Oshin and Rahaman (1984) interpreted these result to indicate significant crustal components in the magma that crystallized the older Granites by crustal remobilization is that the melts from which the older Granites were derived could be enriched in uranium by anatexis of crustal rocks of moderate to high uranium contents. Uranium may be further concentrated in the granites by magmatic differentiation. Most granitic rocks of similar older Granite (Pan-African) such as Damara-Katanga belt in Zaria (Dahlkamp, 1980) are known to host uranium deposits. Also, there is the possibility of finding vein type uranium mineralization in Zaria area of the north central Nigeria (Oshin and Rahaman, 1984). Based on these geological considerations, Kufena a certain area within the Damara Katanga belt in Zaria show some promise for uranium mineralization

1.4 Uranium Minerals Associated with Common Rocks

Uranium never occurs naturally in the free state but is found as a variety of ores in association with other elements, the ores are always contaminated by rare earth elements for example cerium, thorium and lead (Wooley, 1978). Other primary uranium ores in terms of economic importance include Davidite, Autinite, Torbenite, Brannerite and Coffinite (Roberts et al., 1978). Uranium crystallizes in the isometric system and usually occurs in massive formation as a constituent of granite rocks and pegmatites. The important thorium minerals are thorianite (ThO_2), monazite (ThPO_4) and thorite (ThSiO_4). The larger deposits occur mainly as thorium oxide, ThO_2 , in the monazite sands (Wooley, 1978).

Except in some shale and igneous metamorphic deposits, uranium is not found in sufficient quantity in the common rocks in the earth's crust to be extracted economically (Uwah, 1984). The average uranium in common rocks is 3.5 ppm in felsic granites and 3 ppm in syenites (Uwah, 1984). The average crystal abundance of uranium is about 2 ppm (Rich et al., 1972). The relative abundance of uranium in common rocks of the earth crust is shown in Table 1.1.

Table 1.1: Mean Contents of Radio elements in various rock types.

(Adapted from Galbraith and Saunders, 1983)

<i>ROCK TYPE</i>	<i>Th</i> (ppm)	<i>U</i> (ppm)	<i>K</i> (%)	$\frac{U}{Th}$	$\frac{U}{K}$	$\frac{Th}{K}$
IGNEOUS						
Ultra Basic	3.4	0.8	1.0	0.23	0.76	3.4
Basic	6.1	1.7	1.9	0.28	0.91	3.2
Basic-Intermediate	9.8	3.0	2.4	0.30	1.25	4.1
Intermediate-Acidic	16.0	3.6	3.0	0.23	1.25	5.3
Acidic	21.9	4.1	3.5	0.29	1.11	6.3
SEDIMENTARY						
Evaporites	0.4	0.1	0.1	0.25	1.0	4.0
Carbonate	1.6	1.6	0.3	1.0	5.0	5.9
Sandstones	5.7	1.9	1.2	0.33	1.67	4.8
Shale	11.2	3.7	2.7	0.32	1.43	4.1
METAMORPHIC						
Amphibolite	2.0	0.9	0.6	0.45	1.43	3.3
Graywackes	6.7	2.1	2.8	0.31	0.78	2.4
Gneiss	10.6	2.3	3.4	0.22	0.67	3.1
Schist	13.5	4.1	4.1	0.30	1.67	5.5

1.5 Radiometric Anomalies

Geological information is the basic key to the interpretation of all radiometric data collected in the field (Uwah, 1984; Ahmed, 2006). The task of characterizing a radiometric anomaly involves the initial reconnaissance survey of the area. The purpose of initial reconnaissance is to decide whether it is worthwhile to make a systematic gamma ray survey of the area in question (Uwah, 1984).

The three principal natural radioactive elements of the earth crust are potassium (K-40), uranium (U-238) and thorium (Th-232). The most abundant of the three is K, found mainly in alkali feldspar, mica, nepheline and leucites (Galbraith and Saunders; 1983). Most crustal rocks contain at least in trace quantities, the three radioactive elements. Since changes in radioactivity level are reflections on radioisotope contents of the rock (and hence, geological contact), it is possible for correlation to be made between radioactivity of an area and rock types (Galbraith and Saunders, 1983). Such correlation is however seriously affected by the presence or absence of soil and also by the type of soil. Radioactivity of the bed rock is reflected only if the bedrock is exposed or has very thin overburden of few centimeters. The characteristic of a great majority of economic uranium deposits is the preferential enrichment of uranium relative to thorium and potassium. This preferential enrichment may exceed the relative abundance found in normal rock by several orders of magnitude (Darnley, 1973).

For any radioelement's to be extracted economically, they have to be located where they have already been concentrated by geological processes to many times the average figures shown in Table 1.1. According to Darnley (1972) this must be about 250 times the average content in normal rock and in addition their ratios must reflect preferential enrichment of the particular element to the other (Uwah, 1984).

According to Berreta (1981), there are more techniques for uranium prospecting than can be found for any other class of minerals. Because of (for example) presence of faults and joints to enhance radon migration (Soonawala, 1974) and other environmental effects that affect uranium mineralization. Most radiometric anomalies require thorough investigations before conclusions are made as to their economic importance (IAEA, 1980).

1.6 Geology of Kufena Area

The rocks in the Kufena area are mostly of Precambrian in age. These have been subjected to several deformation the latest being the Pan-African orogeny (McCurry, 1975). This thermotectonic event has virtually obliterated the imprints of events but left its own structural landmarks, which includes folding, fracturing, shearing, granitic emplacement and granitization. Rahaman (1976) recognized five petrological units within the Basement complex of Nigeria namely;

1. Migmatites – Gneiss complex;
2. Slightly migmatized to non migmatized para-schist and metaigneious;
3. Charnockitic rocks, metagabros dolerite dikes and hypabysal intrusive.

The Pan-African orogeny is the second orogeny characterized by total magmatization, mobilization, and intrusion of granite. Granitic rocks emplaced during orogeny are collectively referred to as the older granites (Grant 1970; Rahaman et al., 1983). Most granitic rocks of similar older granite (Pan-African) age in the Damara-Katanga belt in Zaria (Dahlkamp, 1980) are known to host uranium deposits (Oshin and Rahaman, 1984). These granitic rocks are believed to be anatectic bodies formed by the mobilization of pre-existing basement.

Older granites strongly to non porphyroblast and variably foliated forms groups of inselbergs. Foliations, where present is defined by generally regional alignment of

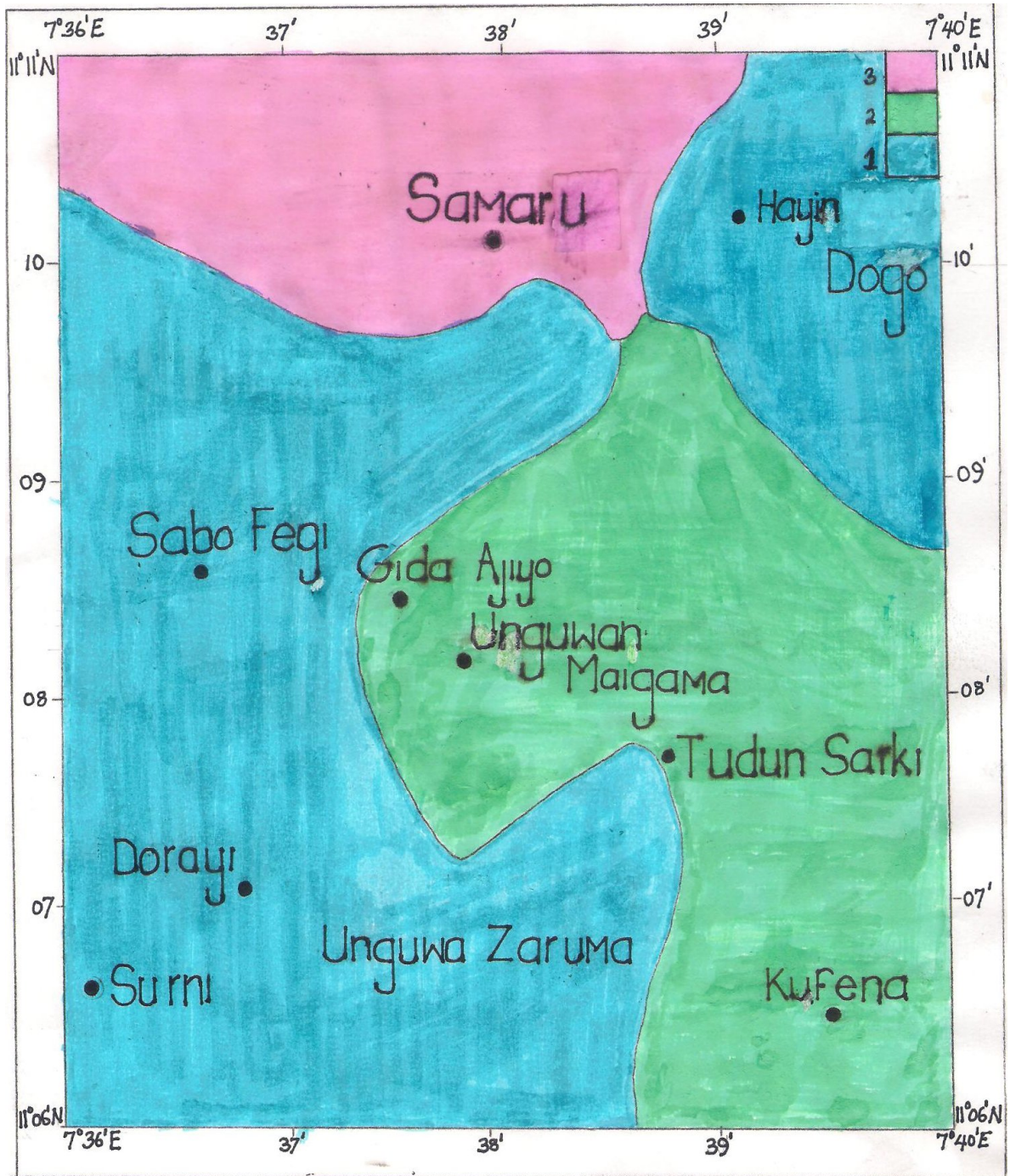
tabular microcline porphyroblasts up to 2 inches long, and biotite. Flakes local deviations are common, and in some exposures the porphyroblasts are randomly oriented. The geology map of the study area is shown in Figure. 1.3

1.6.1 Physiography, Drainage and Structures

The Kufena area is a part of the dissected portion of the Zaria-Kano plains extensive peneplain developed/crystalline metamorphic rocks of the Nigeria basement complex. A large residual granite inselberg (Kufena hill), provide the main relief.

Basement structures in the area appear to be relatively simple because of the uniform regional foliations trends. Lineation and minor isoclinal fold axes have highly variable trend and plunge, however especially among the metasediments. More than one deformational phase was probably involved in the lower Paleozoic orogenesis to produce isoclinal fold pattern typical of the metasediments in other areas, and generally concordant with surrounding gneisses.

Under the pressure temperature conditions of lower Paleozoic orogenesis, large masses of metasomatic granite developed in the original basement by selective extraction of low melting constituents which migrated to regions of lower pressure. Being just below the melting point the granites were both less dense and more mobile than the surroundings.



Explanation: 1. Medium Grained Granite 2. Porphyritic Granite 3. Biotite Gneiss

Figure 1.2: Geological showing the survey area (Kufena) (adopted from Lawal, 2000).

They could thus move upwards under the influence of regional stress field as very viscous and slow moving masses, to be finally emplaced as partly or wholly concordant intrusions (McCurry, 1975).

Deviations of porphyroblast from the regional trend, mark local disturbances in the otherwise generally uniform viscous flow pattern of granitic emplacement. Younger alluvium is the product of most recent erosion cycle; consist of grey brown sands, silts and clays over 30 feet thick in many places. Large quantities of dust are spread over the country annually by the seasonal harmattan winds and it has been suggested that alluvial deposits may contain substantial Aeolian components.

1.6.2 Rock types in the Area

The study area which lies to the north western of Zaria city is composed of Precambrian rocks of the Gneiss – migmatite complex intruded by the Pan-African Older granites. Rocks units observed in the area includes from the oldest to the youngest older granite. This rock type is the most common in the study area occupying the whole area. It outcrops as dome inselbergs, low whalebacks inselbergs, and also as low lying outcrops called ruwares (Lawal, 2000). In hand specimen, orthoclase, biotite and quartz are observed. The rocks are typical of older granites described elsewhere. In all sections of the study area are the “porphyroblastic” biotite granite (McCurry, 1975).

1.6.3 Economic Geology of Kufena

Building materials in the area include crushed stones from the older granites, non porphyroblastic varieties being preferred for crushing. Quartzite might also prove suitable especially more massive varieties except for tendency to splinter. Superficial deposits, mainly of older alluvium, are extensively dug and made locally into bricks for house building.

Porphyroblastic older granites could make ornamental stone, and is available in large quantities. Dark green and pink garnetiferous amphibolites might also have potentials as decorative materials, but quantities so far found are not readily accessible for pottery manufacture appears to be confined to rather small pockets. Kaolinitic clays of variable quantity are obtained from deeply laterite.

1.7 Objectives of the Present Study

The objectives of the present study are to apply gamma ray spectrometry technique to;

- Determine the radioelement (K, U and Th) content in the area;
- Determine on which rock types do the anomalies occur;
- Delineate the most favourable areas of radiometric anomalies;
- Identify the source of radioactivity;

CHAPTER TWO

PRINCIPLES OF GAMMA RAY SPECTROMETRY

2.1 Introduction.

Total gamma radiation and spectral measurements can be made using portable crystals. Generally, total count, uranium, thorium and potassium channels of data are acquired to identify specific sources of radiation. Radiometric survey involves the measurements of gamma radiation resulting from natural radioactive sources. Instruments are available to measure either total count or provide spectral information on individual elements. Modern multispectral meters capable of measuring up to 256 channels are primarily used in environmental mapping (Christillin, 1986). There are basically two radiometric survey techniques, the ground and air-borne radiometric surveys. The air-borne radiometric survey can normally be recommended in circumstances where the terrain is not easily accessible and/or large areas need to be covered/ prospected. The technique becomes particularly advantageous because other geophysical techniques can be carried out simultaneously. The aero surveys are superior to ground surveys for regional reconnaissance work because large areas can be covered in relatively small time.

For reconnaissance survey, gross counts may be adequate to delineate areas of higher than normal radioactivity using the gross count scintillometer. However, where the contribution due to individuals' radioelement is required spectrometric

surveys are employed. In this technique individuals contribution due to K, Th, and U, are obtained in addition to the total count. Determination of the radioelement concentration can then be made assuming secular equilibrium.

2.2 Decay Chain

The daughter nuclide of a decay event may also be radioactive. In this case, it will also decay producing radiation. The second daughter nuclide may also be unstable. This leads to a sequence of several decay events. Eventually a stable nuclide is produced. Each of the particles emitted during radioactive decay has its own characteristics and the gamma rays are characteristics of the element which emits them.

Natural sources of gamma radiation in rocks originate from the decay of radioactive products in the uranium and thorium decay chains and the decay chains of potassium. In Table (2.1), (2.2) and (2.3), the minor branches of decay (with the branching ratio of less than 0.0001%) are omitted. The energy release includes the total kinetic energy of all the emitted particles (electrons, alpha particles, gamma quanta, neutrines, Auger electron and X-rays) and the recoil nucleus, assuming that the original nucleus was at rest. The chain of U-238 (uranium series) begins with naturally occurring uranium-238, and includes astatine, bismuth, lead, thallium and thorium. All are present, at least transiently in any uranium containing ore or mineral. The chain of Th-232 begins with naturally occurring thorium-232 and includes actinium, bismuth, lead, polonium,

Table 2.1 The U-238 decay chain. (After Hoffman et al., 1971).

Nuclide	historic name (short)	historic name (long)	decay mode	half life	MeV	product of decay
^{238}U	U	Uranium	α	$4.468 \cdot 10^9 \text{ a}$	4.270	^{234}Th
^{234}Th	UX ₁	Uranium X1	β^-	24.10 d	0.273	^{234}Pa
^{234}Pa	UZ	Uranium Z	β^-	6.70 h	2.197	^{234}U
^{234}U	U _{II}	Uranium two	α	245500 a	4.859	^{230}Th
^{230}Th	Io	Ionium	α	75380 a	4.770	^{226}Ra
^{226}Ra	Ra	Radium	α	1602 a	4.871	^{222}Rn
^{222}Rn	Rn	Radon	α	3.8235 d	5.590	^{218}Po
^{218}Po	RaA	Radium A	α 99.98 % β^- 0.02 %	3.10 min	6.115 0.265	^{214}Pb ^{218}At
^{218}At			α 99.90 % β^- 0.10 %	1.5 s	6.874 2.883	^{214}Bi ^{218}Rn
^{218}Rn			α	35 ms	7.263	^{214}Po
^{214}Pb	RaB	Radium B	β^-	26.8 min	1.024	^{214}Bi
^{214}Bi	RaC	Radium C	β^- 99.98 % α 0.02 %	19.9 min	3.272 5.617	^{214}Po ^{210}Tl
^{214}Po	RaC'	Radium C'	α	0.1643 ms	7.883	^{210}Pb
^{210}Tl	RaC''	Radium C''	β^-	1.30 min	5.484	^{210}Pb
^{210}Pb	RaD	Radium D	β^-	22.3 a	0.064	^{210}Bi
^{210}Bi	RaE	Radium E	β^- 99.99987% α 0.00013%	5.013 d	1.426 5.982	^{210}Po ^{206}Tl
^{210}Po	RaF	Radium F	α	138.376 d	5.407	^{206}Pb

Table 2.2 The U-235 decay chain. (After Hoffman et al., 1971).

Nuclide	historic name (short)	historic name (long)	decay mode	half life	energy released, MeV	product of decay
^{239}Pu			α	$2.41 \cdot 10^4$ a	5.244	^{235}U
^{235}U	AcU	Actin Uranium	α	$7.04 \cdot 10^8$ a	4.678	^{231}Th
^{231}Th	UY	Uranium Y	β^-	25.52 h	0.391	^{231}Pa
^{231}Pa			α	32760 a	5.150	^{227}Ac
^{227}Ac	Ac	Actinium	β^- 98.62% α 1.38%	21.772 a	0.045 5.042	^{227}Th ^{223}Fr
^{227}Th	RdAc	Radioactinium	α	18.68 d	6.147	^{223}Ra
^{223}Fr	AcK	Actinium K	β^-	22.00 min	1.149	^{223}Ra
^{223}Ra	AcX	Actinium X	α	11.43 d	5.979	^{219}Rn
^{219}Rn	An	Actinon	α	3.96 s	6.946	^{215}Po
^{215}Po	AcA	Actinium A	α 99.99977% β^- 0.00023%	1.781 ms	7.527 0.715	^{211}Pb ^{215}At
^{215}At			α	0.1 ms	8.178	^{211}Bi
^{211}Pb	AcB	Actinium B	β^-	36.1 min	1.367	^{211}Bi
^{211}Bi	AcC	Actinium C	α 99.724% β^- 0.276%	2.14 min	6.751 0.575	^{207}Tl ^{211}Po

Table 2.3 The Th-232 series decay chain. (After Hoffman et al., 1971).

Nuclide	historic name (short)	historic name (long)	decay mode	half life	energy released, MeV	product of decay
^{252}Cf			α	2.645 a	6.1181	^{248}Cm
^{248}Cm			α	3.4×10^5 a	6.260	^{244}Pu
^{244}Pu			α	8×10^7 a	4.589	^{240}U
^{240}U			β^-	14.1 h	.39	^{240}Np
^{240}Np			β^-	1.032 h	2.2	^{240}Pu
^{244}Cm			α	18 a	5.8048	^{240}Pu
^{240}Pu			α	6561 a	5.1683	^{236}U
^{236}U			α	$2.3 \cdot 10^7$ a	4.494	^{232}Th
^{232}Th	Th	Thorium	α	$1.405 \cdot 10^{10}$ a	4.081	^{228}Ra
^{228}Ra	MsTh ₁	Mesothorium 1	β^-	5.75 a	0.046	^{228}Ac
^{228}Ac	MsTh ₂	Mesothorium 2	β^-	6.25 h	2.124	^{228}Th
^{228}Th	RdTh	Radiothorium	α	1.9116 a	5.520	^{224}Ra
^{224}Ra	ThX	Thorium X	α	3.6319 d	5.789	^{220}Rn
^{220}Rn	Tn	Thoron	α	55.6 s	6.404	^{216}Po
^{216}Po	ThA	Thorium A	α	0.145 s	6.906	^{212}Pb
^{212}Pb	ThB	Thorium B	β^-	10.64 h	0.570	^{212}Bi
^{212}Bi	ThC	Thorium C	β^- 64.06%	60.55 min	2.252	^{212}Po
			α 35.94%		6.208	^{208}Tl
^{212}Po	ThC'	Thorium C'	α	299 ns	8.955	^{208}Pb
^{208}Tl	ThC''	Thorium C''	β^-	3.053 min	4.999	^{208}Pb
^{208}Pb		.	stable	.	.	

radium and radon. All are present, at least transiently, in any thorium containing mineral (Lederer et al., 1968).

It is possible to relate measurements of intensities in three selected regions of spectrum to the K, Th and U, content of the rock since each of the radioisotopes emits gamma radiation of characteristics energy and the gamma ray spectrum of rock exhibit peaks of varying intensities corresponding to these characteristics energies. U-235 is only about 0.72 % of the natural uranium, while U-238 is 99.8 %. The gamma ray intensities originating from U-235 series will therefore be lower than those originating from U-238 series. Each of the decay chains of the U-235 and U-238 has an intermediate nuclide of atomic number 86, which is a gas under normal condition decaying by α -emission to a solid daughter radium. The 1.76 MeV peak in the natural rock spectrum though of relative low intensity is pronounced and has minimum interference from other rays (Doig, 1968). The combination of the 1.76 MeV and 1.12 MeV gamma rays emitted by Bi-214 has been used for uranium measurements (Uwah, 1984). The decay of Th-208 to Pb-208 by β -emission results in the emission of 2.62 MeV gamma rays. The 2.62 MeV peak in the natural rock spectrum is pronounced and free from interference and is therefore considered as the most suitable for uranium concentration measurements in geologic samples using gamma ray spectrometry (Figure 2.1).

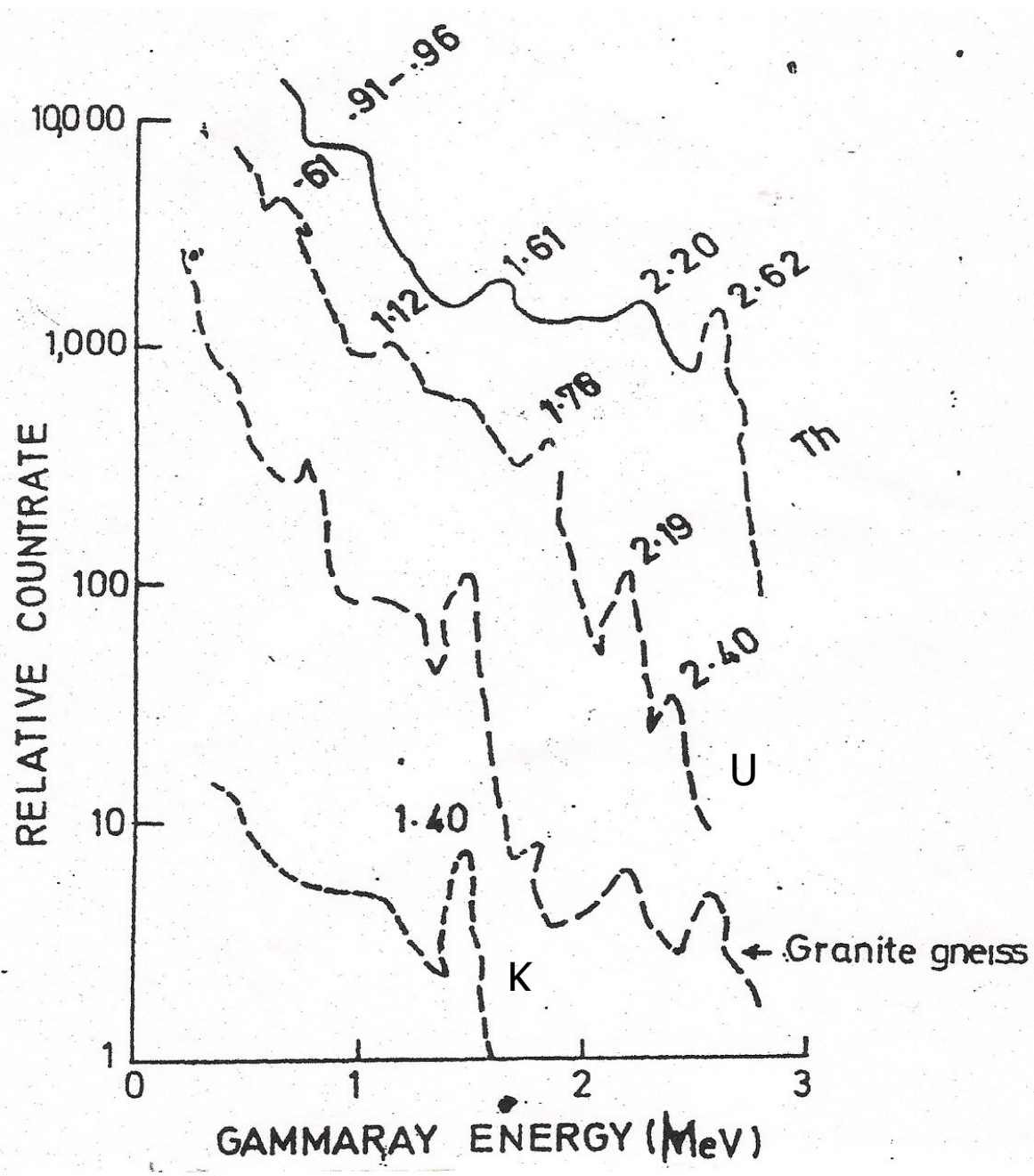


Figure 2.1: Spectrograms obtained from K, Th, and U samples and on a granite gneiss outcrop. (After Doig, 1968).

2.3 U Series Disequilibrium

Disequilibrium in the uranium decay series is a source of error in gamma ray spectrometry. Disequilibrium occurs when one or more decay products in a decay series are completely or partially removed or added to the system. Thorium rarely occurs out of equilibrium in nature, and there is no disequilibrium with potassium. However, in the uranium decay series disequilibrium is common, and can occur at several positions in the U-238 decay series. U-238 can be selectively leached relative to U-234; U-234 can be selectively leached relative to U-238; Th-230 and Ra-226 can be selectively removed from the decay chain; Finally Rn-222 (radon gas) is mobile and can escape from soils and rocks into the atmosphere. Uranium concentration estimates are based on the measurement of Bi-214 and Pb-214 isotope abundances. These occur far down in the radioactive decay chain and may not be in equilibrium with uranium. Estimates of uranium concentration are therefore usually reported as "equivalent Uranium", eU as these estimates are based on the assumption of equilibrium conditions. Thorium is also usually reported as "equivalent thorium" (eTh), although the thorium decay series is almost in equilibrium.

Methods to determine the existence of equilibrium in the U Series from gamma spectrometric and chemical analysis have been suggested. Comparison of the results of chemical analysis and the determination of equivalent uranium (eU) from gamma spectrometry is one of such methods (Dewu, 1989).

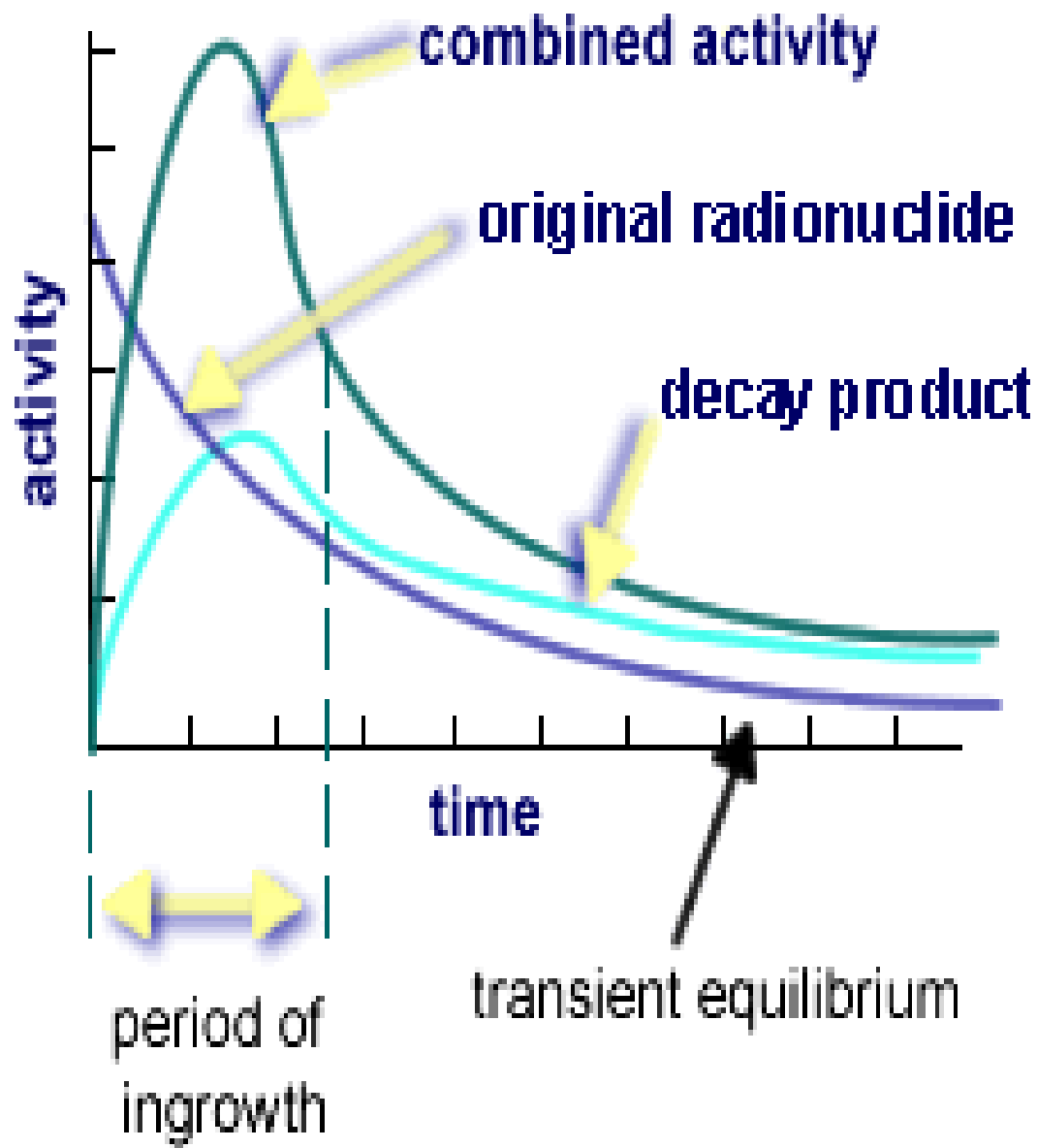


Figure 2.2: Graph of activity versus time of radionuclide and decay product. It is assumed that the parent nuclide has the longest half life.

The graph (Figure 2.2) shows that the maximum activity for a particular decay product occurs when its activity is equal to that of its original radionuclide. Where the activities of all the members of the series are equal, the ratio of activities is unity. The situation where the rates of decay of all members of a radioactive series are equal is described as secular equilibrium.

The radioactive atoms (for example U-238) at this point is said to be in secular equilibrium with its disintegration products since the activity of any of the member series in the equilibrium is equal to that of the original radionuclide, the activity of one of the decay products can be measured by monitoring the particle or photon it emits provided interference from other daughter nuclides and other external sources are checked. Since t , the length of time between the time of deposition of the mineral and the time of observation must be higher than half of the daughter products, and then the time to reach equilibrium will be determined by the half life of the longest lived daughter of the series. This is U-234 ($t_{1/2} = 24,500$ years) in the U-238 series and Ra-228 ($t_{1/2} = 5.75$ years) in the Th-232 (Uwah, 1984). Thus, while a pure Th-source will reach secular equilibrium in approximately 50 years, a U-source requires up to 2×10^6 years to reach equilibrium. Since Th-232 reaches equilibrium in about 50 years, it is often assumed that for most geological samples, the Th-decay series will be in equilibrium and the equivalent thorium (eTh) that is, the amount of Th that would be present if secular equilibrium was established is equal to Th concentration (Dickson et al., 1982). However, Ra-228 which is the immediate daughter of Th-232 has been found separate from Th-232 because of

mobility of radium in the ground water (Dickson et al., 1982). Then the rocks in contact with ground water may have lost Ra-228 and Ra-224 and the Th will not be in equilibrium. Thus, the equivalent concentration of uranium/thorium estimated.

2.5 Gamma Ray Spectrometry

Gamma ray spectrometry (GRS) provides a direct measurement of the surface of the earth and with no significant depth of penetration. GRS measures the spatial distribution of K, Th, and U in the top 30-45 cm of the earth's crust (Grasty, 1975). The abundances of K, Th and U are measured by detecting the gamma rays produced during the natural decay of these elements.

All rocks and soils are naturally radioactive and contain various proportions of variety of radioactive elements. Natural decay of these elements produces a variety of types of radiation (alpha, beta, and gamma) at specific energy level but only gamma ray radiation has sufficient energy to be useful for geological mapping or exploration (Tom, 2002). Individual radionuclide emits gamma rays of specific energies that are characteristics for an element and isotope. Gamma ray measurements can be conducted in two modes. Total counts measurements register gamma rays of all energies. These are used to monitor the gross level of gamma radiation field and to detect the presence of anomalous sources. On the other hand, spectrometers measure both the intensity and energy of radiation, and this enables the source of the radiation to be diagnosed. A gamma ray spectrometer is designed to detect the gamma rays associated with radioactive elements, it accurately sort the detected gamma rays by their respective energies. It's this sorting ability that distinguishes the spectrometer from instruments that measure only total radioactivity (Tom, 2002).

All spectrometers used for measuring gamma ray intensity in geophysics consist of two principal parts. The detector which senses or detects the gamma rays, and the analyzer which analyzes the signal and displays the result. There are three major categories of the gamma ray spectrometry, namely, threshold (integral), multichannel, and window (Darnley, 1973). Multichannel spectrometry involves obtaining counts rates from the full spectrum in a series of discrete steps or channels. Threshold spectrometry such as is used in this work involves summing the counts from the spectrum in a series of overlapping steps by varying the energy threshold at which counting commence, for example, threshold of 1.36, 1.66, and 2.42 MeV could be used respectively to measure the sums K+U+Th, U+Th, and Th alone. Window spectrometry which is the most commonly used in most air borne, ground surveys, and laboratory analyses (Grasty, 1975) involves measuring count rates only from portion of spectrum encompassing the photo peaks of interest.

The major component of gamma ray spectrometer is the detector crystal. The most widely used detectors for gamma ray spectrometry especially for in-situ radiometric surveys are thallium activated sodium iodide crystals (NaI(Tl)) (Lovborg et al., 1971). Lithium drifted germanium, Ge(Li), is most useful in laboratory analysis where high energy resolution and low energy measurements may be required. Hyperpure Germanium detectors (HPGE), have excellent resolution and are better than Ge(Li) detectors. They need to be cooled only when in use unlike the later which must be cooled continually even when not in use to temperature of

nitrogen. Sodium iodide crystals are preferred because they have good resolution of the energies in the 0.3 to 3 MeV ranges, a high transparency (even weak flashes of light can be detected), are relatively easy to grow large crystals of NaI, and relatively economical detector.

CHAPTER THREE

SCINTILLOMETER FIELD SURVEY

3.1 Background

The scintillometer survey was conducted from 28th May to 8th June 2008. The survey covered all the area for possible indication of radioactive mineralization. It was not possible to determine the type of source of radioactivity in-situ, since scintillometer measures gross counts only.

3.2 Field Instrumentation/Procedure

The field scintillometer used was Exploranium model GR-101A, manufactured by Geometrics Inc. California. The model GR-101A total count scintillometer is a complete field system designed for man carrying applications requiring accurate and reliable determination of the total gamma ray intensities from the radioactive elements, potassium (K-40), uranium (as Bi-214), and Thorium (as Th-232). The inherent simplicity of the GR-101A allows rapid accurate measurements to be obtained from a compact field instrument.

The GR-101A scintillometer is an instrument that transforms incident gamma radiation into visual readout of radioactive intensity as a function of the natural radioactive material present in geologic phenomena. A sodium iodide crystal converts gamma rays into faint flashes of light whose brilliance is proportional to

the energy level of the gamma radiation measured. These light flashes are detected by high gain photomultiplier tube (PMT) amplified and feed circuitry which accepts those signals above certain energy. The accepted signals are average in a rate meter circuit as counts per second and continuously displayed on a 250° meter on the instrument front panel. The frequency or signal count rate displayed is the intensity of all gamma ray energy above the preset threshold. The detector crystal was a sodium thallium activated NaI (Ti) cylinder of dimensions 38.1mm x 38.1mm. The instrument recorded total count only for all gamma rays of energies above 0.05 MeV (McDermott, 1977). Readings were taken along profiles aligned in the NW-NE direction spaced at 50 m interval from each other. Along each profile, readings were taking at interval of 50 m. Each profile was 1800 m long and there are a total of 18 profiles. The coordinates (latitudes and longitudes) of points where readings were taken was measured using the Global Positioning System (GPS).

In order to estimate the cosmic ray contribution to the ground activity measured in the field, readings were taken at an area of very thick over burden located which was a pool of water in about 300 m from the study area. Measurements were normally made at 600 and 1800 hours each for five days. The average cosmic background (spectrum when no source is present) estimated was used to correct for the background.

3.3 Data Reduction

The background corrected data were contoured using the surfer program. The observation in the field was that areas of high activities coincided with areas with the outcrops, while areas depicting the lowest activities correlate with areas of thick overburden. These anomalies observed may be significant in terms of radioactive mineralization.

3.3.1 Data Analysis

Because geologic formations are not necessarily uniform in radioactivity calculations of average values and of standard deviations of field activities can be in error. A better method of determining the average value of activity for a geologic unit is to plot a frequency distribution of the number of data points with a given activity versus the activity (Uwah, 1984). The mean activity is the mode of the frequency distribution. The expected or normal mean value of activity for the site was obtained from the frequency plot (Figure 3.1) as follows.

The mode = 8 cps

The full width at half maximum (FWHM);

$$\frac{1 + 2 + 2 + 2 + 2 + 2 + 4 + 6 + 2 + 2 + 4 + 7 + 4}{13} = \frac{40}{13} = 3.1$$

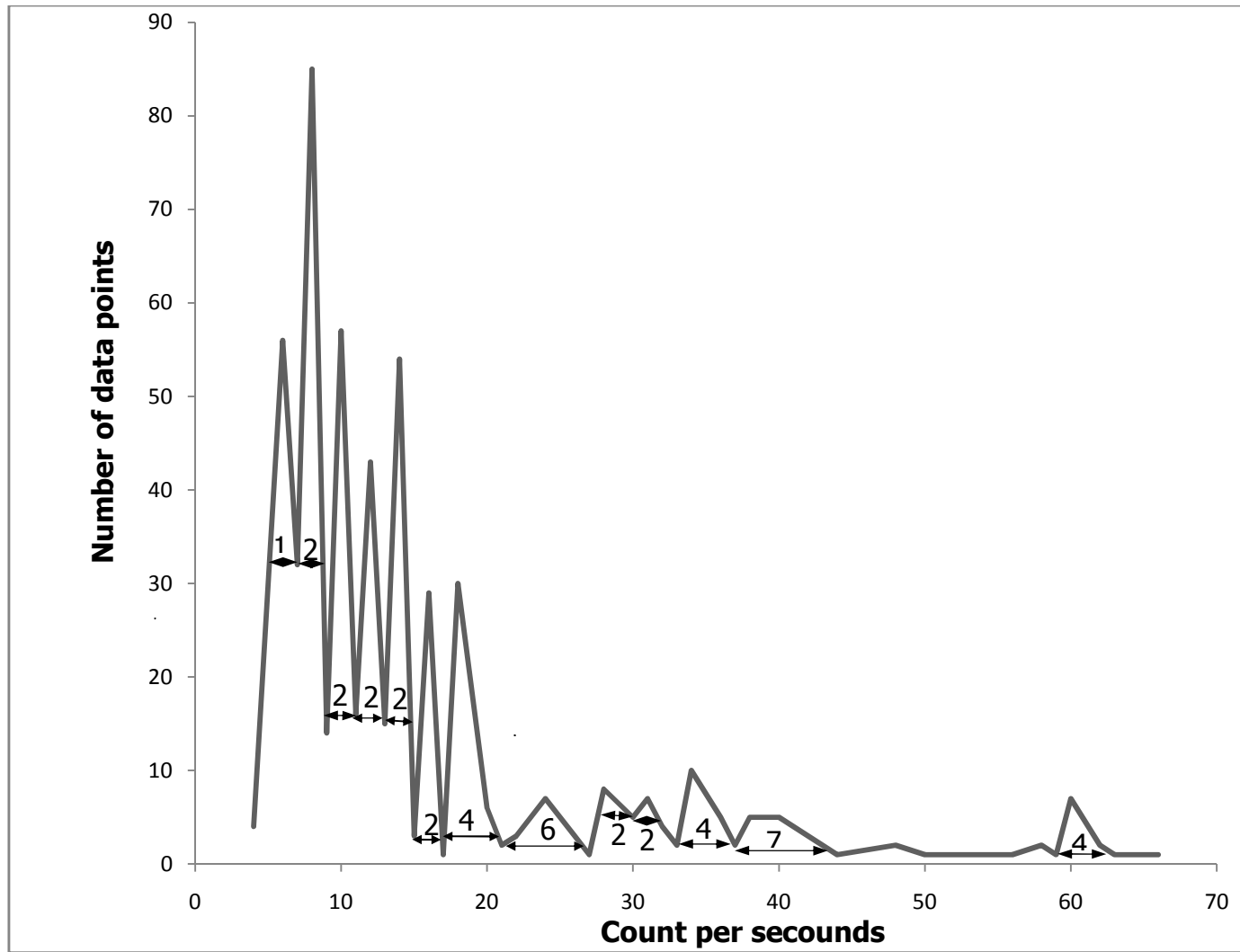


Figure 3.1: Frequency distribution curve of count rates (corrected data)

The Standard Deviation (SD) in accordance to Duval, (1979) is

$$SD = FWHM \times 0.75$$

Therefore,

$$SD = 3.1 \times 0.75$$

$$SD = 2$$

The normal or the expected mean value of activity, LB is then given by:

$$LB = \text{mode} \pm SD$$

$$LB = 8 \pm 2$$

Figure 3.2 is the contour map of count rates (uncorrected data). Figure 3.3 is the contour map of count rates (corrected data). All other values higher than the threshold are considered anomalous in Figure 3.3. Thus, the anomalous areas were considered as bounded by the 16 cps contour line in Figure 3.4.

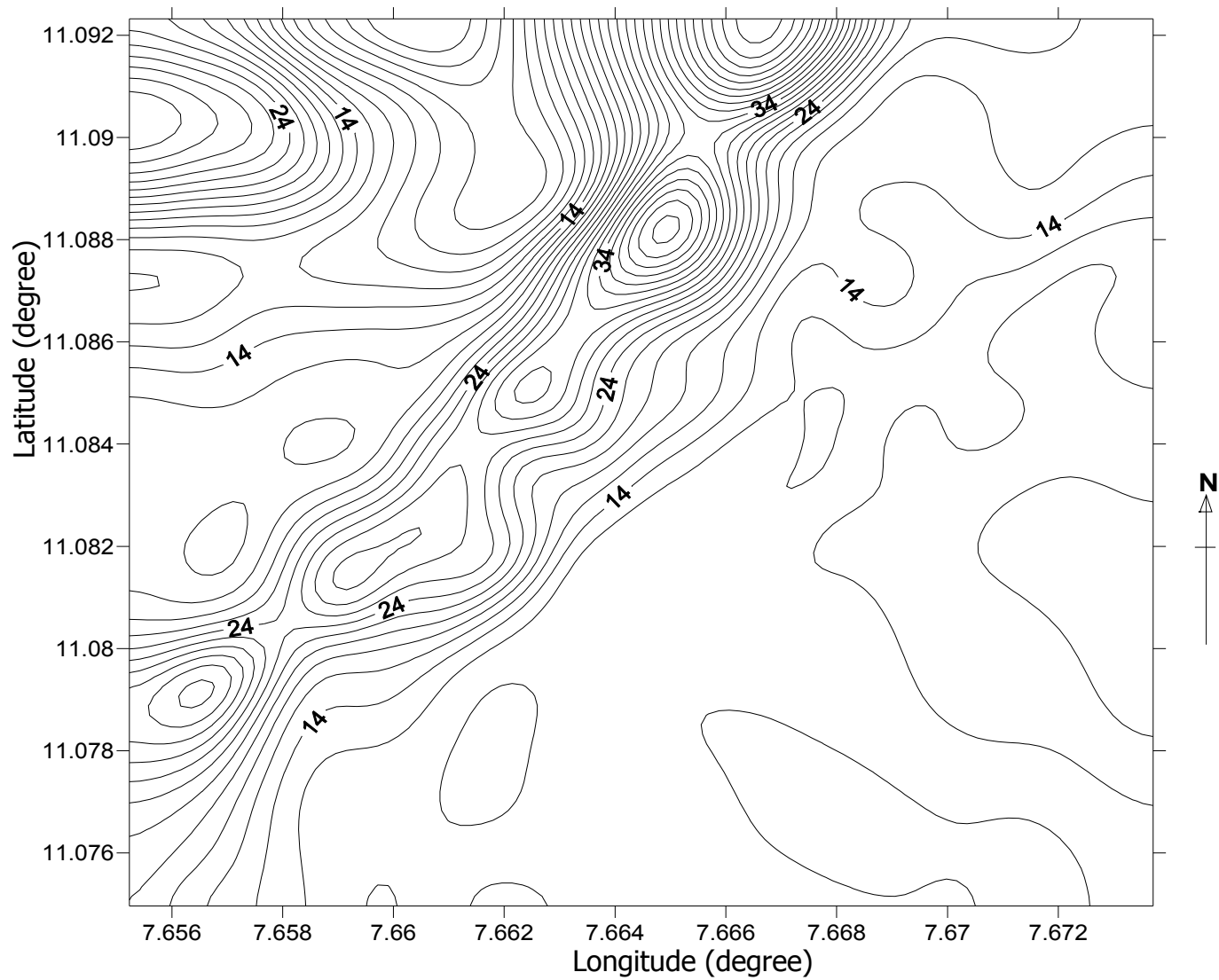


Figure 3.2: Contour map of count rates (uncorrected data). Contour interval is 2 cps.

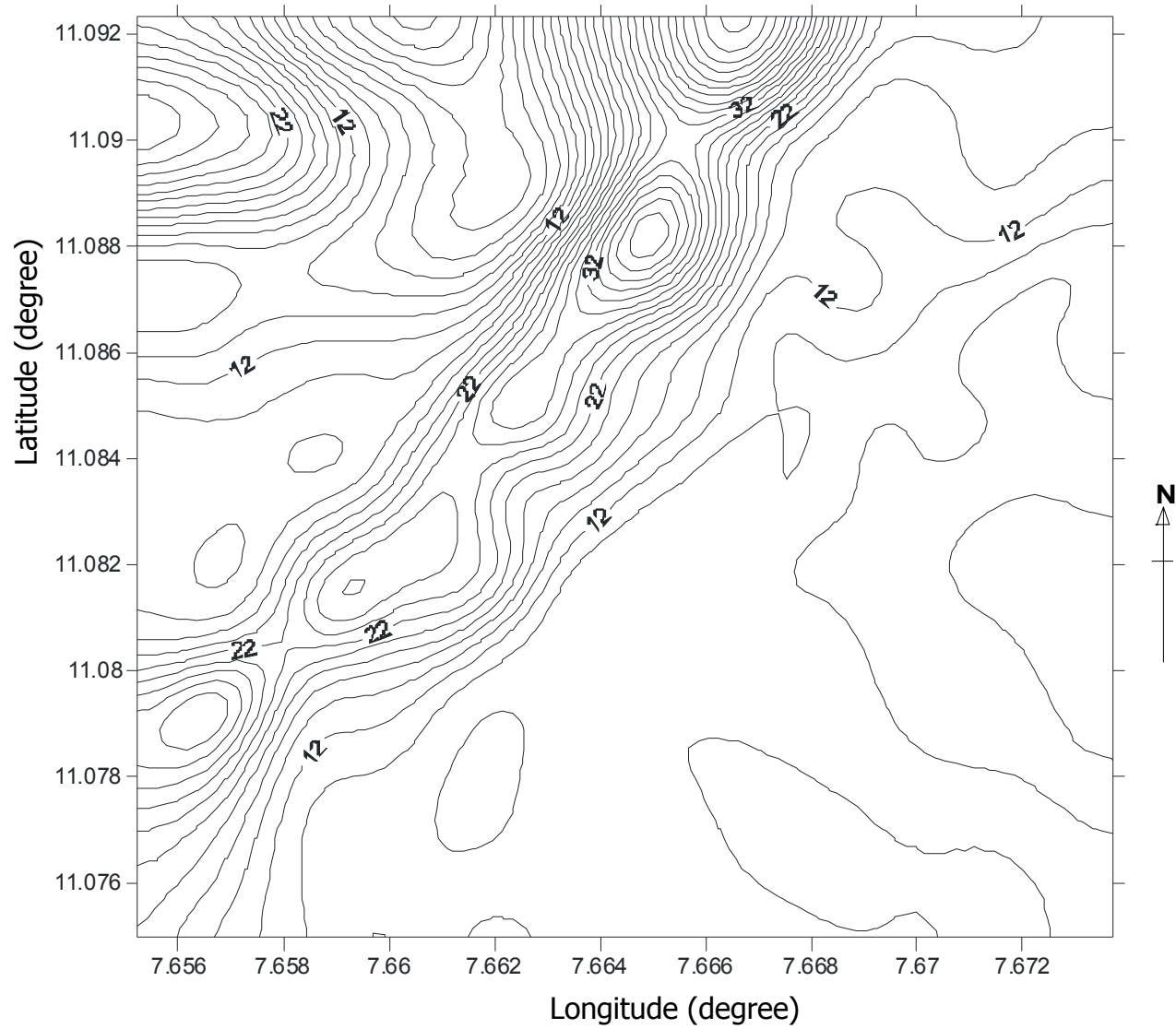


Figure 3.3: Contour Map of count rates (corrected data). Contour interval is 2 cps.

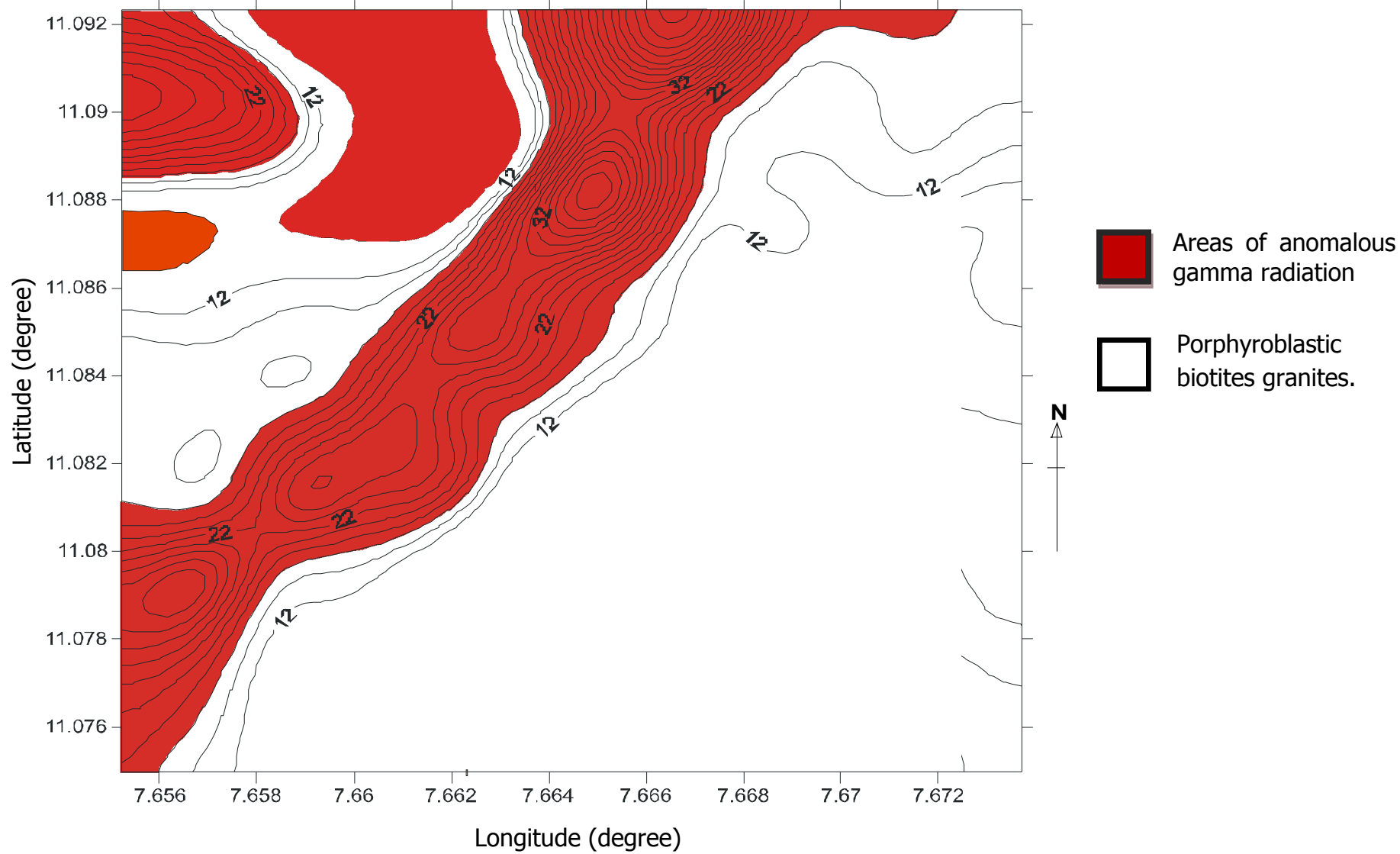


Figure 3.4: Contour map of count rates showing areas of anomalous gamma radiation.

CHAPTER FOUR

GAMMA-RAY SPECTROMETRY SURVEY

4.1 Background

The outcrops including the flat land within the area of study was surveyed between 28th May to 8th June, 2008 with a Digital integral analyzer (DISA-300) gamma ray spectrometer. This survey was conducted in order to determine radioelement (K, Th, and U) content, and identify the source of radiation.

4.2 Field Procedure

An in-situ gamma ray spectrometric survey of the area was carried out. This involves taking readings on the surface of a square grid of 50 m interval. A total area of approximately 2.0 km² was covered. The spectrometer was calibrated every day before the start of the measurements during the course of the survey to ensure that channel drift due to temperature/drift characteristics of the photomultiplier tube was eliminated. Since the spectrometer was used to identify a source of unknown composition, its energy scale must be calibrated first. This was achieved using the peaks of a known source Co-60. Due to the presence of radioactivity everywhere, the spectrum when no source is present (background) was determined. The routine for collection of data involved placing the spectrometer on the ground (or outcrop) at each predetermined point and taking readings in the four channels. A global positioning system (GPS) was used to

measure the geographical coordinates of each point. The measurements were taken along profiles aligned in the NW-NE direction, and a spacing of 50 m was used. The radioactive background was measured twice daily at a particular area of thick overburden located 300 m from the survey site

4.3 Data Processing

Gamma ray field measurements yield a number of counts. For a threshold spectrometer such as the one used in this work, the relationship between the count rates and element concentration is such that the concentration in parts per million (ppm) is directly proportional to the background corrected and stripped count rate. Using the following conversion equations provided by the Exploranium (the instrument manufacturers) the background corrected counts rates were converted to relative surface concentrations.

$$eTh \text{ (ppm)} = K_1 (Th_c - Th_b) \quad 4.1$$

$$eU \text{ (ppm)} = K_2 [(U_c - U_b) - S_2 (Th_c - Th_b)] \quad 4.2$$

$$K \text{ (\%)} = K_3 [(K_c - K_b) - S_2 (U_c - U_b) - S_3 (Th_c - Th_b)] \quad 4.3$$

Where Th_b , U_b , and K_b , are the average background reading in the thorium, uranium and potassium channels respectively K_1 , K_2 , and K_3 , S_1 , S_2 , and S_3 are the sensitivity constants and stripping ratios for their respective spectrometer channels. Using the constants supplied by manufacturers, equation 4.1, 4.2 and 4.3 becomes.

$$eTh \text{ (ppm)} = 1.33 \times (Th_c - Th_b) \quad 4.4$$

$$eU \text{ (ppm)} = 200 \times [(U_c - U_b) - 0.62 (Th_c - Th_b)] \quad 4.5$$

$$K \text{ (\%)} = \frac{[(K_c - U_c) - K_b - 0.68(U_c - Th_c) - U_b - 0.83(Th_c - Th_b)]}{154} \quad 4.6$$

The estimated equivalent surface concentrations eTh , eU , and $K \%$ were obtained using equation 4.4, 4.5 and 4.6 respectively. The total count, eU , eTh and $K \%$ concentrations derived from both the corrected and uncorrected data were contoured using the surfer 8.0 program.

The maps shown in Figure 4.1, is the total count contour map. Figure 4.2, 4.3 and 4.4 are the contour maps of eU , eTh and $K \%$ derived from the background corrected data. The map shown in Figure 4.5, is the total count contour map, Figure 4.6, 4.7, and 4.8, are the contour maps of eU , eTh and $K \%$ derived from uncorrected data.

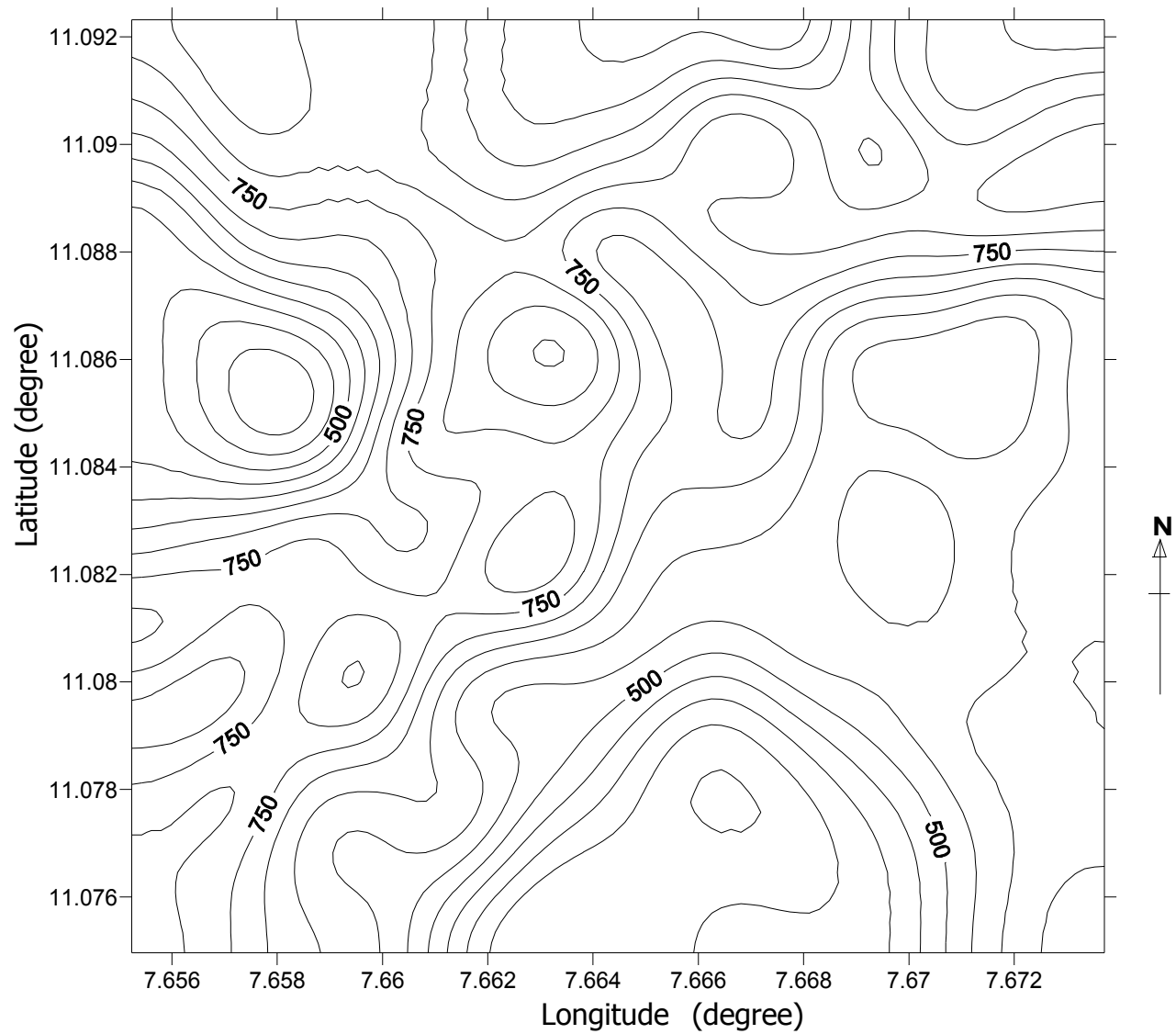


Figure 4.1: Contour map of total count (corrected data). Contour interval is 50 cps.

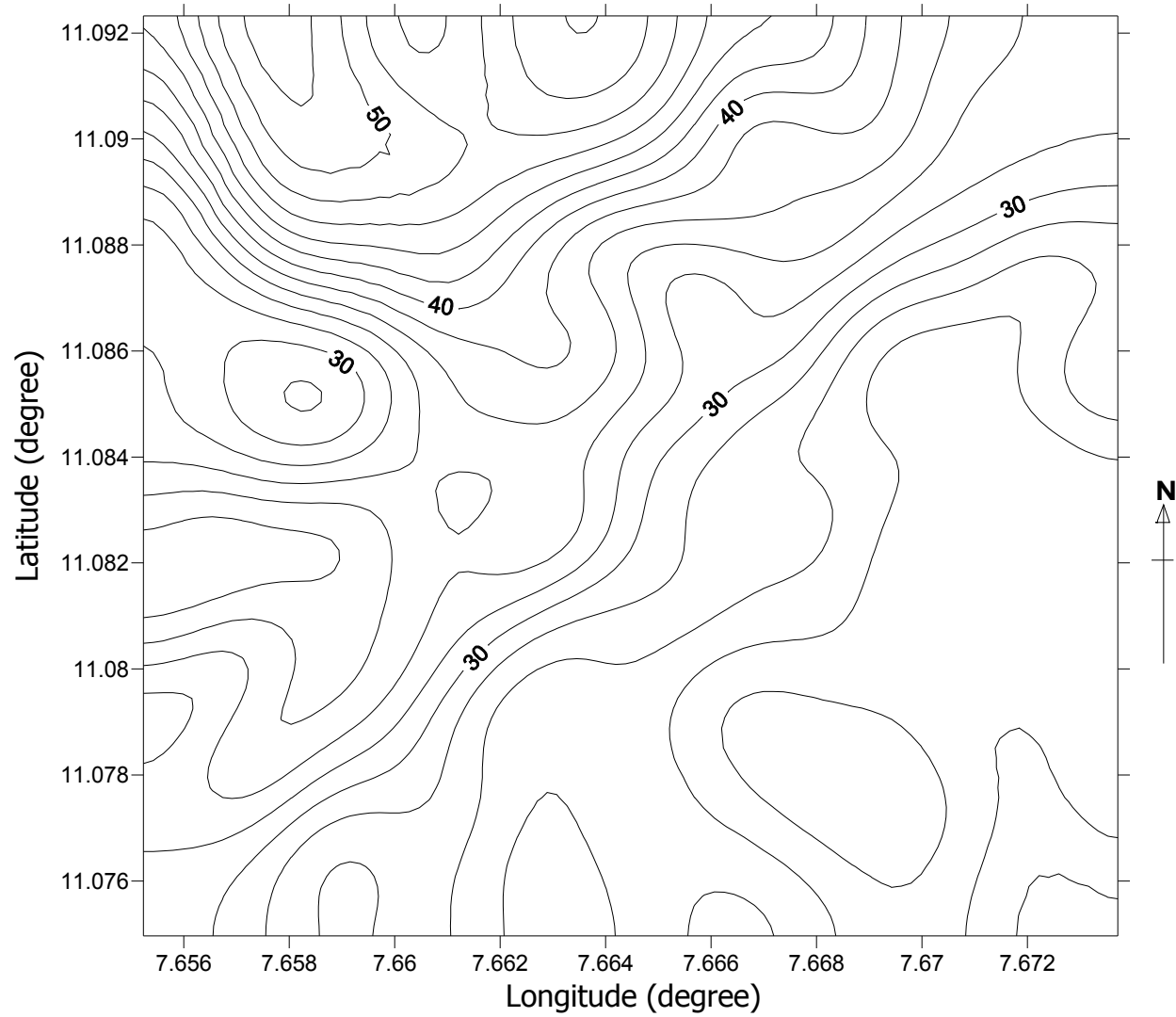


Figure 4.2: Contour map of eU (corrected data).Contour interval is 2 ppm.

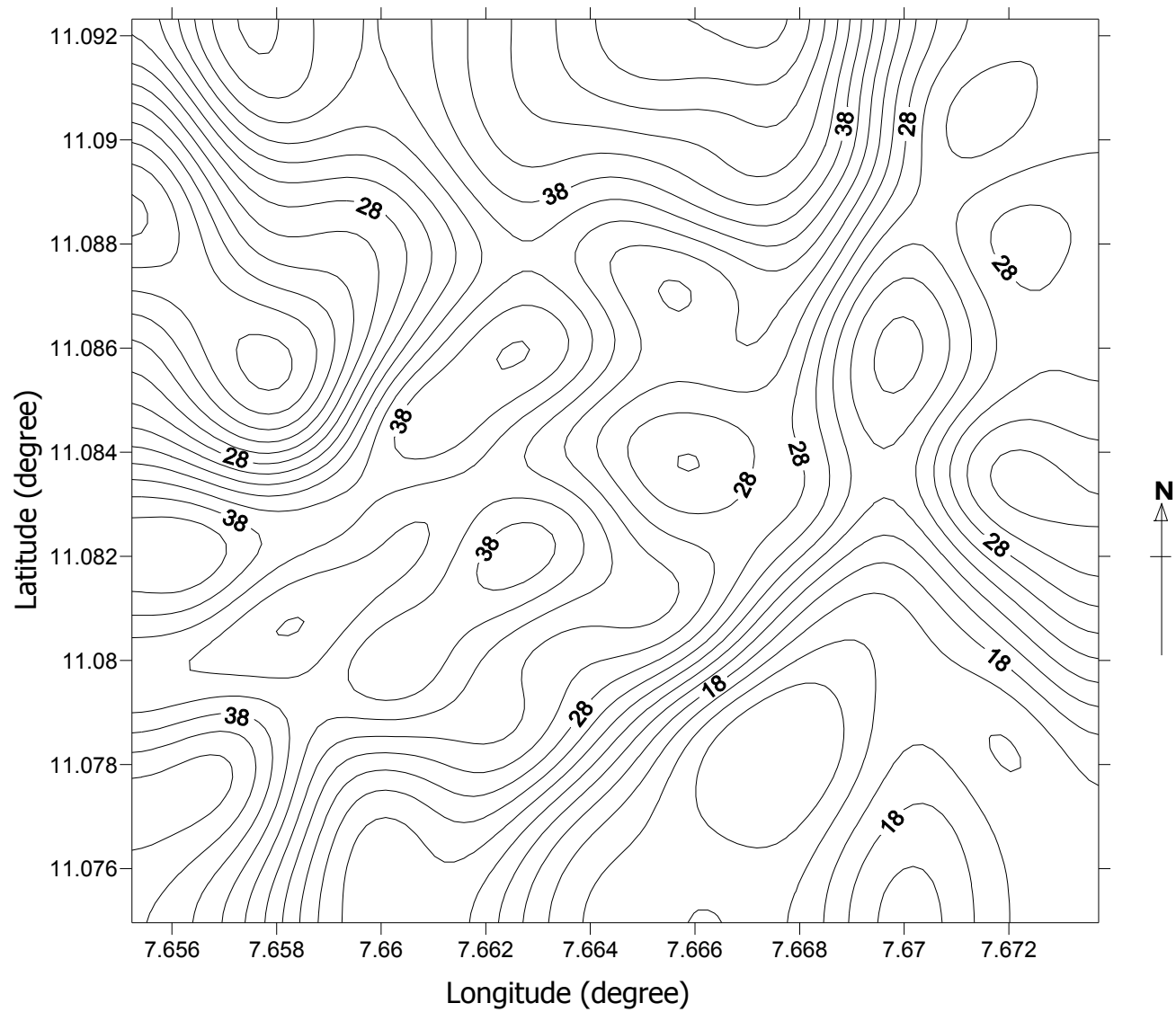


Figure 4.3 Contour map of eTh (corrected data). Contour interval is 2 ppm.

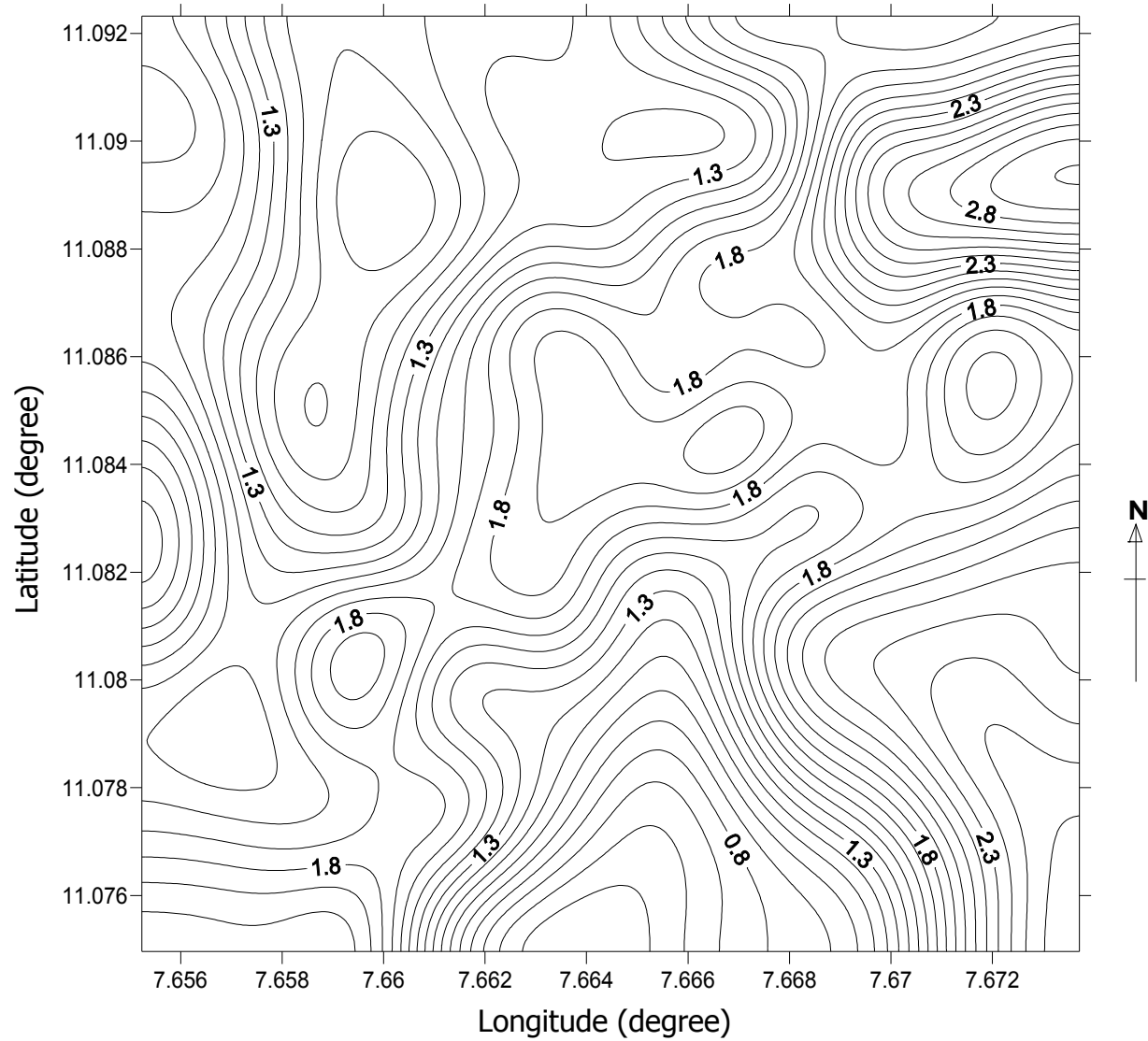


Figure 4.4: Contour map of K % (corrected data). Contour interval is 0.1 %.

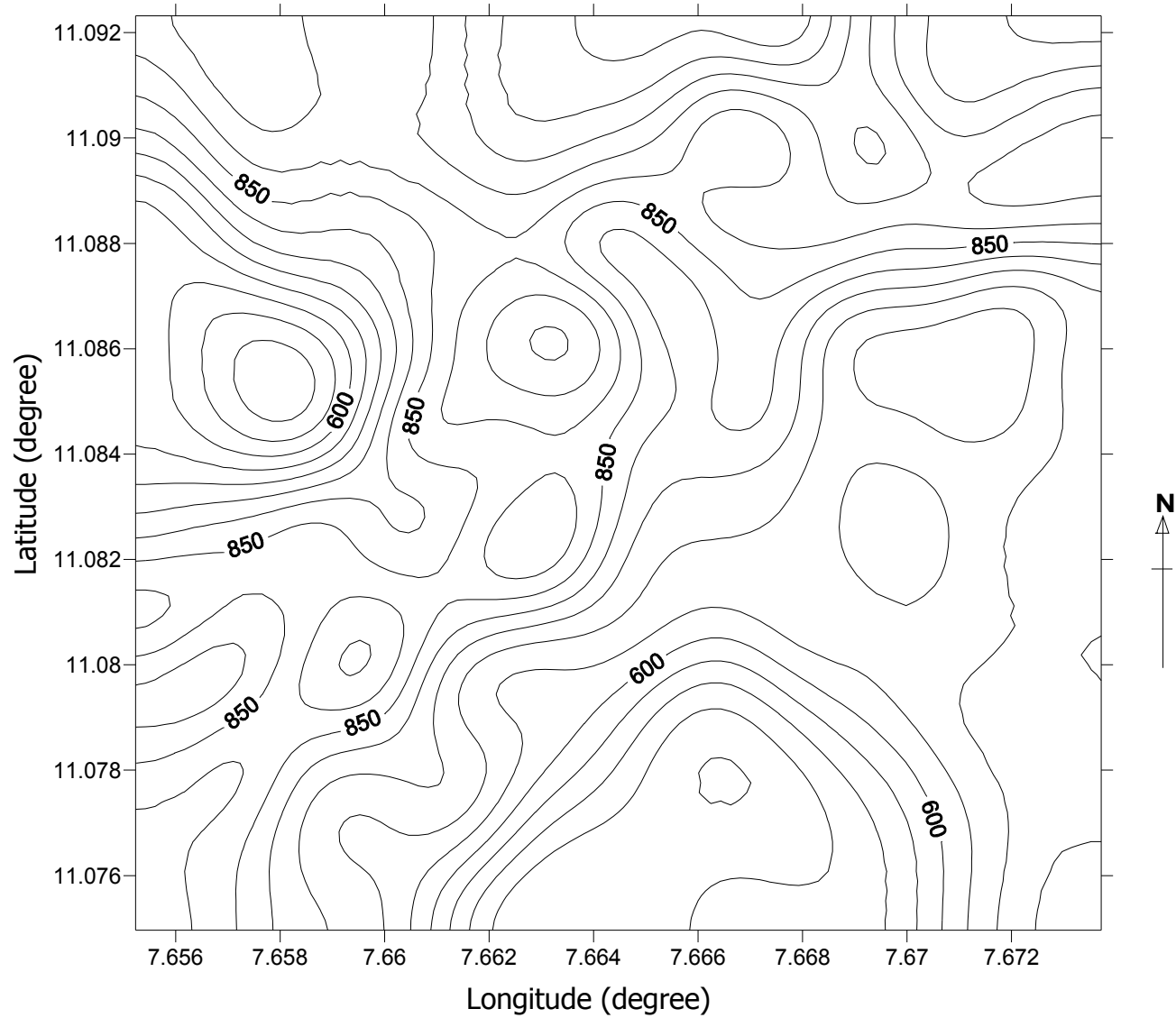


Figure 4.5: Contour map of total count (uncorrected data). Contour interval is 50 cps.

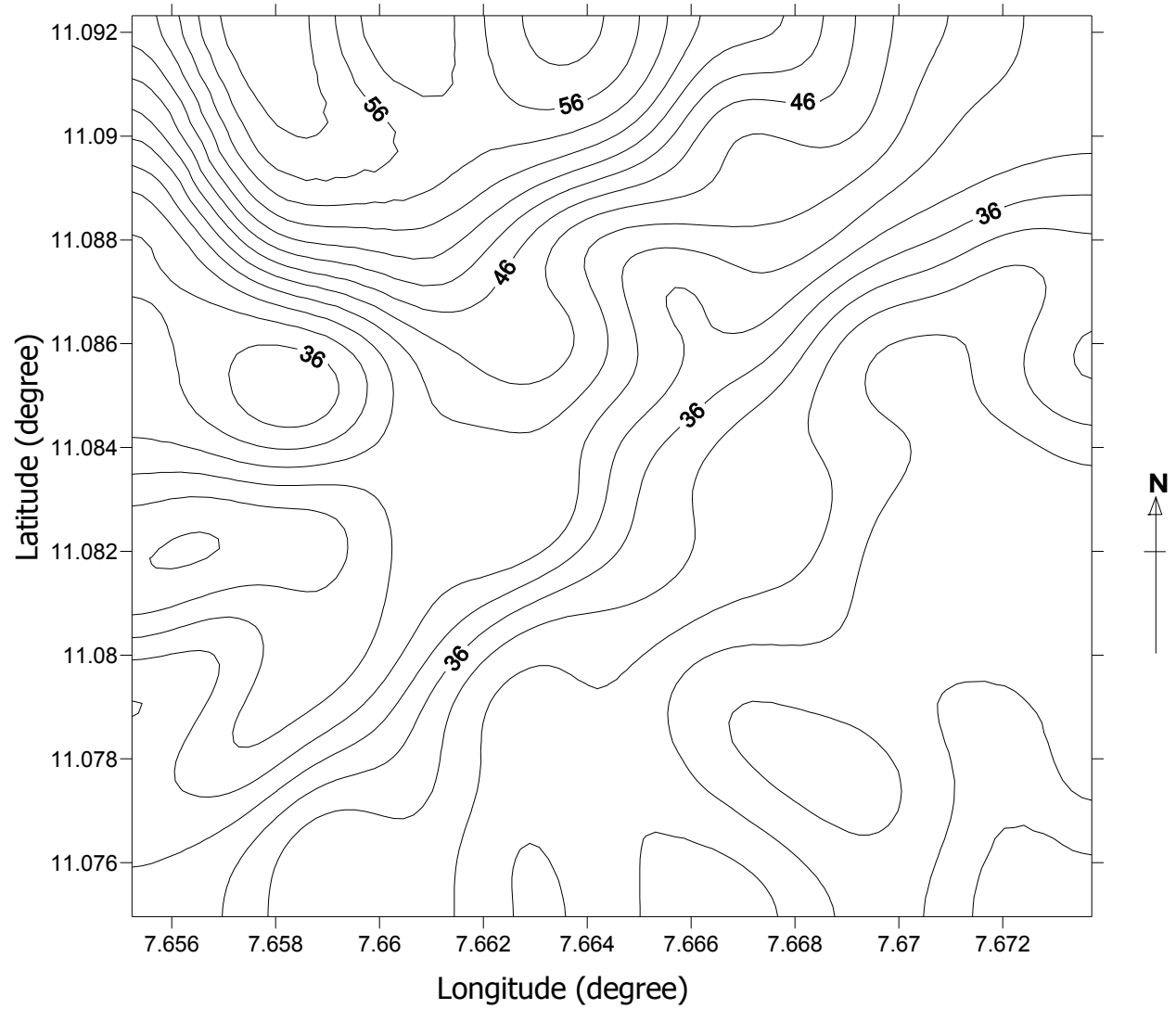


Figure 4.6: Contour map of eU (uncorrected data). Contour interval is 2 ppm.

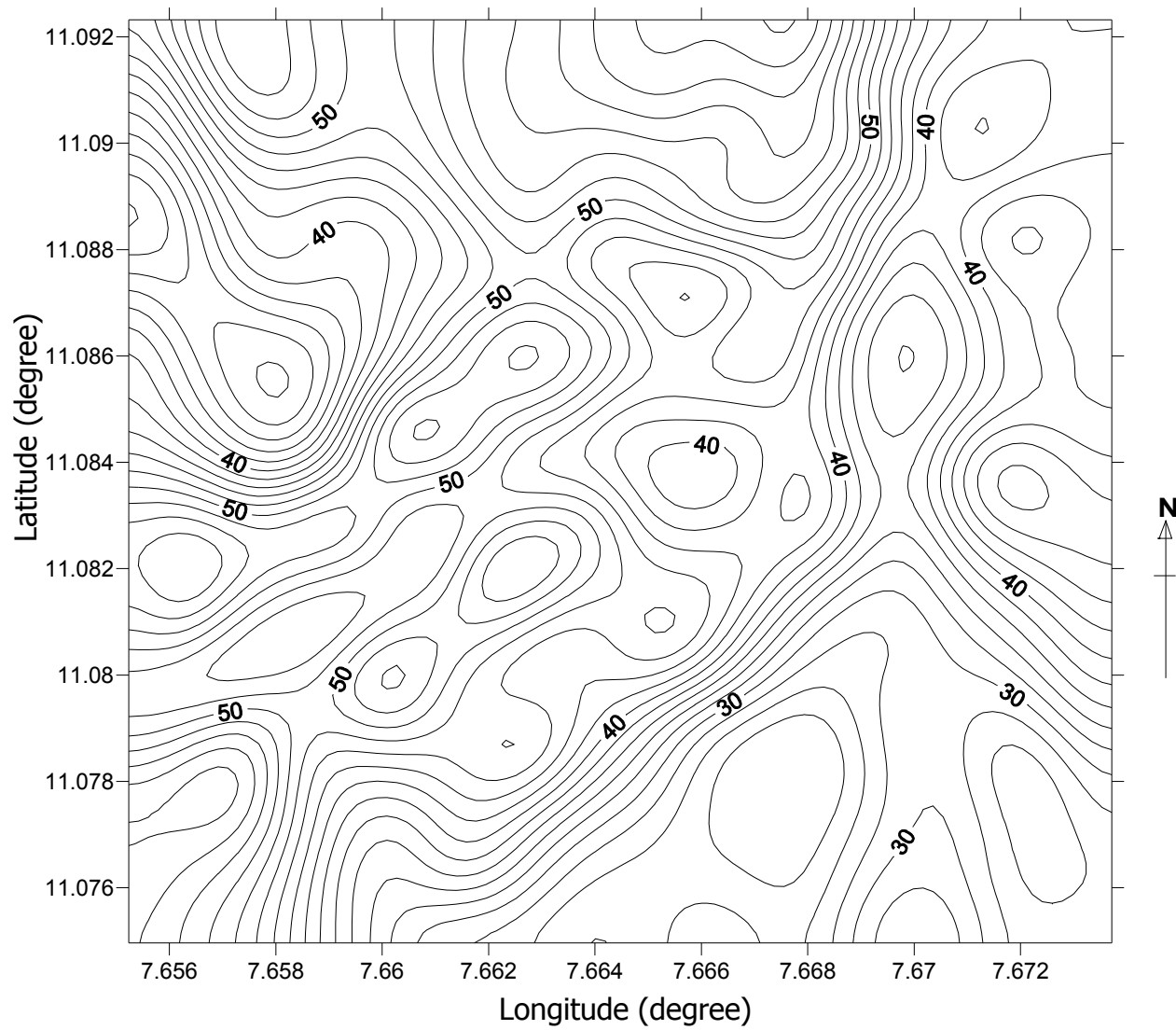


Figure 4.7: Contour map of eTh (uncorrected data). Contour interval is 2 ppm.

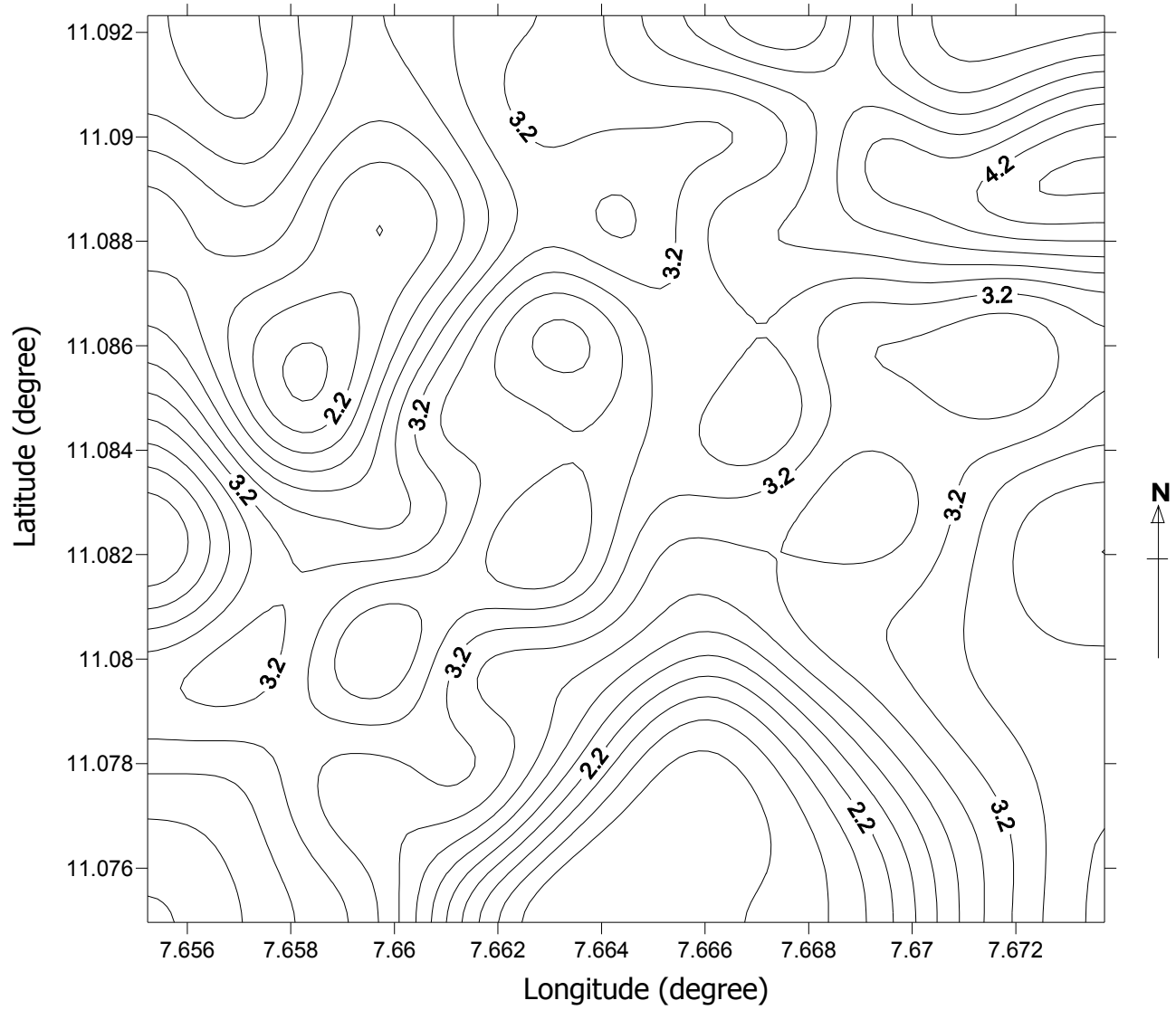


Figure 4.8: Contour map of K % (uncorrected data). Contour interval is 0.2 %

CHAPTER FIVE

DATA ANALYSIS AND INTERPRETATION OF SPECTROMETRY DATA

To characterize the major radioactive areas of the site the total count contour map (Figure 4.2) was used. This was possible by determining a reference background count and anomalies selected on the basis of areas with readings above the reference background (Dewu, 1986). The reference background was deduced using a frequency distribution curve (Figure 5.1). The mode gave a count of 539.5cps and this was taken as the reference background for the site.

The total count contour map revealed one defined anomaly centered at (11.083°, 7.658°) degrees whose peak intensity (highest contour value) is 1458 cps. The contour which is mid way the reference background and the peak intensity is approximately 800 cps contour line. Therefore, the approximate areas of sources of radiations which produce this anomaly were bounded by 800 cps contour line.

5.1 Probable Areas of Radiometric Mineralization

In order to map out the most probable areas of radiometric mineralization, threshold values of eU, eTh and K% concentrations were determined statistically as described below. The median (L) of eU, eTh and K% were taken as their mean values (Uwah, 1984). Both the median (L) and the standard deviation(S) from the median were obtained from standard statistical formulae (Spiegel, 1961).

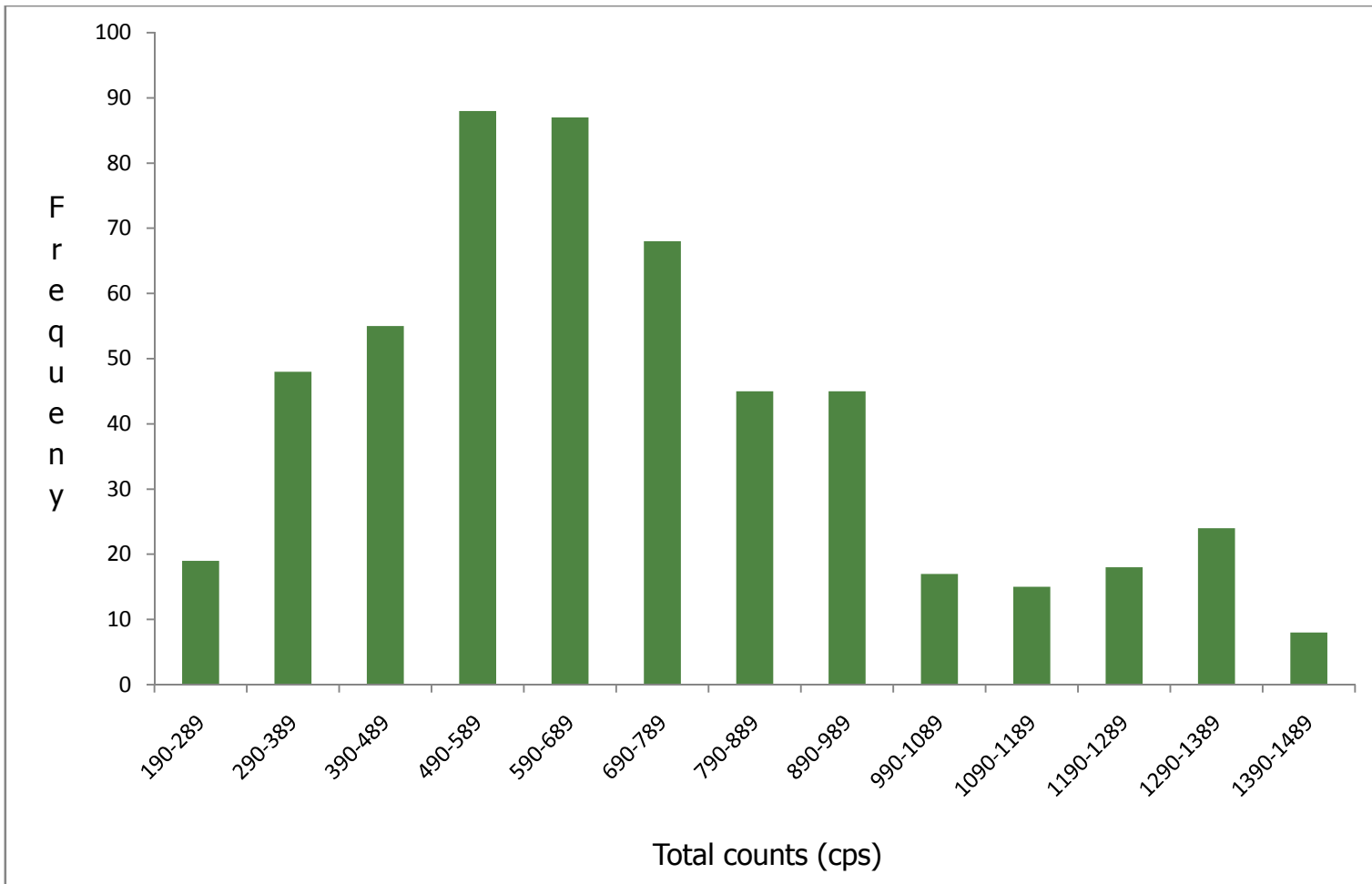


Figure 5.1: Frequency distribution curve of total count.

In order not to underestimate the threshold values, and hence over estimate the size of the anomalies characterized from the data, those areas where e U, eTh, or K % could not be measure were excluded in determining L and S. Frequency distribution table (Table 5.1–5.6) were drawn from which I and S were calculated using standard statistical formulae.

For class interval with equal size C, the median (\bar{L}) obtained by interpolation is given by;

$$\bar{L} = L_i + \frac{\frac{N}{2} - (\sum f)_N \times C}{f_{Med}} \quad 5.1$$

Where: L_i = lower class boundary of the median class.

f_{med} = frequency of the median class.

$(\sum f)_N$ = Sum of frequencies of all classes lower than the median.

C = Size of median class interval (spiegel, 1961).

The 90% confidence interval for the mean values was obtained from the equation:

$$L = \bar{L} \pm \frac{Z \cdot S}{\sqrt{N}} \sqrt{\frac{N_p - N}{N_p - 1}} \quad 5.2$$

Where: N_p = total number of points at the survey site.

N = Number of points where eU, eTh or K % could not be measured.

$Z = 1.645$ for 90 % confidence (Spiegel, 1961)

$S =$ Standard deviation

The standard deviation from the median, S is given by;

$$S = \sqrt{\frac{f_i (L_i - \bar{L})^2}{N - 1}} \quad 5.3$$

Where: $L_1 =$ Lower limit of class intervals

$$\bar{L} = L_i + \frac{\frac{N}{2} - (\sum f)_N \times C}{f_{Med}} \quad 5.4$$

Equation 5.2 can be written as

$$L = \bar{L} \pm \Delta \quad 5.5$$

The threshold value L_B was taken as the upper range of equation 5.5.

$$\text{Therefore, } L_B = L \pm \Delta \quad 5.6$$

The value of eU , eTh , and K % exceeding their threshold values were considered anomalous.

Table 5.1: Frequency Distribution of eU concentration (corrected data).

Class Interval eU(ppm)	L_i (ppm)	Frequency (f_i)	Cumulative frequency	f_i(L_i-\bar{L})²
16 – 20	18	74	74	773.2974
21 – 24	22.5	74	148	93.25808
25 – 28	26.5	69	217	1869.321
29 – 32	30.5	83	300	7048.606
33 – 36	34.5	75	375	13106.57
37 – 40	38.5	48	423	14236.11
41 – 44	42.5	37	460	16665.43
45 – 48	46.5	22	482	13997.46
49 – 52	50.5	17	499	14519.36
53 – 56	54.5	22	521	24286.04
57 – 60	58.5	13	534	18014.65
61 – 64	62.5	1	536	1699.574
65 – 68	66.5	1	536	2045.405
				128355.1

Table 5.2: Frequency Distribution of eTh concentration (corrected data).

Class Interval eTh(ppm)	L_i (ppm)	Frequency (f_i)	Cumulative frequency	f_i(L_i-\bar{L})²
8 – 12	10	10	10	4000
13 – 16	14.5	83	93	17436.31
17 – 20	18.5	35	128	3854.341
21 – 24	22.5	34	162	1433.849
25 – 28	26.5	73	235	454.0626
29 – 32	30.5	69	304	156.4945
33 – 36	34.5	27	331	818.533
37 – 40	38.5	25	356	2259.101
41 -44	42.5	60	416	10944.72
45 – 48	46.5	18	434	5516.281
49 – 52	50.5	23	457	10637.68
53 – 56	54.5	26	483	16914.46
57 – 60	58.5	17	500	14800.27
61 – 64	62.5	5	505	5613.26
65 – 68	66.5	8	513	11253.6
69 – 72	70.5	14	527	24118.47
73 – 76	74.5	1	528	2070.796
77 – 80	78.5	2	530	4901.688
81 – 84	82.5	3	533	8588.676
85 – 88	86.5	2	535	6613.88
89 – 92	90.5	1	536	3782.988
				156169.5

Table 5.3: Frequency Distribution of K concentration (corrected data).

Class Interval K (%)	L_i (ppm)	Frequency (f_i)	Cumulative frequency	f_i(L_i-\bar{L})²
0.06 - 0.75	0.405	124	124	115.4719
0.76 - 1.46	1.11	161	285	10.8836
1.47 - 2.16	1.815	110	395	21.78275
2.17 - 2.86	2.515	64	459	83.9056
2.87 - 3.56	3.215	36	495	122.5449
3.57 - 4.26	3.915	19	514	123.0635
4.27 - 4.97	4.62	10	524	105.625
4.98 - 5.66	5.32	5	529	78.0125
5.67 - 6.36	6.015	3	532	64.72808
6.37 - 7.06	6.715	1	533	28.56903
				754.5868

Table 5.4: Frequency Distribution of eU concentration (uncorrected data)

Class Interval eU (ppm)	L_i (ppm)	Frequency (f_i)	Cumulative frequency	f_i(L_i-\bar{L})²
23 - 27	25	75	75	1995.937
28 - 31	29.5	84	159	36.44972
32 - 35	33.5	63	222	703.3374
36 - 39	37.5	83	305	4473.222
40 - 43	41.5	74	379	9518.206
44 - 47	45.5	48	427	11297.02
48 - 51	49.5	34	461	12718.88
52 - 55	53.5	23	484	12530.74
56 - 59	57.5	17	501	12708.27
60 - 63	61.5	21	522	20627.78
64 - 67	65.5	13	535	16237.07
68 - 71	69.5	1	536	1547.736
				104394.6

Table 5.5: Frequency Distribution of eTh concentration (uncorrected data)

Class Interval eTh (ppm)	L_i (ppm)	Frequency (f_i)	Cumulative frequency	$f_i(L_i - \bar{L})^2$
4 – 8	6	1	1	1376.41
9 – 12	10.5	0	1	0
13 – 16	14.5	0	1	0
16 – 20	18	0	1	0
21 – 24	22.5	2	3	848.72
25 – 28	26.5	32	35	8817.92
29 – 32	30.5	79	114	12542.04
33 – 36	34.5	31	145	2292.76
37 – 40	38.5	40	185	846.4
41 – 44	42.5	98	283	35.28
45 – 48	46.5	33	316	381.48
49 – 52	50.5	30	346	1642.8
53 – 56	54.5	49	395	6368.04
57 – 60	58.5	33	428	7826.28
61 – 64	62.5	24	452	9032.64
65 – 68	66.5	14	466	7665.84
69 – 72	70.5	29	495	21772.04
73 – 76	74.5	8	503	7887.68
77 – 80	78.5	7	510	8772.12
81 – 84	82.5	10	520	15523.6
85 – 88	86.5	8	528	15068.48
89 – 92	90.5	1	529	2246.76
93 – 96	94.5	3	532	7925.88
97 – 100	98.5	3	535	9207.48
101 – 104	102.5	1	536	3528.36

151609

Table 5.6: Frequency Distribution of K % concentration (uncorrected data)

Class Interval K (%)	L_i (ppm)	Frequency (f_i)	Cumulative frequency	f_i(L_i-\bar{L})²
0.87 - 1.57	1.22	10	10	63.78236
1.58 - 2.27	1.925	109	119	361.2568
2.28 - 2.97	2.625	137	256	172.0115
2.98 - 3.67	3.325	116	372	20.51281
3.68 - 4.37	4.025	68	440	5.311531
4.38 - 5.07	4.725	44	484	42.21303
5.08 - 5.77	5.425	23	507	64.87525
5.78 - 6.47	6.125	14	521	79.26715
6.48 - 7.17	6.825	10	531	94.83216
7.18 - 7.87	7.525	5	536	71.42246
				975.485

5.2 Interpretation of Results

5.2.1 Total Count

The approximate areas of the source of radiations which produce the anomaly on the total count map were bounded by 800 cps contour line in Figure 5.2. Observations from the survey points indicated 800 cps and above were recorded mostly on the outcrops of the survey area. Also, comparison of the gross count map revealed that over 60 % of the area delineated as sources of radiation (in the gross count map obtained using the spectrometer) coincided with areas of anomalous radiation (in the gross count map obtained using the scintillometer). This is an indication that the major radiations were actually from the outcrops of the porphyroblastic biotite granites.

5.2.2 Uranium (eU)

The contour map of eU concentrations derived from background corrected counts is shown in Figure 4.2. The map revealed some defined anomalies in the area. Using Table 5.1 and equations 5.1-5.6, the threshold value of corrected eU concentrations was found to be 28.8 ppm. Those areas where eU concentrations exceeded 28.8 ppm were considered anomalous. Therefore, all areas bounded by 30 ppm contour line in Figure 5.3 were considered anomalous.

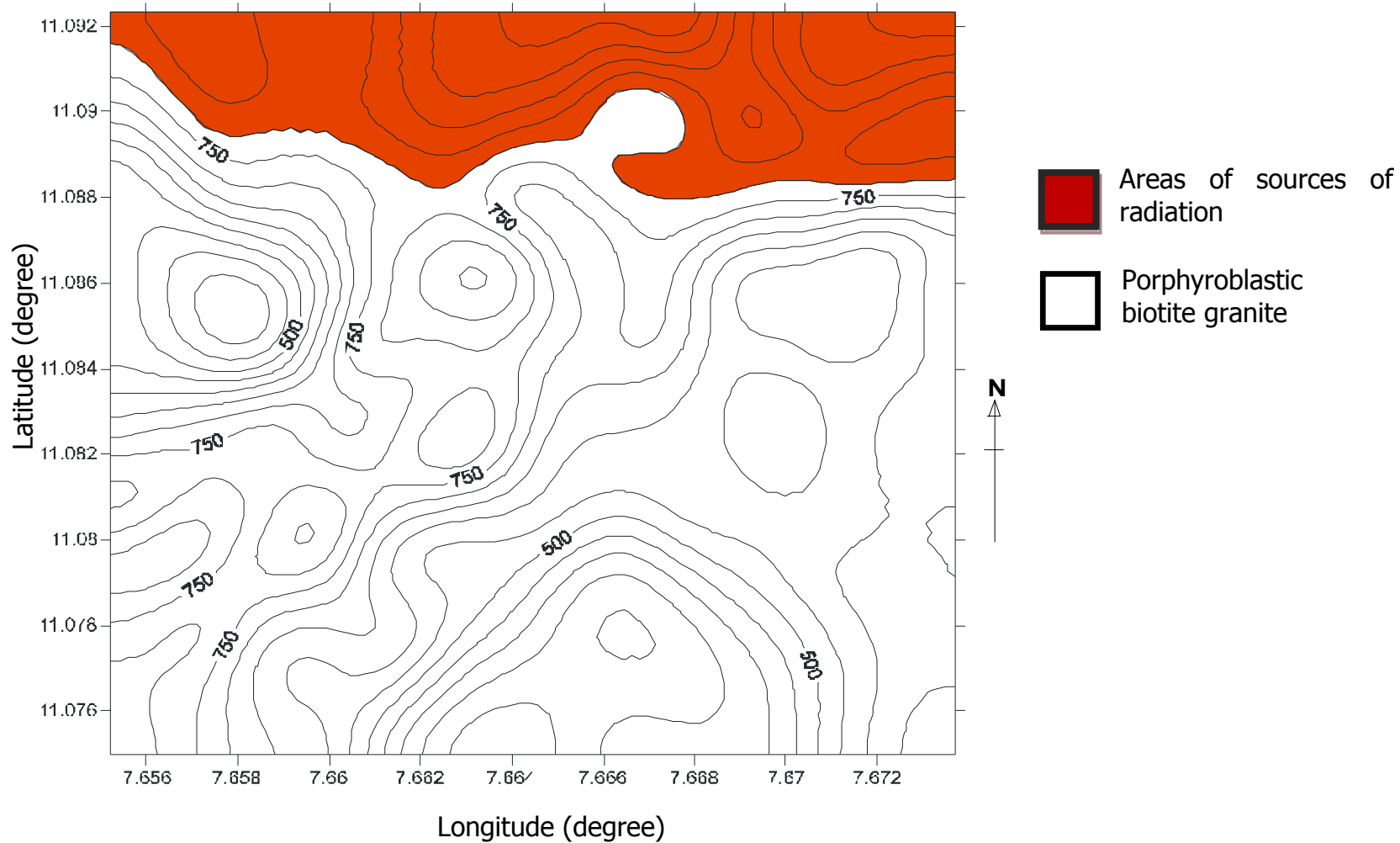


Figure 5.2: Contour map of total count (corrected data) showing areas of sources of radiation. Contour interval is 50 cps.

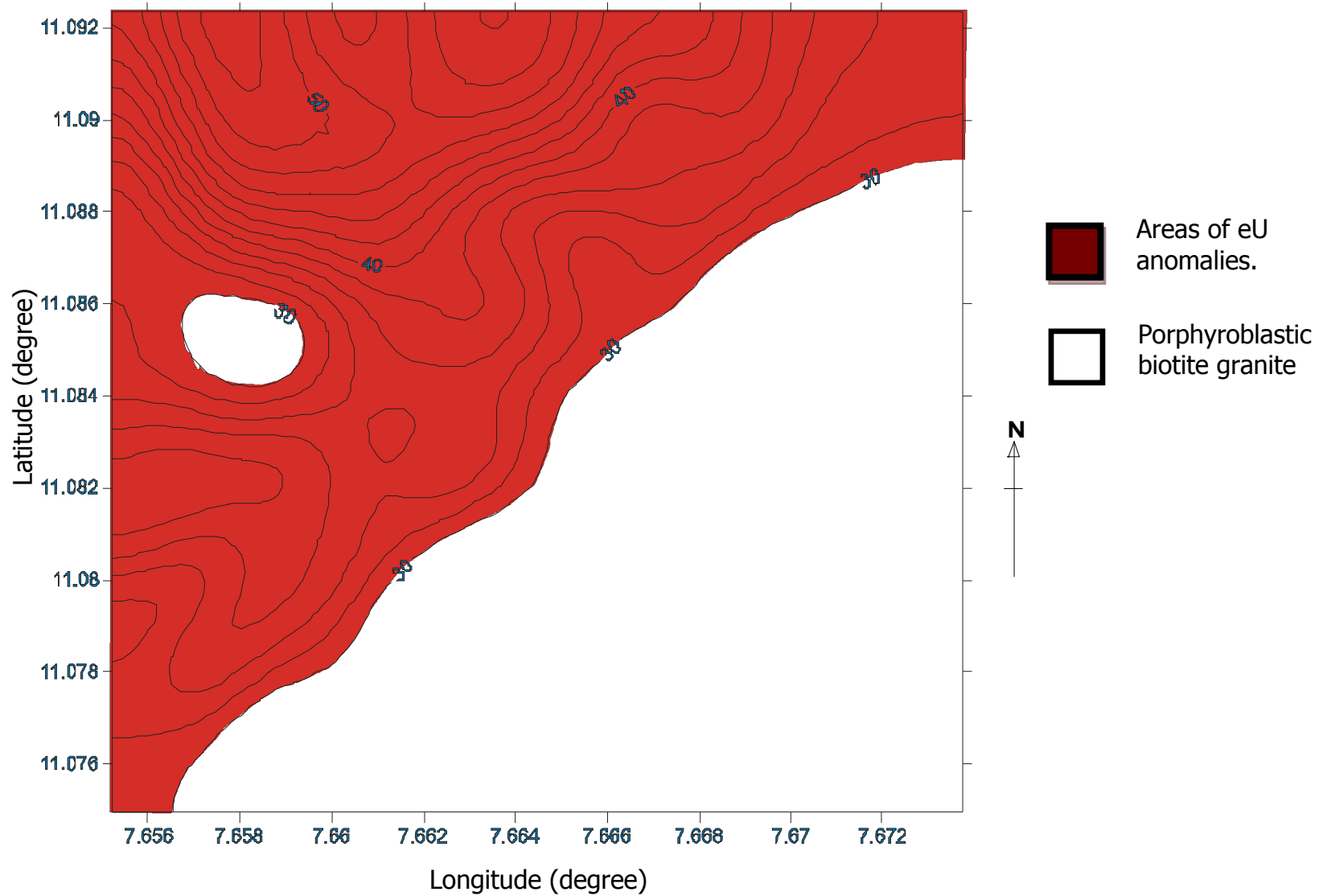


Figure 5.3: Contour map of eU showing areas of anomalies. Contour interval is 2ppm.

5.2.3 Thorium (eTh)

The contour map of eTh concentration derived from background corrected count rates is shown in Figure 4.3. The map revealed some defined anomalies in the area. Using Table 5.2 and equations 5.1–5.6, the threshold value of eTh for the corrected data was found to be 19.3 ppm. Those areas where eTh concentration exceeded 19.3 ppm were considered anomalous. In this case, the areas bounded by 20 ppm contour line in Figure 5.4 were considered anomalous.

5.2.4 Potassium (K %)

The contour map of K % concentrations derived from the background corrected count rates is shown in Figure 4.4. The map revealed some defined anomalies in the area. Using Table 5.3 and equations 5.1–5.6, the threshold value for the corrected K % concentration was found to be 1.9 %. Those areas where K % concentrations exceeded 1.9 % were considered anomalous. Therefore, all areas in Figure 5.5 bounded by 2.0 % contour line were considered anomalous. The map showing areas of eU, eTh, and K % anomalies is shown in Figure 5.6.

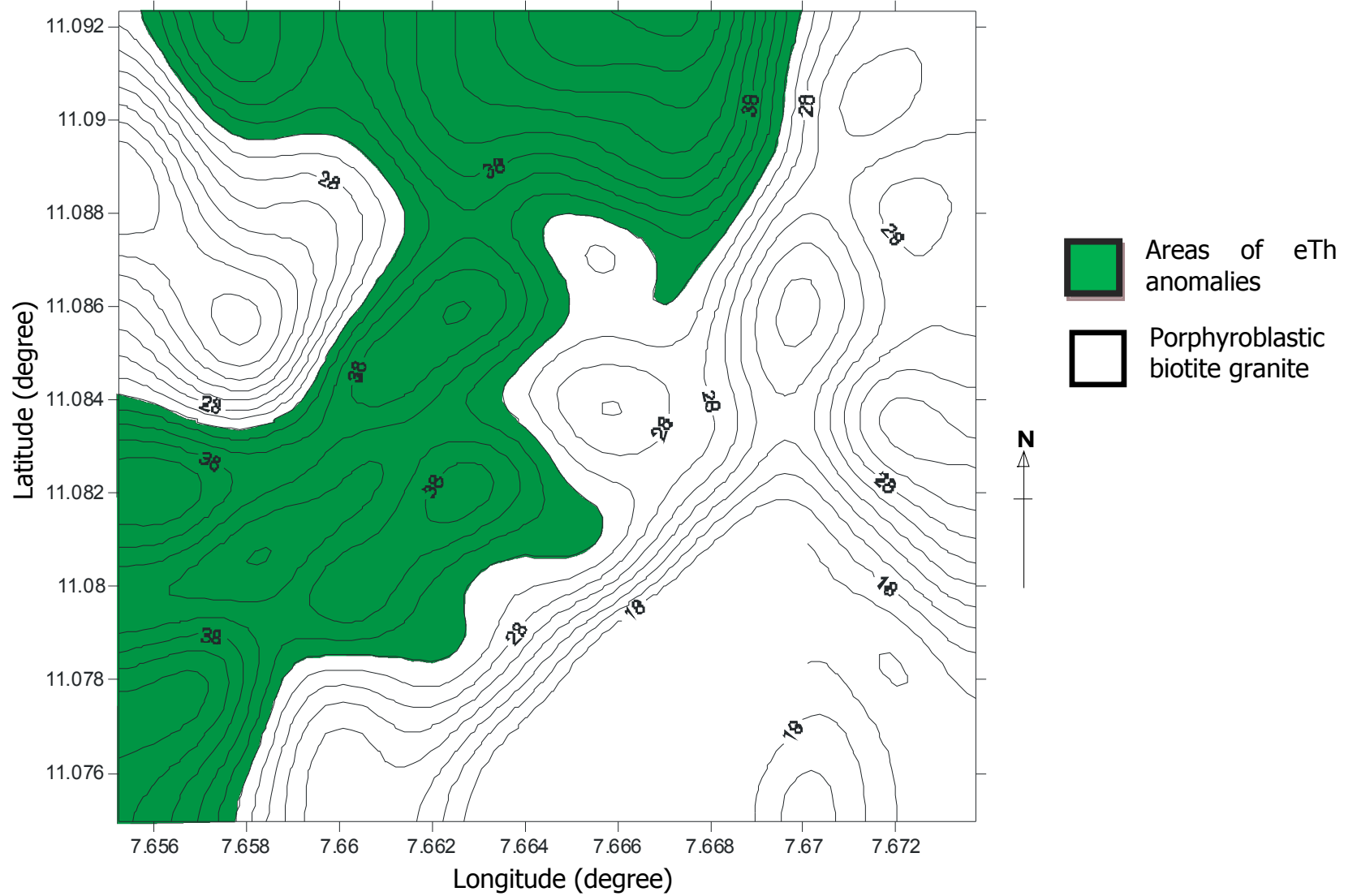


Figure 5.4: Contour map of eTh showing areas of anomalies. Contour interval is 2ppm.

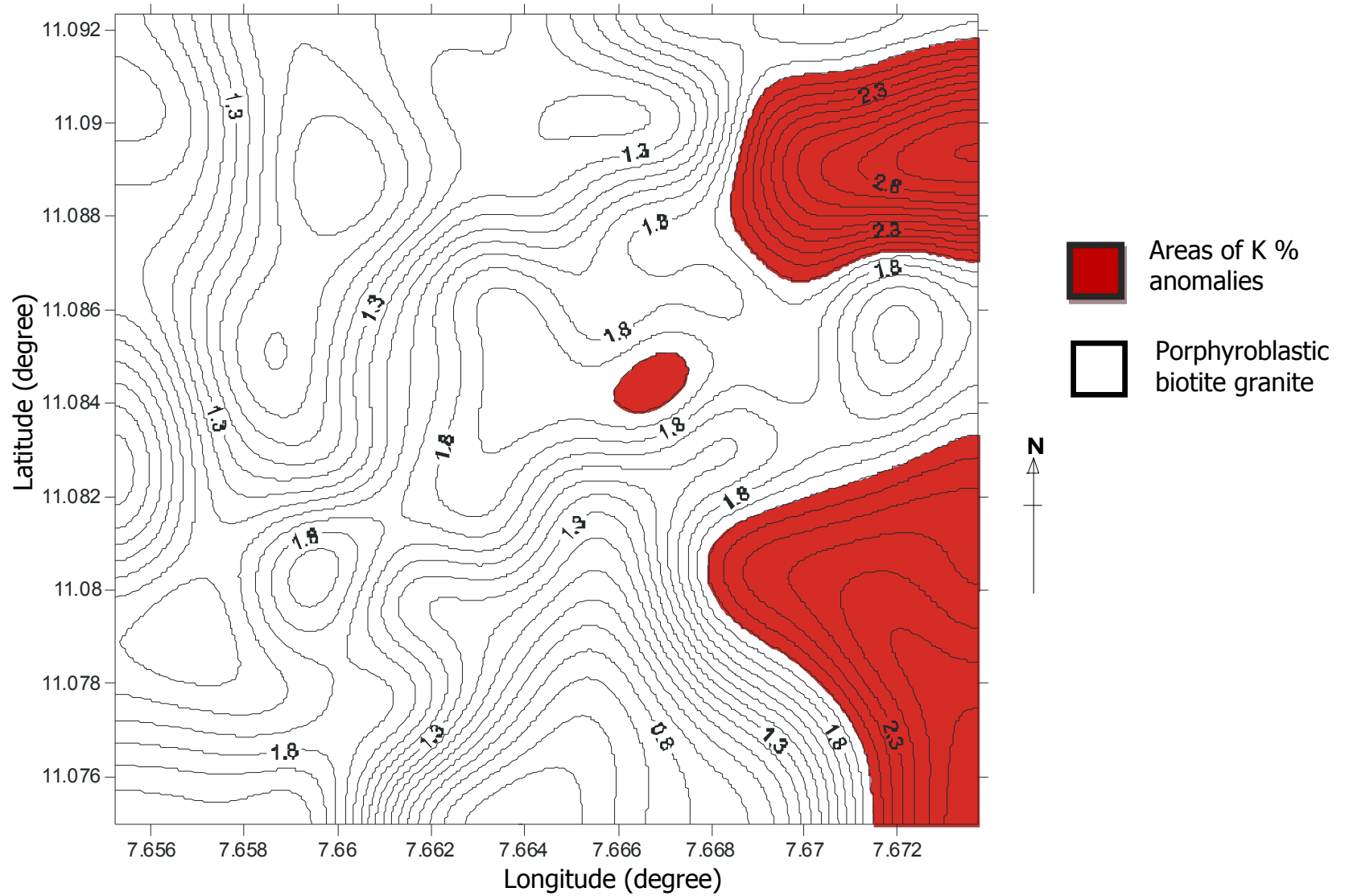


Figure 5.5: Contour map of K% showing areas of anomalies. Contour interval is 0.1 %.

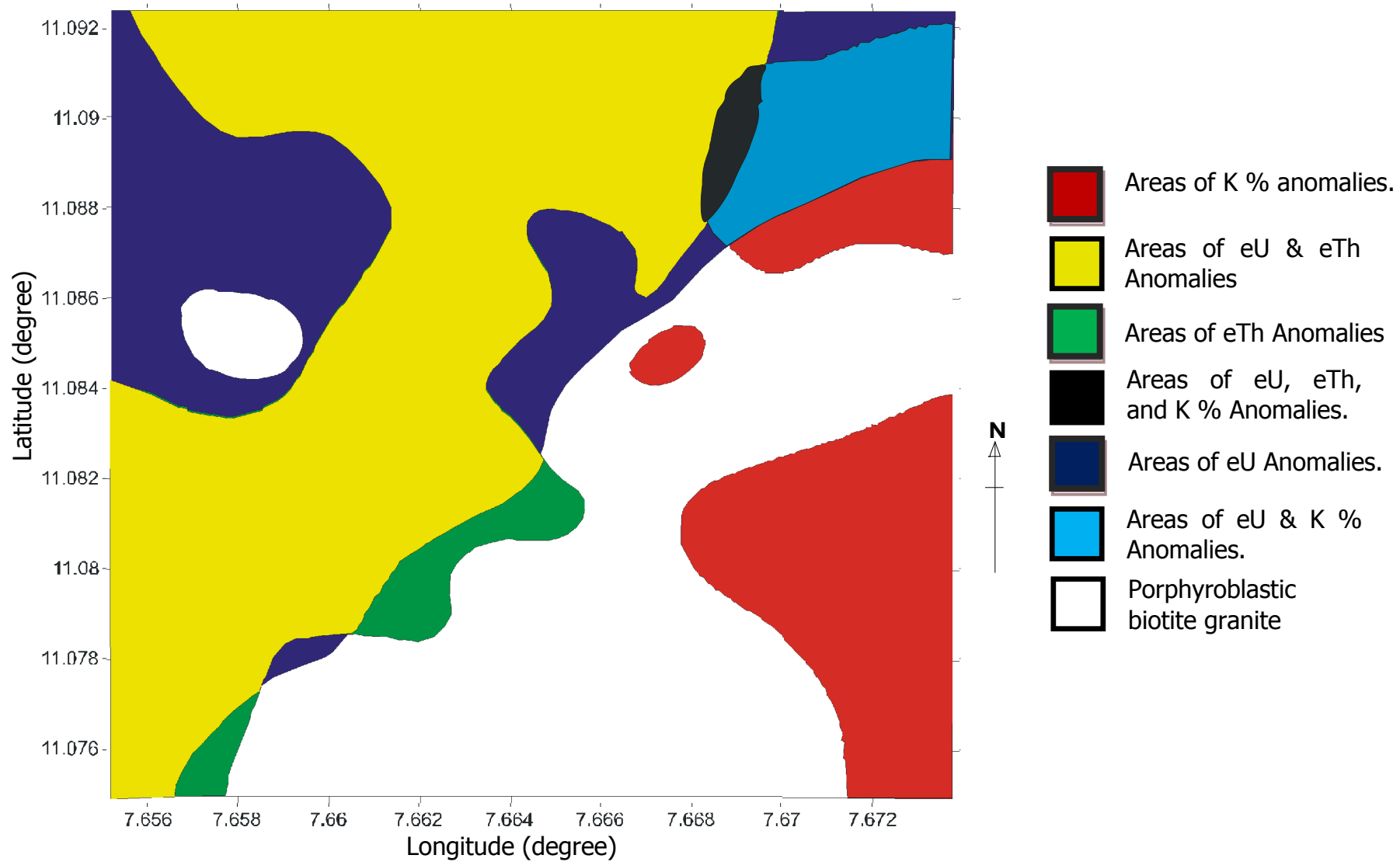


Figure 5.6: Map showing areas of eU, eTh, and K % Anomalies.

5.3 Isolation Of Residual Anomalies

In this study the Regional-Residual Separation was done by fitting a two-dimensional polynomial (trend) surface to the total count, eU, eTh and K% field data by the method of the Least Squares: in the manner outlined by Davis (1973).

In the least square method, we are interested in the general tendency of the data, this tendency is used to interpolate between data points extrapolate beyond the data sequence, infer the presence of trends, or estimate characteristics that may be of interest to the geologist and the geophysicist (Davis, 1973).

The least square criterion of Regional-Residual Separation is such that the Residual is the squared of the deviation of the Regional from the Observed (measured). The Regional, usually a second order polynomial exposes the Residual features as deviation from the Observed field. The separation of a data into two component is done by fitting a trend (plane) surface, which may be defined as linear function of the geographic coordinates of a set of observations (in this case our data) so constructed that the squared deviations from the trend are minimized.

The definition above may explain in three parts:

It is based on the geographic coordinates: this mean that an observation (our data) is considered to be in part a function of the location of the observation.

The surface is a linear function: it has the form

$Y = b_0 + b_1 X_1 + b_2 X_2 \dots$, where the b's are coefficients and the x's are some combination of the geographic coordinates.

The specific linear function chosen for the trend must minimize the square deviation from the trend.

Hence a linear function is an equation of this type

$$Y = b_0 + b_1 X_1 + b_2 X_2 \tag{5.7}$$

Where the b's are coefficients and the X's are some combination of the geographic coordinates. Equation (5.7), thus yield values (\hat{Y}), which are the Regional Components of the data (observation). equation (5.7) is a geologic observation, which may be regarded as a linear function of some constant value b_0 related to the mean observation of the observations, plus an east west (b_1) component (in this case, the latitudes) and north-south (b_2) component (that is, the longitudes).

Hence, we obtained three normal equations

$$\begin{aligned} \sum Y &= nb_0 + b_1 \sum X_1 + b_2 \sum X_2 \\ \sum X_1 Y &= b_0 \sum X_1 + b_1 \sum X_1^2 + b_2 \sum X_1 X_2 \\ \sum X_2 Y &= b_0 \sum X_2 + b_1 \sum X_1 X_2 + b_2 \sum X_2^2 \end{aligned} \tag{5.8}$$

In matrix form equation (5.8) becomes

$$\begin{bmatrix} n & \sum X_1 & \sum X_2 \\ \sum X_1 & \sum X_1^2 & \sum X_1 X_2 \\ \sum X_2 & \sum X_1 X_2 & \sum X_2^2 \end{bmatrix} \times \begin{bmatrix} b_0 \\ b_1 \\ b_2 \end{bmatrix} = \begin{bmatrix} \sum Y \\ \sum X_1 Y \\ \sum X_2 Y \end{bmatrix} \tag{5.9}$$

5.3.1 Application and Result

The solution to equation (5.9) is obtained by solving the series of simultaneous equation that evolved from the substitution of the sums, sums of powers, and sums of cross-products required in equation (5.8) are shown in Table 5.7.

Where;

$$n = 536$$

$$\Sigma X_1 = 4108.117$$

$$\Sigma X_2 = 5940.93$$

The coefficients b_0 , b_1 and b_2 are found by solving the resulting set of simultaneous normal equations, hence Table 5.7 The coefficient of the plane surface determined are then substituted into equation (5.7) and evaluated to obtain the regional surface (\hat{Y}). The regional data computed was then used to produce the contour maps of the regional field of total count, eU, eTh and K % of the study area (Figure 5.7).

The differences between the measured or observed data (field) Y and the regional data (field) \hat{Y} gives the residual data (field), $\Delta T(x,y)$. These residuals are contoured (Figure. 5.8). The residual obtained normally consist of positive and negative values.

Table 5.7: Sum of powers, sum of cross product and coefficients of plane surface calculated for the survey area.

	Total count	eU	eTh	K%
b₀	702.91	31.8574	33.3420	1.619
b₁	0.16011	0.16021	0.16013	0.16012
b₂	-0.1021	-0.1011	-0.1012	-0.1013
ΣY	376753.24	17076.22	17871.34	867.83
ΣX₁²	31486.25	31486.25	31486.25	31486.25
ΣX₂²	65848.29	65848.29	65848.29	65848.29
ΣX₁X₂	45533.67	45533.67	45533.67	45533.67
ΣX₁Y	2887586.60	130874.10	198087.4	6651.21
ΣX₂Y	4175868.64	189274.60	2195618.0	9619.10

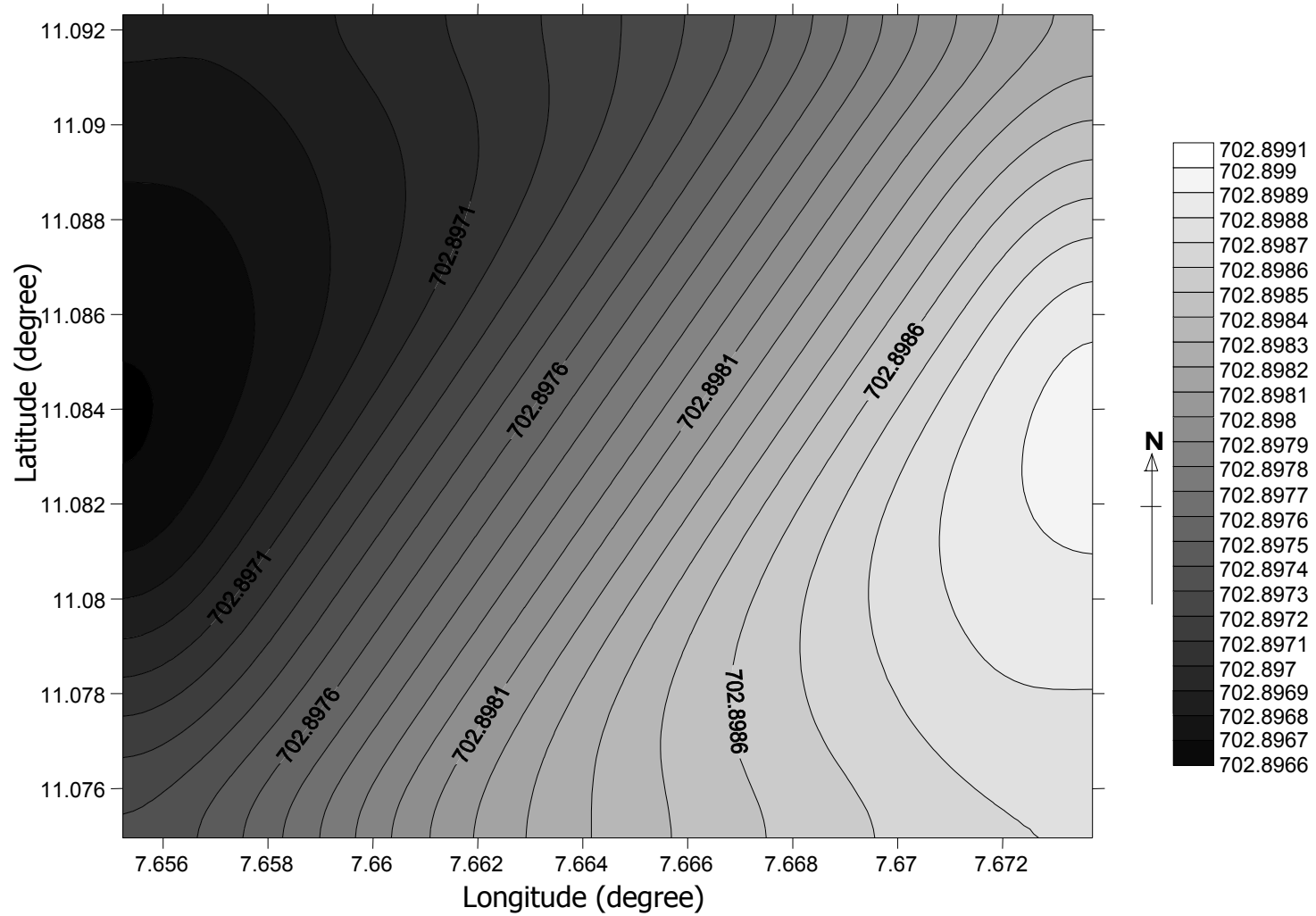


Figure 5.7a: Regional field map of total count (cps) anomalies of the study area.

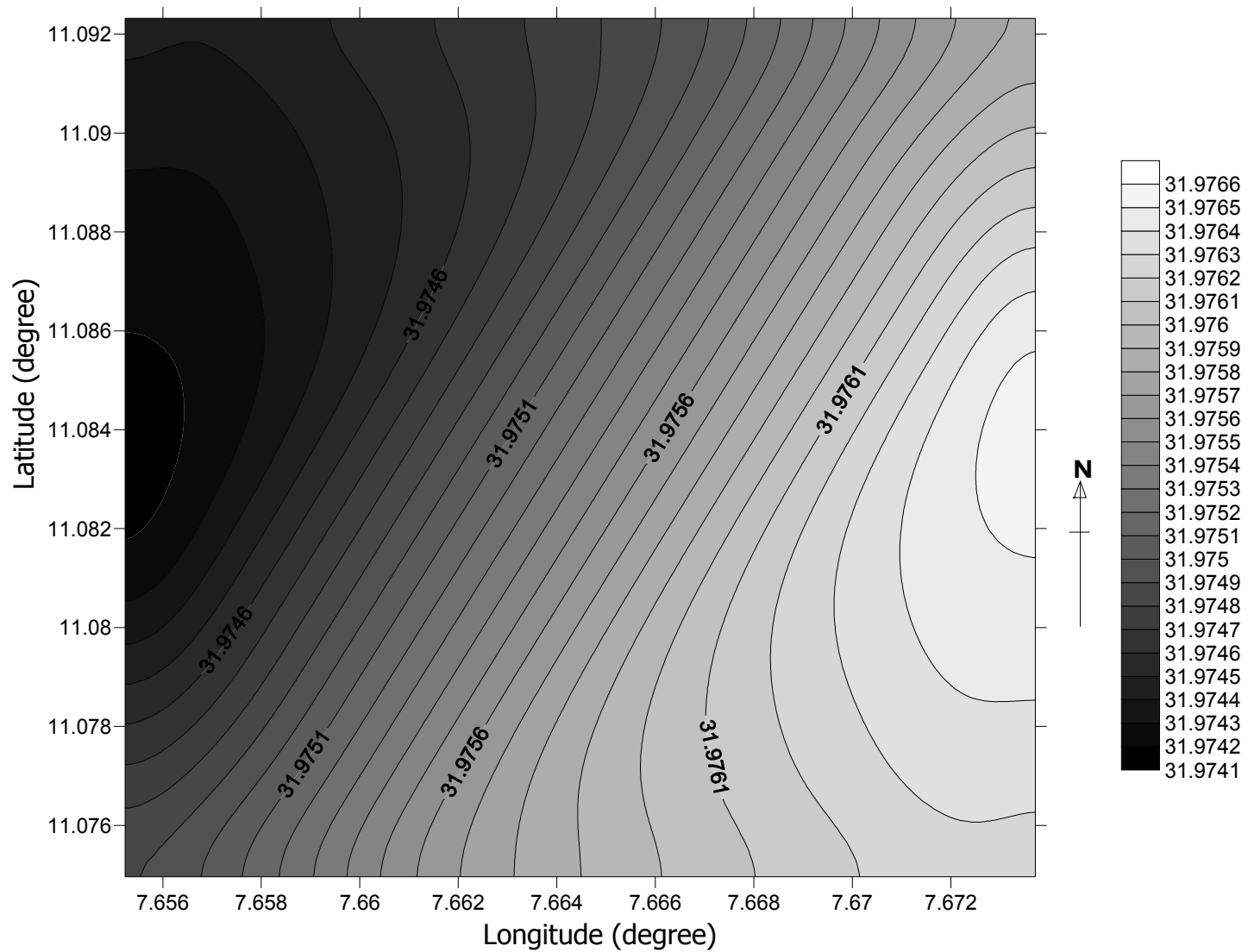


Figure 5.7b: Regional field map of eU (corrected data) anomalies of the study area.

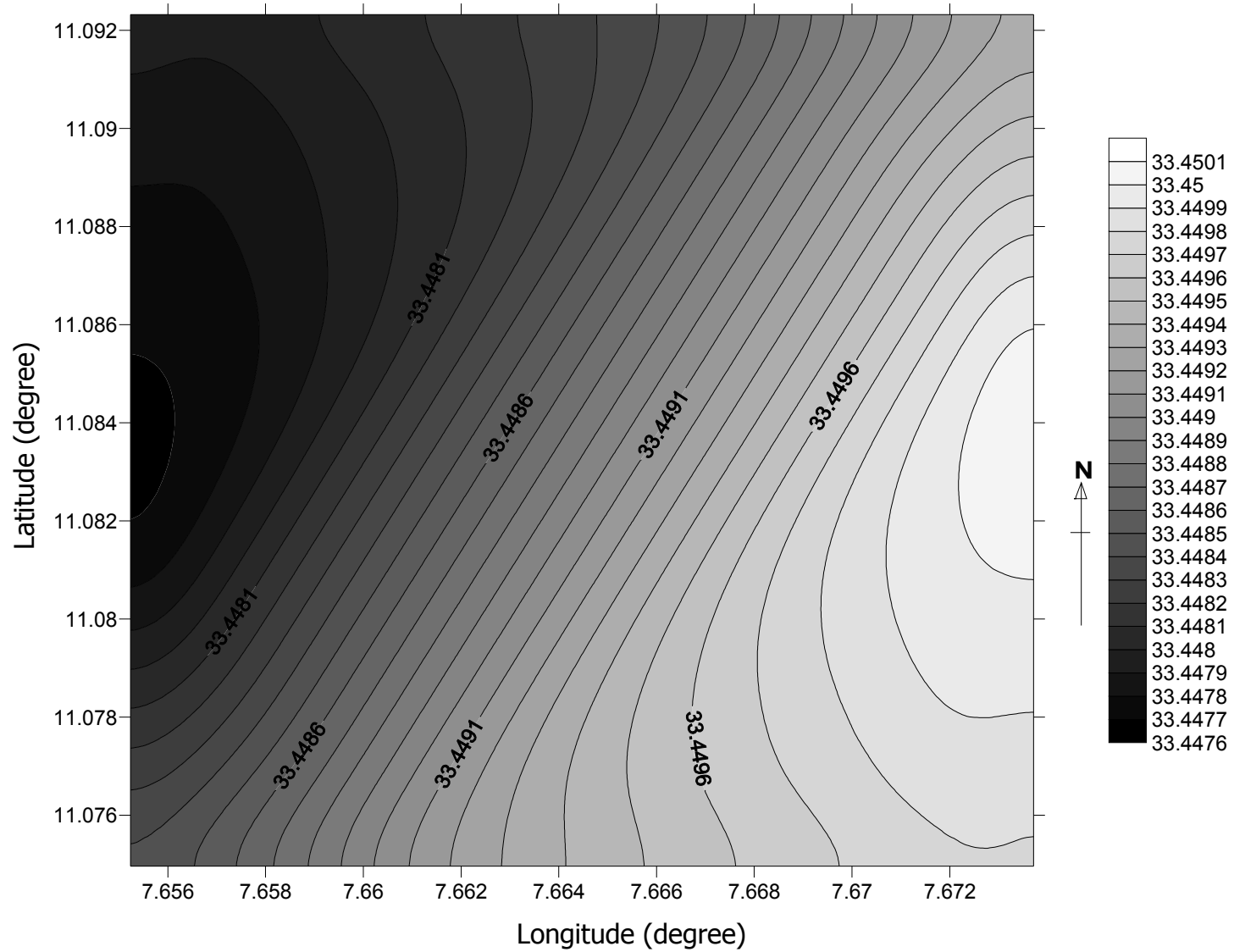


Figure 5.7c: Regional field map of eTh (corrected data) anomalies of the study area.

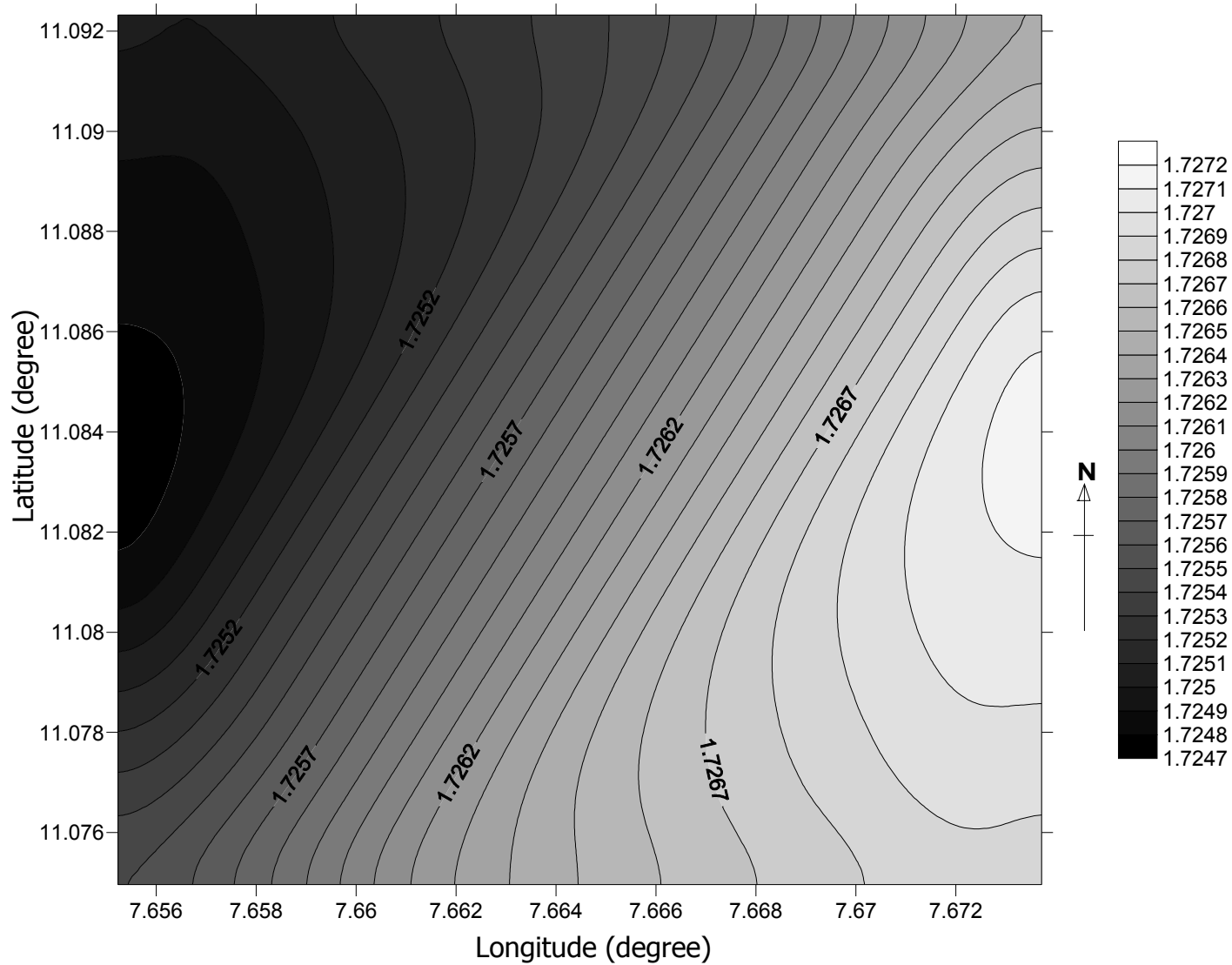


Figure 5.7d: Regional field map of K (corrected data) anomalies of the study area.

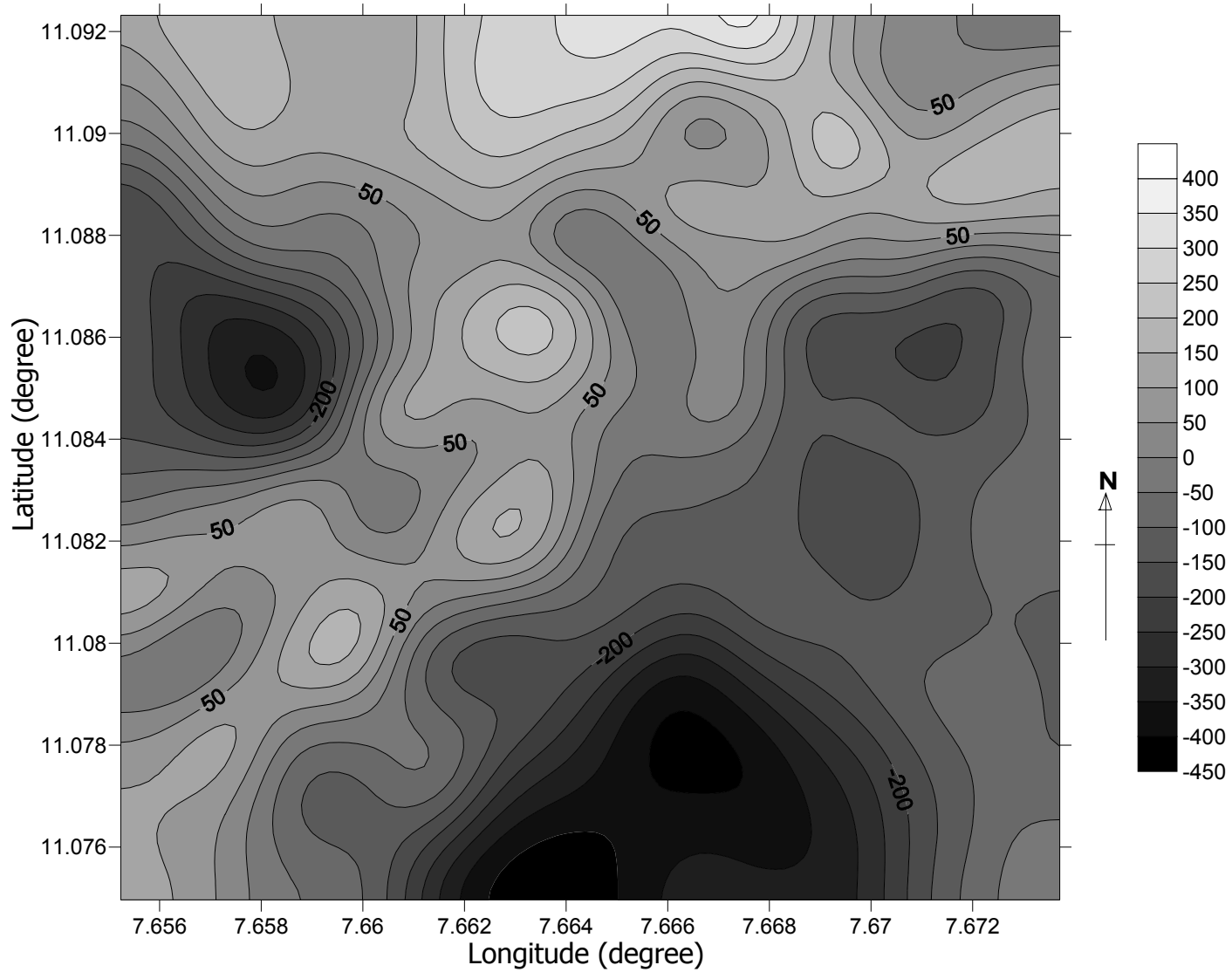


Figure 5.8a: Residual field map of total count (corrected data) anomalies.

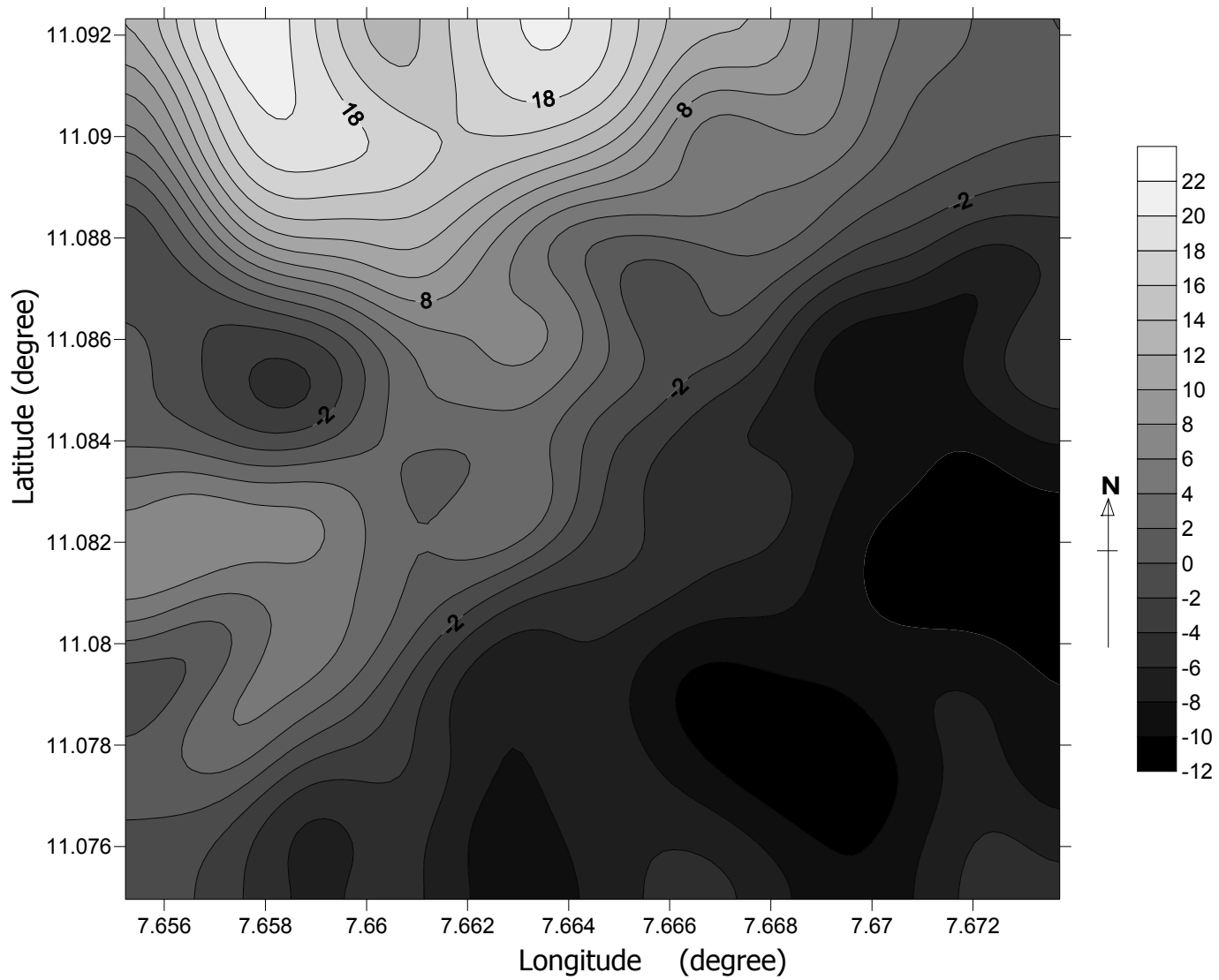


Figure 5.8b: Residual field map of eU (corrected data) anomalies of the study area.

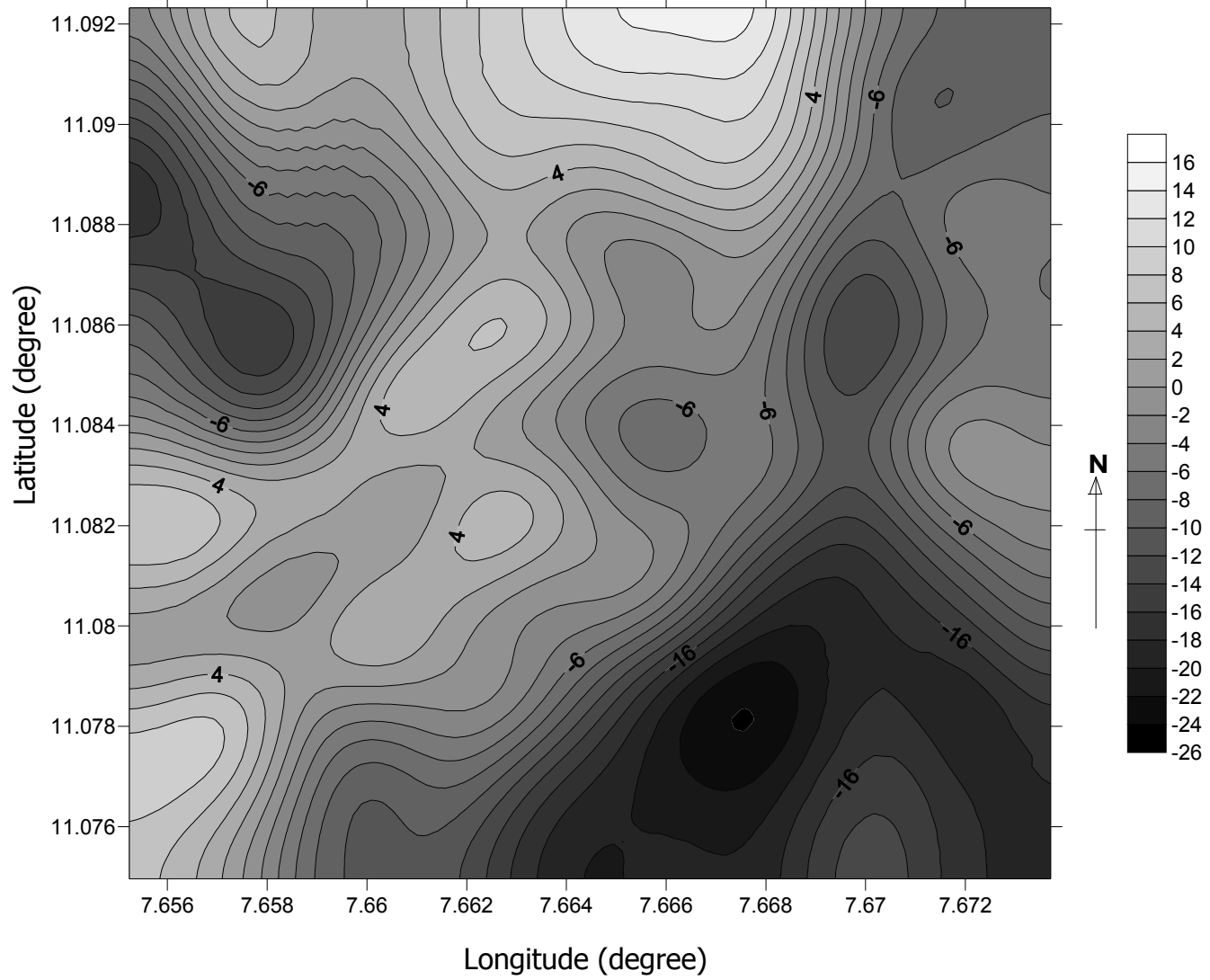


Figure 5.8c: Residual field map of eTh (corrected data) of the study area.

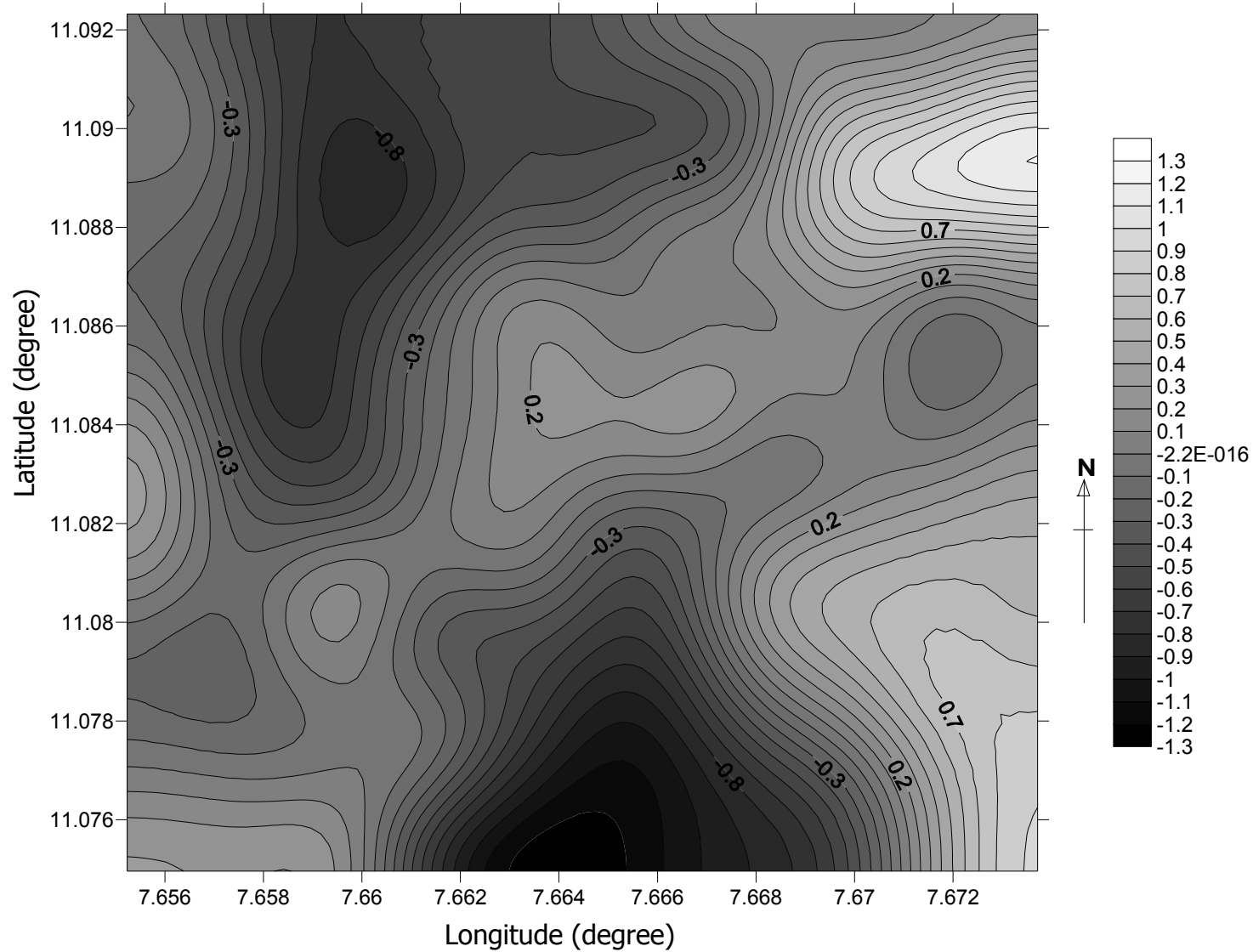


Figure 5.8d: Residual field map of K% (corrected data) of the study area.

CHAPTER VI

DISCUSSION, CONCLUSION AND RECOMMENDATION.

6.1 Discussion of Results

Results of the gamma activity measurements obtained in the course of the scintillometer field survey suggest an existence of anomalous gamma radiation in the region. Activities of 16 cps and above that are twice the average mode for the entire area were recorded at 157 of stations. This means that the anomaly characterized at the area is promising in terms of radioactive mineralization (Levinson, 1974). A comparison of the two total count maps reveals that 59 % of areas of sources of radiation (spectrometer gross count) coincided with areas of anomalous radiation (scintillometer gross count).

The results from the four- channel gamma ray spectrometry field survey identified uranium and thorium as the main sources of radiation. Potassium is a minor contributor to the gamma activity observed in the area. The U concentrations derived from the background corrected data ranges from 23.4 – 64.1 ppm, Th concentrations from 8.3 - 89.1 ppm, and K concentrations 0.03 – 6.5 %. eU, eTh and K concentrations derived from the uncorrected data were however higher than those derived from the corrected data. Both results could be reliable as there is no much difference between them due to low background values used to correct for cosmic ray contribution to the ground activities.

The results of the analysis of the rocks in the area so far indicate they contain as much as 64.1 ppm U, 89.1 ppm Th, and 6.5 % K. 64.1 ppm U is about 15 times as much as the average concentrations of uranium in normal granitic rocks and suggest a possible low grade uranium mineralization (Rahaman et al., 1984).

The total count map Figure 4.1 revealed an anomaly. The sources of radioactivity in the area surveyed were identified from the contour map of the total count. Some of these sources correspond with areas of eU, eTh, and K anomalies for both corrected and uncorrected data. eU map compares well with the total count map than eTh and K % map. This may suggest a predominant contribution of U and daughter nuclides in the gamma activity in the area. A comparison of the characterized anomalies showed that the anomalies obtained from the uncorrected data were larger than the corrected data though having the same centre.

The regional field maps of total count, eU, eTh, and K % (Figure 5.7) revealed the tendency (trends) of the data running approximately in the NW – NE of the study area. The residual field maps (Figure 5.8) delineate the regions of large deviation of the observed field data from the regional field data in the area. This could indicate alteration/mineralization or other geological processes such as magma differentiation or weathering in these regions (IAEA, 2003).

The residual field map of eU, and eTh compares well with the residual field map of total count than the residual field map of K %. This could be due to inability to

delineate units of similar radiometric character that is, similar concentration of K, U, and Th in the survey area (IAEA, 2003).

6.2 Conclusion

Analyses and interpretation of K, U, and Th elemental data in their local geological context is best done in conjunction with other data, such as bulk and clay mineralogy, porosity, and other major and minor elemental data obtained from the same samples. Such analysis is beyond the scope of this study, which is focused on the potential use of the gamma ray spectrometry device to obtain meaningful data from natural gamma ray spectra. We therefore limit ourselves to a few general comments.

The result of the present study demonstrates the accuracy of ground radiometric data as well as the suitability of the gamma ray spectrometry technique for exploration of radioactive materials. Also, this study revealed that using gamma ray spectrometry in an area where calibration facilities are lacking and where cosmic background cannot be measured accurately, systematic ground gamma ray spectrometry technique can be used to determine the concentrations of K, Th, and U for the survey area.

The results so far indicates predominant contribution of U and daughter nuclides in the gamma activity in the area. This conclusion is derived from the observation that eU anomaly map compares well with the total count anomaly map than eTh

and K % anomaly maps. The areas of anomalous eU and eTh characterized correlated with the areas of exposed outcrops which are identified as the main sources of high activities in the study area. Thus, there is good agreement between uranium and vegetation in the study area that is, area of low uranium concentration coincided with areas of thick vegetation.

We believed the significance of the results to be the indication of the possibility of the existence of radiometric mineralization in the area.

6.3 Recommendation

Because of poor sensitivity of instruments due to small crystal volume, excessive channel fluctuations and the inability to measure accurately the cosmic background, it is recommended that a detailed spectrometry and geochemical survey of this study area should be carried out. Such a survey will help assess the extent of uranium mineralization in porphyroblastic biotite granites.

REFERENCES

- Ahmed, A.L. (1994). Ground follow up of surveys of some radiometric anomalies Jingir, Plateau State, using gamma ray spectrometry. *Unpublished M.Sc Thesis, Department of Physics, Ahmadu Bello University, Zaria*, pp 1-9.
- Ahmed, A.L (2006). Detailed radiometric surveys of the Albite Riebeckite granites of Dutsen Wai Ring Complex, Northern Nigeria. *Unpublished Ph.D Thesis, Department of Physics, Ahmadu Bello University, Zaria*, pp 1-116.
- Barretta, P.M. (1981). Recent development in uranium exploration. *International atomic energy agency (IAEA) Bulletin*, vol. **23**, No.2, pp 15-20.
- Christillin, P. (1986). Nuclear Compton scattering. *J Phys. G: Nuclear Phys.*, Vol. **12**, pp 837-851.
- Darnley, A.G. (1972). Airborne gamma-ray survey techniques. In: Bowie et al. (Editors), *Uranium Prospecting Handbook*. Institute of Mining and Metallurgy, London, pp 174-211.
- Darnley, A.G. (1973). Airborne gamma-ray survey techniques – present and future. *Uranium Exploration methods*. IAEA, Vienna, pp 67-108.
- Davis, J.C. (1973). Statistics and Data Analysis in Geology. *John Wiley & Sons Inc., N.Y.*, p 550.
- Dahlkamp, F.J (1980). The time related occurrence of Uranium deposits. *Mineral Deposits* **15**, pp 69-79.
- Dewu, B.B.M (1986). A geophysical ground follow-up of an aeroradiometric anomaly at Bisichi area of Plateau State Nigeria. *Unpublished undergraduate Thesis, Department of Physics, Ahmadu Bello University, Zaria*, pp 1-85
- Dewu, B.B.M (1989). Distribution of Uranium in granites and mobility of Uranium during low temperature alteration processes. *Unpublished Ph.D Thesis of Department of Geophysics, University of Exeter, U.K*, pp 63-83
- Dickson, B.L., Christiansen, E.M. Luborg, L. (1982). Reference materials for calibration of laboratory gamma-ray analyses. *Uranium exploration Methods* IAEA, Vienna, pp 687-698.

- Doig, R. (1968). The natural gamma-ray flux: in-situ analysis. *Economic geology*, Vol. **33**, pp. 311-328.
- Galbraith, J.H. and Saunders, D.F. (1983). Rock classification by characteristics of aerial gamma-ray measurements. *Journal of geochemical exploration*, Vol.**18**, No. 1., pp.49-73.
- Garba, I. (1988). Introduction to Geology and Mineral Deposits of Nigeria. *Ganuwa Publishers Limited, Zaria, Nigeria*, pp 7&15.
- Grant, N.K. (1970). Geochronology of Precambrian basement rocks from Ibadan, South Western Nigeria. In: *Earth Planet Science Letter*, 10, pp 19-38.
- Grasty, R.L. (1975). Uranium measurement by airborne gamma-ray spectrometry. *Geophysics*, **40**:503–519.
- Hoffman, D.C., Lawrence, F.O., Mewhetter, J.L., and Rourke, F.M. (1971). Detection of plutonium-244 in nature. In: *nature No. 34*, pp 132-138
- IAEA (2000). *Technical Reports: No 186*, p 86
- IAEA- TECDOC, (2003). Guidelines for radioelement mapping using gamma ray spectrometry. *Technical Report Series, 1363*, pp 1-148.
- Jones, H.A and Hockey, R.D. (1964). The geology of part of South - Western Nigeria . *Bull Geological survey of Nigeria* No. 31, pp 1-101.
- Lawal, G. M. (2000). Lead (Pb) Concentration in the water of Kubanni River Dam, Zaria. *Unpublished M.Sc Thesis, Department of Geology, Ahmadu Bello University, Zaria*, pp 8-9.
- Lederer, C.M., Hollander, J.M., and Parلمان, I. (1968). Tables of isotopes. *6th edition*, p 46.
- Levinson, A.A (1974). Introduction to Exploration Geochemistry. *Applied publishing Ltd. Maywood Illinois*, p 614.
- Lovborg, L., Wollenberg, H., Sorensen, P. and Rose - Hansen, J. (1971). Field determination of uranium and thorium by gamma-ray spectrometry, exemplified by measurements in the ilimaussa alkaline intrusive, south Greenland. *Economic geology*, Vol. 66, pp 68-378.

- Mackay, R.A. and Beer, K.E. (1952). The Albite – Riekerbites Granites of Nigeria. *Geological Survey of Great Britain S.W.*, PP 1-25.
- McCurry, P. (1975). The Geology of Degree Sheet 21 (Zaria). *Unpublished M.Sc Thesis, Department of Geology, Ahmadu Bello University, Zaria*, p 103.
- McDermott, A. (1977). Field Experiments with Exploranium Model GR-101. *Geometrics Exploranium Model GR-101 Users Manual*, p 10.
- Oshin, I.O. and Rahaman, M.A. (1984). Uranium favourability study in Nigeria. *Journal of African Earth Sciences*, Vol. 5, No. 2, pp 167-175.
- Rahaman, M.A. (1976). Review of the Basement Geology of South Western Nigeria. *In: Geology of Nigeria Edited by Kogbe, Elizabethan, Lagos*, pp. 41-58.
- Rahaman, M.A., Emofurieta, W.O. and Caen – Vanchette, M. (1983). The potassic Granites of the Igbedi Area. In: Further evidence of the Polycyclic evolution of the Pan – African belt in South Western Nigeria. *Precambrian Res.*, 22, pp 75-92.
- Rahaman, M.A., Van Breemen, O., Bowden, P. and Bennett, J.N. (1984). Age migrations of anorogenic ring complexes in Northern Nigeria. *Journal of Geology*, 92: 173-184.
- Rich, R.A., Holland, H.D. and Peterson, U. (1972). Hydrothermal Uranium deposits. *Elsevier*, pp 26-30.
- Roberts, K.U. and Major, P.O. (1978). Future for uranium prospecting on the ground. *Uranium exploration methods*. IAEA, Vienna, pp 114-125.
- Rogers, J.W., Ragland, P.C. and Nishimori, R.K. (1980). Varieties of granitic uranium deposits and favourable exploration areas in eastern United States. *Economic Geology*, **73**:1539-1955
- Spiegel, M.R (1961). Theory and problems of statistics. *Schaums outline series*; McGraw Hill, pp 45-73.
- Soonawalla, N.M. (1974). Data processing techniques for the radon method of Uranium exploration. *Canadian Institute of Mining Bulletin*, 67, pp 110-116.

- Tom, J.T. (2002). Use of radiometric data for the mapping of Uranium in groundwater. In: *Publication of centre for water research and policy, University of South Africa*, pp 1-20.
- Uwah, J.E. (1984). Investigation of radiometric anomalies by nuclear and other methods. (A case study of the Sokoto basin of Nigeria). *Unpublished Ph.D Thesis, Department of Physics, Ahmadu Bello University, Zaria*, pp 1-135.
- Van Breeman, O., Pidgeon, R.T. and Bowden, P. (1977). Age and isotopic studies of some Pan-African granites from north central Nigeria. *Precambrian Res.*, Vol 4, pp 307-319.
- Wooley, A (1978) (Editor). The Illustrated Encyclopedia of the Mineral kingdom. *Hamlyn pub. Co.*, p. 240.

APPENDICES

Appendix 1. Total counts (TC), equivalent surface concentration of uranium (eU), thorium (eTh) and potassium (K%)
(corrected data)

Longitude	Latitude	eU(ppm)	Th(ppm)	K%
7.660302	11.07496	33.3585	28.196	0.62
7.660782	11.07536	28.52625	28.329	0.95
7.661155	11.07571	24.04756	27.93	0.54
7.661555	11.07597	23.44172	15.96	0.82
7.662435	11.07669	16.41252	22.61	0.53
7.662755	11.07704	28.62752	15.295	1.17
7.663155	11.07736	21.35442	21.945	1.69
7.663555	11.07771	19.73444	15.96	0.68
7.663982	11.07797	33.58269	20.482	1.17
7.664328	11.07829	28.35152	23.142	0.40
7.664728	11.07877	24.04152	28.196	0.34
7.665128	11.07907	24.54512	14.63	0.51
7.665555	11.07936	19.18459	10.108	1.01
7.665982	11.07979	19.74049	15.694	0.77
7.666435	11.08008	19.57493	27.265	0.50
7.666728	11.08045	19.39639	17.955	0.75
7.667155	11.08075	28.90361	24.605	2.73
7.667582	11.08104	24.7497	16.359	2.97
7.668008	11.08144	31.09374	14.098	2.33
7.668355	11.08168	23.66103	14.896	1.83
7.668728	11.082	24.11254	16.492	1.60
7.669048	11.08227	23.68981	22.211	2.18
7.669422	11.08256	24.04142	11.039	1.91
7.669768	11.08288	18.61777	11.438	1.11
7.670115	11.0832	21.74651	15.428	1.56
7.670488	11.08355	28.23357	28.329	1.97
7.670862	11.08381	22.33656	40.964	1.06
7.671208	11.08408	18.90957	56.525	1.75
7.671555	11.0844	19.65736	27.93	0.99
7.671955	11.08472	23.61772	44.688	1.39
7.672382	11.08504	23.32825	12.369	0.87
7.672675	11.08531	28.89415	22.876	1.54
7.673048	11.08557	28.55991	28.994	1.43
7.673715	11.08616	33.9862	26.334	3.02
7.673422	11.08656	26.88968	31.654	1.45

Longitude	Latitude	eU(ppm)	Th(ppm)	K%
7.672702	11.08595	29.13776	37.905	2.25
7.672408	11.0856	27.81728	35.91	0.56
7.672008	11.08536	33.35615	15.428	0.73
7.671688	11.08509	28.44684	27.531	1.27
7.671262	11.08469	21.8271	22.61	1.57
7.670968	11.08445	22.52856	23.94	0.84
7.670595	11.08416	28.73005	25.802	1.57
7.670248	11.08389	34.25917	18.62	1.18
7.669848	11.08355	27.41826	21.28	0.58
7.669502	11.08323	32.13373	32.718	0.29
7.669155	11.08296	17.83807	15.694	0.89
7.668675	11.08269	20.22829	15.694	0.87
7.668462	11.08245	29.72604	20.615	0.72
7.668088	11.08205	27.98431	15.694	1.56
7.667688	11.08176	23.84757	34.58	0.38
7.667288	11.08139	18.40421	27.265	1.82
7.666835	11.08109	30.08146	13.566	1.67
7.666462	11.0808	27.02119	17.29	0.59
7.666088	11.08045	27.98782	34.846	0.96
7.665662	11.08008	20.56604	28.728	0.22
7.665262	11.07973	24.91917	26.068	1.08
7.664408	11.07907	22.32436	24.339	2.01
7.663955	11.07872	18.6885	14.763	1.24
7.663635	11.0784	24.38561	25.935	0.65
7.663235	11.07803	17.48909	24.605	1.56
7.662782	11.07773	17.56129	19.285	0.80
7.662408	11.07741	26.82461	25.935	0.66
7.662035	11.07709	17.22402	25.536	2.26
7.661608	11.07672	26.17623	48.013	2.61
7.661208	11.0764	28.0646	37.905	0.20
7.660782	11.07605	33.52796	37.905	1.22
7.660408	11.07573	28.55045	27.265	2.31
7.659955	11.07539	21.8709	12.103	2.97
7.659795	11.07576	26.34813	21.147	3.90
7.660142	11.07608	22.44417	12.635	2.02
7.660542	11.07637	28.6763	15.295	1.82
7.660942	11.07672	31.75168	10.906	2.15
7.661795	11.07744	29.03073	36.176	2.85
7.662142	11.07773	30.90886	20.083	1.58
7.662488	11.07808	23.41128	49.476	0.45
7.662942	11.07843	20.65628	71.953	1.49
7.663368	11.07872	34.02054	14.098	2.20

Longitude	Latitude	eU(ppm)	Th(ppm)	K%
7.664168	11.07939	29.32829	29.526	0.69
7.664542	11.07976	36.26461	48.412	1.09
7.664915	11.08008	24.89009	33.782	0.96
7.665395	11.08043	34.74687	67.963	0.49
7.665822	11.0808	32.10368	68.362	1.84
7.666142	11.08112	27.72363	57.19	0.35
7.666568	11.08144	24.3059	40.166	1.23
7.666995	11.08176	28.45796	54.929	0.88
7.667342	11.08211	23.20952	13.3	1.90
7.667742	11.0824	27.90021	55.86	0.70
7.668115	11.08272	37.16773	68.761	1.32
7.668435	11.08296	28.17777	56.525	2.18
7.668835	11.08331	27.67924	31.255	2.22
7.669182	11.08357	18.85679	18.088	1.30
7.669475	11.08387	23.29538	15.96	2.87
7.669875	11.08416	24.48385	13.034	4.40
7.670248	11.08451	23.2784	23.142	2.88
7.670622	11.0848	21.83198	15.96	1.44
7.670942	11.08507	19.072	27.93	0.99
7.671342	11.08539	23.93859	15.561	1.41
7.671688	11.08568	24.55341	9.975	1.94
7.672062	11.08597	26.82139	58.254	0.56
7.672408	11.08632	18.68128	8.645	1.17
7.672808	11.08661	18.60801	24.738	0.57
7.673128	11.08691	23.88718	17.822	1.61
7.672808	11.08723	26.3372	28.063	0.21
7.672168	11.08664	21.64154	41.496	0.81
7.671768	11.08635	16.7851	42.693	0.79
7.668888	11.08389	23.57518	12.236	1.30
7.668542	11.08357	26.58071	25.935	0.44
7.668168	11.08328	32.17304	30.989	1.42
7.667875	11.08299	33.9381	13.433	1.58
7.667502	11.08267	28.71259	13.699	2.60
7.667128	11.08243	24.26454	14.098	1.13
7.666675	11.08211	23.89781	25.935	1.86
7.666275	11.08173	24.34932	27.531	1.89
7.665902	11.08139	22.5028	16.492	0.47
7.665555	11.08109	22.07851	13.699	0.80
7.665048	11.08072	16.74276	44.555	2.18
7.664702	11.08037	17.31446	36.575	0.92
7.664248	11.08	23.76464	14.63	1.06
7.663928	11.07973	22.06983	16.226	1.86

Longitude	Latitude	eU(ppm)	Th(ppm)	K%
7.663075	11.07901	23.66084	47.082	0.90
7.662648	11.07867	28.37357	43.624	2.93
7.662275	11.07832	22.38612	45.22	1.37
7.659475	11.07608	24.80795	18.088	1.85
7.659288	11.07648	23.09684	13.965	2.34
7.659582	11.07672	23.73176	18.221	0.88
7.662382	11.07909	18.76654	41.363	0.46
7.662755	11.07936	19.432	29.26	0.86
7.663128	11.07973	23.15831	49.875	0.38
7.663582	11.08005	28.89991	37.639	1.39
7.663928	11.08037	38.49854	27.398	1.74
7.664355	11.08075	29.04127	27.132	1.52
7.664808	11.08107	32.80377	28.994	1.59
7.665208	11.08144	38.41503	37.506	0.80
7.665635	11.08176	34.19722	29.925	0.81
7.665955	11.08205	28.37659	43.491	1.37
7.666408	11.08243	36.19613	40.698	2.19
7.666755	11.08277	33.94698	45.22	1.88
7.667155	11.08309	34.33488	32.452	0.20
7.667528	11.08339	28.64098	55.461	0.91
7.667848	11.08365	22.24319	47.215	0.55
7.668195	11.084	32.86699	41.23	1.02
7.668515	11.08429	28.43698	23.674	0.50
7.671768	11.08704	24.1859	17.556	2.16
7.672195	11.08733	17.0452	31.255	1.33
7.672488	11.0876	19.07991	21.147	3.75
7.672222	11.08795	16.67359	49.742	2.50
7.671848	11.08768	18.33991	25.802	1.82
7.671128	11.08707	24.75614	18.221	0.91
7.668275	11.08464	19.05083	28.861	1.54
7.667928	11.08437	21.80642	42.826	1.91
7.667528	11.08403	16.64325	33.915	2.85
7.667208	11.08381	18.78908	14.63	1.33
7.666835	11.08347	18.80118	14.098	1.62
7.666462	11.08315	19.57678	20.748	0.58
7.666062	11.0828	18.60723	20.482	1.21
7.665635	11.08245	23.96025	33.915	0.97
7.665262	11.08213	34.02971	30.856	0.21
7.664888	11.08181	27.99728	36.575	0.27
7.664462	11.08141	28.37084	28.728	1.10
7.664008	11.08109	28.73279	40.698	1.52
7.663635	11.08075	18.60196	25.004	1.02

Longitude	Latitude	eU(ppm)	Th(ppm)	K%
7.662835	11.08005	18.40304	20.881	0.72
7.662462	11.07979	19.37142	14.763	0.76
7.662088	11.07947	29.29883	35.112	0.42
7.661688	11.07912	19.09015	27.132	1.68
7.658968	11.07688	18.70147	35.644	1.28
7.658782	11.0772	21.77305	27.132	1.44
7.659022	11.07744	32.37382	28.595	1.61
7.661795	11.07979	26.82227	13.167	0.75
7.662142	11.08008	22.02222	22.61	0.97
7.662515	11.0804	25.7094	12.768	1.28
7.662968	11.0808	23.72874	18.354	2.17
7.663342	11.08109	24.48424	15.162	1.75
7.663795	11.08141	24.26122	29.26	1.86
7.664142	11.08179	33.26064	43.225	1.01
7.664568	11.08216	18.51162	31.122	1.53
7.664942	11.08248	30.97471	30.058	1.01
7.665315	11.0828	29.57892	16.359	3.02
7.665795	11.08315	23.26669	25.802	2.47
7.666515	11.08384	23.44738	13.566	2.90
7.666862	11.08413	23.74123	19.95	4.10
7.667208	11.0844	23.75069	21.679	2.19
7.667528	11.08472	27.92577	28.994	2.69
7.667875	11.08499	29.23415	31.521	1.15
7.671182	11.08776	28.3523	27.398	0.89
7.671502	11.08808	28.43484	45.22	1.05
7.671875	11.0884	35.25184	28.595	3.08
7.671502	11.08872	32.6265	43.225	5.65
7.671182	11.08843	28.03631	49.875	3.98
7.670835	11.08808	40.39911	33.915	4.40
7.670435	11.08776	37.72411	27.132	5.07
7.667635	11.08536	27.04168	29.26	3.37
7.667262	11.08509	39.95062	32.186	4.70
7.666888	11.08477	28.81893	28.329	5.97
7.666568	11.08448	29.13922	29.26	5.93
7.665795	11.08384	41.25178	28.595	4.85
7.665448	11.08347	33.64581	15.561	0.86
7.665022	11.08317	23.79566	17.556	2.68
7.664648	11.08285	29.20537	24.206	0.90
7.664302	11.08253	22.90797	48.013	2.38
7.663795	11.08216	21.95188	21.413	2.32
7.663395	11.08179	31.13549	42.294	4.99
7.662968	11.08147	22.85802	41.629	5.10

Longitude	Latitude	eU(ppm)	Th(ppm)	K%
7.662222	11.08083	28.53767	40.698	3.38
7.661848	11.08048	41.77422	67.83	0.60
7.661475	11.08016	29.9197	29.26	0.72
7.661022	11.07981	28.20411	33.915	0.18
7.658382	11.07752	23.98064	28.728	1.57
7.658088	11.07784	38.58674	42.826	0.40
7.658382	11.07816	29.10859	28.462	0.33
7.661155	11.08045	27.94538	19.551	0.42
7.661555	11.0808	42.47333	56.392	2.02
7.661928	11.08115	27.93484	28.595	0.83
7.662382	11.08149	35.69779	49.742	0.29
7.662702	11.08176	37.88987	49.875	1.74
7.663128	11.08213	39.01259	54.131	1.90
7.663502	11.08248	48.76322	41.496	0.33
7.663982	11.08285	32.81216	41.496	1.07
7.664302	11.08317	28.75776	43.89	1.46
7.664702	11.08349	29.01708	28.196	1.24
7.665128	11.08384	19.68	18.354	1.10
7.665528	11.08419	16.72071	24.073	0.51
7.665875	11.08451	24.26951	24.605	0.18
7.666248	11.0848	23.80132	15.162	0.39
7.666568	11.08509	18.67269	28.329	0.62
7.666942	11.08539	28.51415	28.861	0.78
7.667288	11.08573	28.828	27.93	2.05
7.667635	11.086	37.82743	41.895	2.53
7.668008	11.08632	26.31759	37.506	0.12
7.668408	11.08664	24.00854	14.63	0.98
7.670168	11.08816	27.79601	19.684	0.63
7.670488	11.08845	29.41102	15.162	1.85
7.670862	11.08877	25.02307	10.773	3.02
7.671182	11.08912	33.50893	17.29	1.52
7.670862	11.08941	34.83653	8.246	3.70
7.670542	11.08909	34.28795	25.935	3.69
7.670168	11.08883	33.85947	16.891	2.52
7.669795	11.08851	29.28507	9.975	1.49
7.669448	11.08824	28.65132	12.103	3.33
7.669128	11.08792	23.80435	15.029	2.88
7.668728	11.0876	38.64156	42.56	1.74
7.668408	11.08731	28.82196	28.196	1.46
7.668062	11.08704	32.16592	42.028	1.82
7.667715	11.08667	37.45231	41.23	2.07
7.667315	11.08643	29.31512	40.831	0.83

Longitude	Latitude	eU(ppm)	Th(ppm)	K%
7.666595	11.08579	29.53288	31.255	1.13
7.666248	11.08555	19.02693	14.896	1.92
7.665928	11.0852	45.55135	49.742	0.71
7.665502	11.08485	43.14747	41.762	0.75
7.665155	11.08461	34.76434	13.566	1.50
7.664782	11.08424	34.35302	31.654	2.48
7.664355	11.08392	38.87064	28.196	3.22
7.663982	11.08357	38.28528	28.196	3.65
7.663582	11.08328	52.44533	70.49	1.69
7.663155	11.08288	54.14756	42.826	3.23
7.662755	11.08259	49.10468	41.496	0.96
7.662355	11.08219	52.96874	81.795	0.45
7.661982	11.08187	64.06375	85.12	0.60
7.661555	11.08157	34.76336	41.496	1.99
7.661182	11.08123	30.9434	42.161	1.31
7.660782	11.08091	31.3192	29.925	2.38
7.660382	11.08056	45.64032	69.426	0.40
7.660008	11.08024	45.82335	69.958	3.56
7.659635	11.07989	33.61118	42.826	2.29
7.659208	11.07955	38.50927	52.668	2.08
7.658808	11.07925	39.59326	28.595	2.48
7.658382	11.07888	33.50893	17.29	2.47
7.658035	11.07859	29.75853	14.896	1.87
7.657635	11.07824	47.96996	54.929	2.75
7.657288	11.07867	47.17367	68.495	0.37
7.657715	11.07893	42.30475	68.096	1.06
7.658115	11.07925	42.30475	68.096	0.30
7.658488	11.07955	39.9476	32.319	1.96
7.658862	11.07992	52.9862	27.398	3.85
7.659288	11.08024	37.07114	40.831	4.78
7.659662	11.08059	28.39503	27.664	2.95
7.660035	11.08093	33.96503	27.265	4.15
7.660462	11.08125	37.00041	37.506	4.77
7.660835	11.0816	24.34024	27.93	2.51
7.661235	11.08195	24.5818	15.162	2.97
7.661635	11.08227	24.09517	21.546	3.67
7.661982	11.08253	24.454	16.492	4.87
7.662435	11.08293	19.73229	37.506	0.58
7.662808	11.08325	18.70674	31.122	0.77
7.663235	11.08365	23.8622	14.63	4.51
7.663608	11.08395	18.9842	14.63	1.04
7.663982	11.08427	19.60585	13.034	1.05

Longitude	Latitude	eU(ppm)	Th(ppm)	K%
7.664835	11.08499	23.40396	26.201	6.45
7.665208	11.08528	51.60758	40.831	1.38
7.665555	11.08563	33.60005	15.428	1.31
7.665875	11.08587	27.69904	56.126	0.72
7.666248	11.08619	40.66125	50.274	1.74
7.666595	11.08648	48.02937	63.042	0.55
7.666968	11.08677	59.2119	28.196	3.05
7.667315	11.08712	34.8775	32.186	1.88
7.667688	11.08741	34.12922	41.496	1.01
7.668035	11.08771	53.97292	54.796	1.25
7.668382	11.088	52.13948	81.795	2.25
7.668782	11.08832	57.37308	42.56	3.16
7.669128	11.08861	34.18171	28.462	2.21
7.669448	11.08891	28.69191	33.915	1.83
7.669768	11.08923	37.13475	55.195	4.00
7.670168	11.08955	34.03459	24.206	1.26
7.670488	11.08987	34.16961	28.994	1.65
7.670222	11.09024	24.36815	13.832	2.82
7.669822	11.08992	39.01054	26.334	5.50
7.669475	11.08957	28.72518	32.452	5.84
7.669102	11.08933	35.75067	38.836	4.57
7.668728	11.08899	21.90534	17.024	0.68
7.668408	11.08867	39.03278	14.63	3.51
7.668035	11.08837	18.65913	37.506	0.50
7.667715	11.08811	23.56728	19.019	3.57
7.667395	11.08781	18.14587	15.029	3.08
7.666995	11.08752	28.56215	24.605	1.44
7.666595	11.08717	24.49029	14.896	3.13
7.666302	11.08683	24.23127	15.561	2.96
7.665875	11.08656	18.99064	16.492	1.14
7.665528	11.08624	20.50887	16.226	1.67
7.665235	11.086	24.44756	14.63	2.02
7.664835	11.08568	43.89244	47.614	0.09
7.664488	11.08536	23.62435	14.364	2.33
7.664115	11.08499	19.44107	28.861	1.63
7.663688	11.08467	56.50148	44.422	2.03
7.663262	11.08429	37.73016	26.866	2.60
7.662915	11.08403	43.74932	15.295	2.55
7.662462	11.08365	47.69104	13.566	2.22
7.662088	11.08328	37.6167	23.275	3.01
7.661635	11.08296	28.37952	26.201	2.03
7.661342	11.08264	38.1605	29.393	1.27

Longitude	Latitude	eU(ppm)	Th(ppm)	K%
7.660542	11.08197	28.43698	23.674	0.33
7.660142	11.08163	28.70625	28.994	0.81
7.659715	11.08131	38.07572	15.96	3.09
7.659395	11.08096	33.54679	24.206	1.77
7.659048	11.08061	33.02533	23.541	1.85
7.658595	11.08032	34.81087	17.955	0.67
7.658168	11.07995	47.46245	47.215	0.72
7.657715	11.07957	39.12966	27.531	3.01
7.657395	11.07928	48.08928	23.94	0.58
7.656995	11.07899	32.47138	28.595	0.97
7.656728	11.07933	29.95872	42.56	0.74
7.657102	11.07971	33.03528	44.555	2.03
7.657475	11.08003	28.86537	15.561	0.65
7.657848	11.08032	17.22471	12.635	1.16
7.658302	11.08069	29.19259	37.639	0.40
7.658648	11.08101	28.39269	14.896	1.32
7.658995	11.08131	32.51675	26.6	1.61
7.659422	11.08163	43.26152	15.295	0.86
7.659848	11.082	44.6577	31.122	1.14
7.660195	11.08235	38.13025	30.723	0.47
7.660622	11.08269	33.59703	15.561	0.92
7.660995	11.08296	44.58102	45.22	1.19
7.661315	11.08331	31.38047	31.521	0.42
7.661768	11.08368	27.84499	53.998	0.41
7.662142	11.08403	18.53474	40.831	0.52
7.662568	11.08437	23.55372	28.196	0.82
7.662968	11.08467	35.09682	31.122	3.44
7.663342	11.08504	40.26652	59.052	1.01
7.663742	11.08539	47.93396	41.496	3.54
7.664195	11.08571	43.07479	27.797	1.97
7.664488	11.08603	37.53475	41.895	1.02
7.667022	11.08819	24.70931	28.861	2.08
7.667368	11.08845	47.8085	55.594	1.07
7.667715	11.08875	34.29136	27.93	0.43
7.668088	11.08909	39.39746	41.496	1.76
7.668435	11.08939	42.8945	42.161	0.65
7.668782	11.08963	42.49421	70.49	0.74
7.669075	11.08997	53.16288	43.225	3.65
7.669502	11.09032	44.45985	16.226	2.40
7.669875	11.09061	34.33634	23.807	1.53
7.669528	11.09093	48.71444	41.496	0.75
7.669155	11.09064	40.53384	53.732	3.76

Longitude	Latitude	eU(ppm)	Th(ppm)	K%
7.668408	11.09005	38.88507	40.432	1.34
7.668088	11.08971	34.47897	36.841	0.59
7.667768	11.08944	35.95223	40.698	0.99
7.667395	11.08915	24.40659	57.19	0.76
7.667048	11.0888	55.33584	72.086	1.60
7.666702	11.08853	58.78136	57.855	2.51
7.664222	11.0864	47.95991	83.258	2.74
7.663875	11.08608	27.30373	28.462	1.78
7.663448	11.08571	52.36318	54.796	2.89
7.663022	11.08536	33.00455	26.6	1.09
7.662622	11.08507	42.15519	33.915	0.62
7.662275	11.08472	37.41406	32.186	0.79
7.661795	11.08432	41.23032	44.555	2.14
7.661448	11.08403	35.72237	50.806	0.69
7.661022	11.08365	18.98576	23.142	2.07
7.660675	11.08336	28.98264	23.275	0.60
7.660302	11.08301	43.61439	27.664	0.34
7.659902	11.08269	42.41811	54.53	0.30
7.659502	11.08235	28.75708	56.791	0.30
7.659102	11.08203	47.81289	29.659	1.43
7.658755	11.08165	58.83717	29.659	3.13
7.657982	11.08101	57.5803	42.028	2.76
7.657582	11.08069	53.45215	41.23	3.14
7.657155	11.08037	20.95999	15.694	1.24
7.656808	11.08	17.48373	11.97	0.95
7.656408	11.07971	16.81671	15.561	0.93
7.656088	11.08003	25.24658	15.96	2.24
7.656862	11.08072	18.98381	12.502	1.24
7.657235	11.08104	19.62439	14.364	0.87
7.657662	11.08141	17.42324	14.63	1.05
7.658062	11.08171	21.911	14.63	1.47
7.658088	11.08195	42.72718	77.406	0.06
7.658435	11.08203	35.95223	40.698	0.97
7.658808	11.08237	30.21804	26.866	0.83
7.659235	11.08272	28.89093	55.195	0.56
7.659635	11.08304	37.1207	45.087	0.67
7.660008	11.08336	17.6607	12.768	1.07
7.660382	11.08371	18.2367	28.196	2.66
7.660702	11.084	31.36456	27.93	3.23
7.661155	11.08437	38.40254	35.91	4.03
7.661528	11.08469	23.83888	37.107	0.83
7.661982	11.08509	50.31628	48.279	1.01

Longitude	Latitude	eU(ppm)	Th(ppm)	K%
7.662728	11.08573	45.8691	70.091	1.75
7.663102	11.08608	26.3731	24.339	0.52
7.663555	11.08645	36.69602	40.166	4.59
7.663902	11.08675	51.07168	27.93	1.87
7.666382	11.08891	45.93632	54.264	0.90
7.666728	11.0892	32.6745	38.969	0.44
7.667075	11.08949	41.20495	39.235	2.52
7.667422	11.08981	28.96283	64.904	1.66
7.667742	11.09005	21.95471	53.466	0.70
7.668115	11.0904	35.72198	48.678	0.30
7.668408	11.09075	53.91536	40.166	3.70
7.668862	11.09109	26.93124	25.536	1.05
7.669208	11.09136	34.95946	13.566	2.59
7.668862	11.09168	34.3058	40.166	2.28
7.668515	11.09141	26.6529	20.615	1.28
7.668115	11.09104	46.01837	52.801	0.09
7.667768	11.09077	42.67509	26.068	0.51
7.667395	11.09045	40.9634	52.003	0.94
7.667128	11.09013	33.84034	45.619	1.38
7.666782	11.08989	36.78295	32.053	0.38
7.666382	11.08957	39.70068	32.452	0.73
7.666035	11.08925	41.00379	39.501	1.66
7.663555	11.08715	50.92193	25.935	2.40
7.663182	11.08683	41.92465	56.924	2.77
7.662782	11.08645	53.69917	58.254	2.34
7.662328	11.08613	54.78677	70.49	1.99
7.662008	11.08576	33.07118	40.831	1.74
7.661635	11.08544	54.31555	61.18	3.25
7.661182	11.08507	43.88785	39.235	1.43
7.660835	11.08472	56.74558	78.736	1.68
7.660008	11.08405	54.57653	71.155	0.17
7.659662	11.08376	52.90962	58.653	0.39
7.659288	11.08339	40.90505	33.117	1.05
7.658888	11.08312	57.71874	48.811	2.61
7.658488	11.08272	53.20698	84.189	2.40
7.658088	11.0824	38.92176	40.964	1.00
7.657715	11.08213	57.18899	52.801	1.69
7.657315	11.08179	53.31313	64.505	0.37
7.656915	11.08141	40.22672	41.496	1.55
7.656542	11.08112	50.26584	89.11	2.12
7.656195	11.08075	53.17849	61.845	2.30
7.655768	11.08045	40.10692	53.2	0.46

Longitude	Latitude	eU(ppm)	Th(ppm)	K%
7.655902	11.08109	43.0303	51.205	1.05
7.656302	11.08141	48.58781	49.21	2.02
7.656648	11.08173	36.10686	36.043	1.03
7.657075	11.08211	41.19354	26.866	1.04
7.657475	11.08243	33.57069	38.171	0.50
7.657822	11.08269	27.18461	27.265	0.39
7.658195	11.08304	46.70344	31.255	1.47
7.658622	11.08341	40.00594	51.205	0.50
7.658995	11.08373	31.62622	25.004	0.72
7.659395	11.08408	17.55036	26.201	1.82
7.659715	11.0844	26.36949	54.53	0.51
7.660088	11.08469	30.38233	58.254	0.93
7.660542	11.08509	48.90478	65.303	1.34
7.660888	11.08541	17.39075	20.349	1.30
7.661342	11.08579	17.66109	14.896	1.33
7.661688	11.08611	16.8652	30.59	2.23
7.662088	11.08645	19.76936	40.166	2.66
7.662488	11.08675	20.43345	53.865	2.14
7.662915	11.08715	45.94374	28.196	4.01
7.663262	11.08744	18.98088	29.792	0.47
7.663635	11.08779	22.36329	20.482	1.10
7.663955	11.08811	16.45974	14.098	0.51
7.664355	11.08837	21.14154	24.871	0.03
7.664648	11.08867	46.79114	27.398	1.44
7.664995	11.08896	55.02082	66.633	1.09
7.665395	11.08931	16.9132	26.334	1.59
7.665768	11.08963	36.87036	43.225	0.80
7.666142	11.08989	17.26373	25.935	0.81
7.666488	11.09024	16.31193	22.743	0.44
7.666782	11.09053	17.07544	29.925	1.17
7.667155	11.09077	52.27772	54.264	0.39
7.667502	11.09109	41.36768	62.111	0.57
7.667795	11.09139	56.83016	57.855	2.74
7.668568	11.09208	50.58525	68.628	1.62
7.668302	11.09232	32.53763	40.698	0.52
7.667902	11.09213	49.66555	57.589	2.82
7.667448	11.09171	51.50222	64.771	3.32
7.667182	11.09147	38.8321	34.181	1.52
7.666755	11.0912	36.53456	40.831	1.54
7.666408	11.0908	35.88989	49.875	0.80
7.666142	11.09061	34.48317	43.092	0.71
7.665795	11.09024	60.0435	40.964	0.03

Longitude	Latitude	eU(ppm)	Th(ppm)	K%
7.665075	11.08965	32.27285	26.6	1.12
7.664702	11.08933	44.17175	24.605	1.05
7.664382	11.08899	46.18276	34.846	1.44
7.664035	11.08875	36.36256	50.54	0.54
7.663662	11.0884	37.17651	16.891	1.35
7.663342	11.08816	32.42729	54.131	1.77
7.662968	11.08779	43.34035	46.151	2.12
7.662622	11.08749	31.96846	29.26	0.83
7.662168	11.08712	27.90226	17.157	0.71
7.661822	11.08677	57.75454	27.93	2.47
7.661422	11.08643	32.95362	48.146	1.06
7.661075	11.08613	56.025	39.634	1.79
7.660622	11.08571	26.56149	37.506	0.93
7.660222	11.08544	17.41719	14.896	1.26
7.659715	11.08504	34.92297	47.348	1.28
7.659422	11.08469	21.9991	12.901	0.39
7.659102	11.08448	21.81042	14.763	0.59
7.658728	11.08397	22.4548	20.748	0.47
7.658328	11.08373	28.58137	13.034	0.05
7.657902	11.08336	29.46175	25.802	1.49
7.657528	11.08304	36.59729	33.782	1.25
7.657208	11.08269	42.20592	44.555	1.50
7.656835	11.08237	52.79801	48.545	2.37
7.656382	11.08203	40.69081	61.845	0.42
7.656008	11.08171	48.35152	57.456	3.84
7.655662	11.08144	36.26822	18.221	1.73
7.655235	11.08109	27.08558	35.91	3.21

Appendix 2: Total counts (TC), equivalent surface concentration of uranium (eU), thorium (eTh) and potassium (K%)

(uncorrected data)

Longitude	Latitude	eU(ppm)	Th(ppm)	K%
7.660302	11.07496	40.06223	42.294	2.073469
7.660782	11.07536	35.22999	4.2427	2.406741
7.661155	11.07571	30.7513	42.028	1.988268
7.661555	11.07597	30.14545	30.058	1.782019
7.662435	11.07669	23.11626	36.708	1.755263
7.662755	11.07704	35.33126	29.393	2.106199
7.663155	11.07736	28.05816	36.043	2.893791
7.663555	11.07771	26.43817	30.058	1.643566
7.663982	11.07797	40.28643	34.58	2.309331
7.664328	11.07829	35.05526	37.24	1.647463
7.664728	11.07877	30.74525	42.294	1.793448
7.665128	11.07907	31.24886	28.728	1.418614
7.665555	11.07936	25.88833	24.206	1.731365
7.665982	11.07979	26.44422	29.792	1.721494
7.666435	11.08008	26.27866	41.363	1.920471
7.666728	11.08045	26.10013	32.053	1.786954
7.667155	11.08075	35.60735	38.703	4.04271
7.667582	11.08104	31.45344	30.457	3.942183
7.668008	11.08144	37.79748	28.196	3.210179
7.668355	11.08168	30.36477	28.994	2.751443
7.668728	11.082	30.81628	30.59	2.577404
7.669048	11.08227	30.39355	36.309	3.389673
7.669422	11.08256	30.74516	25.137	2.666501
7.669768	11.08288	25.3215	25.536	1.883844
7.670115	11.0832	28.45025	29.526	2.501554
7.670488	11.08355	34.93731	42.427	3.426819
7.670862	11.08381	29.04029	55.062	3.031984
7.671208	11.08408	25.6133	70.623	4.349227
7.671555	11.0844	26.3611	42.028	2.431159
7.671955	11.08472	30.32145	58.786	3.51228
7.672382	11.08504	30.03199	26.467	1.689284
7.672675	11.08531	35.59789	36.974	2.780796
7.673048	11.08557	35.26365	43.092	2.921845
7.673715	11.08616	40.68993	40.432	4.403776
7.673422	11.08656	33.59342	45.752	3.041595
7.673102	11.08624	40.35491	42.294	2.878206
7.672702	11.08595	35.8415	52.003	4.098039
7.672408	11.0856	34.52102	50.008	2.325436

Longitude	Latitude	eU(ppm)	Th(ppm)	K%
7.671688	11.08509	35.15058	41.629	2.701309
7.671262	11.08469	28.53084	36.708	2.79768
7.670968	11.08445	29.23229	38.038	2.127499
7.670595	11.08416	35.43379	39.9	2.932496
7.670248	11.08389	40.96291	32.718	2.24543
7.669848	11.08355	34.122	35.378	1.755263
7.669502	11.08323	38.83747	46.816	1.928263
7.669155	11.08296	24.5418	29.792	1.841763
7.668675	11.08269	26.93202	29.792	1.820203
7.668462	11.08245	36.42978	34.713	1.865921
7.668088	11.08205	34.68804	29.792	2.507788
7.667688	11.08176	30.5513	48.678	2.090094
7.667288	11.08139	25.10794	41.363	3.234337
7.666835	11.08109	36.78519	27.664	2.530127
7.666462	11.0808	33.72493	31.388	1.604602
7.666088	11.08045	34.69156	48.944	2.688841
7.665662	11.08008	27.26978	42.826	1.697856
7.665262	11.07973	31.6229	40.166	2.452199
7.664408	11.07907	29.0281	38.437	3.314083
7.663955	11.07872	25.39223	28.861	2.149839
7.663635	11.0784	31.08935	40.033	2.013724
7.663235	11.07803	24.19283	38.703	2.874569
7.662782	11.07773	24.26503	33.383	1.891897
7.662408	11.07741	33.52835	40.033	2.026712
7.662035	11.07709	23.92776	39.634	3.610989
7.661608	11.07672	32.87996	62.111	4.86485
7.661208	11.0764	34.76834	52.003	2.045675
7.660782	11.07605	40.2317	52.003	3.070688
7.660408	11.07573	35.25418	41.363	3.731517
7.659955	11.07539	28.57464	26.201	3.776456
7.659795	11.07576	33.05186	35.245	5.066944
7.660142	11.07608	29.1479	26.733	2.846775
7.660542	11.07637	35.38004	29.393	2.757677
7.660942	11.07672	38.45542	25.004	2.903922
7.661795	11.07744	35.73447	50.274	4.630806
7.662142	11.07773	37.6126	34.181	2.708063
7.662488	11.07808	30.11502	63.574	2.767808
7.662942	11.07843	27.36002	86.051	4.717826
7.663368	11.07872	40.72428	28.196	3.081598
7.663715	11.07904	34.70112	67.83	4.038813
7.664168	11.07939	36.03203	43.624	2.195297
7.664542	11.07976	42.96835	62.51	3.366295

Longitude	Latitude	eU(ppm)	Th(ppm)	K%
7.665395	11.08043	41.45061	82.061	3.560855
7.665822	11.0808	38.80742	82.46	4.922777
7.666142	11.08112	34.42736	71.288	2.978473
7.666568	11.08144	31.00964	54.264	3.167059
7.666995	11.08176	35.1617	69.027	3.423182
7.667342	11.08211	29.91326	27.398	2.750144
7.667742	11.0824	34.60395	69.958	3.276937
7.668115	11.08272	43.87146	82.859	4.418063
7.668435	11.08296	34.8815	70.623	4.783026
7.668835	11.08331	34.38297	45.353	3.802172
7.669182	11.08357	25.56052	32.186	2.348555
7.669475	11.08387	29.99911	30.058	3.827888
7.669875	11.08416	31.18759	27.132	5.239424
7.670248	11.08451	29.98214	37.24	4.126353
7.670622	11.0848	28.53571	30.058	2.401806
7.670942	11.08507	25.77574	42.028	2.432198
7.671342	11.08539	30.64233	29.659	2.354789
7.671688	11.08568	31.25715	24.073	2.661306
7.672062	11.08597	33.52513	72.352	3.233298
7.672408	11.08632	25.38501	22.743	1.831892
7.672808	11.08661	25.31175	38.836	1.883325
7.673128	11.08691	30.59091	31.92	2.647019
7.672808	11.08723	33.04094	42.161	1.657334
7.672168	11.08664	28.34528	55.594	2.808071
7.671768	11.08635	23.48884	56.791	2.836125
7.668888	11.08389	30.27892	26.334	2.108797
7.668542	11.08357	33.28445	40.033	1.808514
7.668168	11.08328	38.87678	45.087	2.986785
7.667875	11.08299	40.64184	27.531	2.44103
7.667502	11.08267	35.41633	27.797	3.465523
7.667128	11.08243	30.96828	28.196	2.016582
7.666675	11.08211	30.60155	40.033	3.22031
7.666275	11.08173	31.05306	41.629	3.319018
7.665902	11.08139	29.20654	30.59	1.450305
7.665555	11.08109	28.78225	27.797	1.669802
7.665048	11.08072	23.4465	58.653	4.297275
7.664702	11.08037	24.0182	50.673	2.716375
7.664248	11.08	30.46838	28.728	1.963331
7.663928	11.07973	28.77357	30.324	2.834306
7.663448	11.07936	30.69452	31.654	2.735598
7.663075	11.07901	30.36457	61.18	3.120302
7.662648	11.07867	35.07731	57.722	5.012654

Longitude	Latitude	eU(ppm)	Th(ppm)	K%
7.659475	11.07608	31.51168	32.186	2.894311
7.659288	11.07648	29.80058	28.063	3.22005
7.659582	11.07672	30.4355	32.319	1.932939
7.662382	11.07909	25.47028	55.461	2.445186
7.662755	11.07936	26.13574	43.358	2.357906
7.663128	11.07973	29.86204	63.973	2.718453
7.663582	11.08005	35.60364	51.737	3.223946
7.663928	11.08037	45.20228	41.496	3.168358
7.664355	11.08075	35.74501	41.23	2.934054
7.664808	11.08107	39.50751	43.092	3.083156
7.665208	11.08144	45.11877	51.604	2.629096
7.665635	11.08176	40.90096	44.023	2.331671
7.665955	11.08205	35.08033	57.589	3.441106
7.666408	11.08243	42.89986	54.796	4.154666
7.666755	11.08277	40.65072	59.318	4.024267
7.667155	11.08309	41.03861	46.55	1.833451
7.667528	11.08339	35.34472	69.559	3.470459
7.667848	11.08365	28.94693	61.313	2.774302
7.668195	11.084	39.57073	55.328	3.006787
7.668515	11.08429	35.14072	37.772	1.775005
7.671768	11.08704	30.88964	31.654	3.185502
7.672195	11.08733	23.74893	45.353	2.907559
7.672488	11.0876	25.78364	35.245	4.91966
7.672222	11.08795	23.37733	63.84	4.831861
7.671848	11.08768	25.04365	39.9	3.178229
7.671128	11.08707	31.45988	32.319	1.957097
7.668275	11.08464	25.75457	42.959	3.023152
7.667928	11.08437	28.51015	56.924	3.959327
7.667528	11.08403	23.34699	48.013	4.535994
7.667208	11.08381	25.49282	28.728	2.238417
7.666835	11.08347	25.50492	28.196	2.504671
7.666462	11.08315	26.28052	34.846	1.738898
7.666062	11.0828	25.31097	34.58	2.353231
7.665635	11.08245	30.66399	48.013	2.659228
7.665262	11.08213	40.73345	44.954	1.773446
7.664888	11.08181	34.70102	50.673	2.067495
7.664462	11.08141	35.07458	42.826	2.582339
7.664008	11.08109	35.43652	54.796	3.486044
7.663635	11.08075	25.3057	39.102	2.344399
7.663342	11.08048	29.62487	50.806	2.741052
7.662835	11.08005	25.10677	34.979	1.883844
7.662462	11.07979	26.07515	28.861	1.6724

Longitude	Latitude	eU(ppm)	Th(ppm)	K%
7.661688	11.07912	25.79389	41.23	3.088092
7.658968	11.07688	25.40521	49.742	3.040816
7.658782	11.0772	28.47679	41.23	2.85171
7.659022	11.07744	39.07756	42.693	3.083936
7.661795	11.07979	33.52601	27.265	1.592134
7.662142	11.08008	28.72596	36.708	2.195556
7.662515	11.0804	32.41314	26.866	2.109316
7.662968	11.0808	30.43248	32.452	3.231739
7.663342	11.08109	31.18798	29.26	2.676372
7.663795	11.08141	30.96496	43.358	3.362398
7.664142	11.08179	39.96438	57.323	3.077442
7.664568	11.08216	25.21536	45.22	3.099781
7.664942	11.08248	37.67845	44.156	2.538699
7.665315	11.0828	36.28266	30.457	3.998551
7.665795	11.08315	29.97043	39.9	3.829707
7.666515	11.08384	30.15111	27.664	3.767104
7.666862	11.08413	30.44496	34.048	5.220981
7.667208	11.0844	30.45443	35.777	3.385257
7.667528	11.08472	34.62951	43.092	4.174148
7.667875	11.08499	35.93788	45.619	2.745209
7.671182	11.08776	35.05604	41.496	2.314007
7.671502	11.08808	35.13858	59.318	3.19849
7.671875	11.0884	41.95558	42.693	4.5508
7.671502	11.08872	39.33024	57.323	7.713119
7.671182	11.08843	34.74004	63.973	6.316129
7.670835	11.08808	47.10285	48.013	6.087021
7.670435	11.08776	44.42785	41.23	6.479518
7.667635	11.08536	33.74542	43.358	4.870565
7.667262	11.08509	46.65436	46.284	6.319506
7.666888	11.08477	35.52267	42.427	7.432578
7.666568	11.08448	35.84296	43.358	7.427642
7.665795	11.08384	47.95552	42.693	6.326
7.665448	11.08347	40.34955	29.659	1.800721
7.665022	11.08317	30.4994	31.654	3.701385
7.664648	11.08285	35.9091	38.304	2.197894
7.664302	11.08253	29.6117	62.111	4.641197
7.663795	11.08216	28.65562	35.511	3.496694
7.663395	11.08179	37.83923	56.392	7.01878
7.662968	11.08147	29.56175	55.727	7.100605
7.662622	11.08115	29.3401	44.023	3.715932
7.662222	11.08083	35.2414	54.796	5.34151
7.661848	11.08048	48.47795	81.928	3.658785

Longitude	Latitude	eU(ppm)	Th(ppm)	K%
7.661022	11.07981	34.90785	48.013	1.865921
7.658382	11.07752	30.68438	42.826	3.044712
7.658088	11.07784	45.29047	56.924	2.446744
7.658382	11.07816	35.81232	42.56	1.795266
7.661155	11.08045	34.64912	33.649	1.529272
7.661555	11.0808	49.17707	70.49	4.619117
7.661928	11.08115	34.63858	42.693	2.297382
7.662382	11.08149	42.40153	63.84	2.616108
7.662702	11.08176	44.5936	63.973	4.073362
7.663128	11.08213	45.71632	68.229	4.41105
7.663502	11.08248	55.46696	55.594	2.326995
7.663982	11.08285	39.5159	55.594	3.063155
7.664302	11.08317	35.4615	57.988	3.548646
7.664702	11.08349	35.72081	42.294	2.70027
7.665128	11.08384	26.38374	32.452	2.156592
7.665528	11.08419	23.42445	38.171	1.795786
7.665875	11.08451	30.97325	38.703	1.48797
7.666248	11.0848	30.50506	29.26	1.316009
7.666568	11.08509	25.37643	42.427	2.084379
7.666942	11.08539	35.21789	42.959	2.263873
7.667288	11.08573	35.53174	42.028	3.497214
7.667635	11.086	44.53116	55.993	4.543527
7.668008	11.08632	33.02133	51.604	1.957876
7.668408	11.08664	30.71228	28.728	1.889299
7.670168	11.08816	34.49975	33.782	1.743834
7.670488	11.08845	36.11476	29.26	2.77586
7.670862	11.08877	31.7268	24.871	3.766585
7.671182	11.08912	40.21267	31.388	2.536881
7.670862	11.08941	41.54027	22.344	4.344551
7.670542	11.08909	40.99169	40.033	5.059151
7.670168	11.08883	40.5632	30.989	3.519034
7.669795	11.08851	35.98881	24.073	2.206986
7.669448	11.08824	35.35506	26.201	4.130249
7.669128	11.08792	30.50809	29.127	3.803211
7.668728	11.0876	45.3453	56.658	3.773598
7.668408	11.08731	35.52569	42.294	2.912754
7.668062	11.08704	38.86966	56.126	3.834902
7.667715	11.08667	44.15605	55.328	4.05284
7.667315	11.08643	36.01886	54.929	2.796641
7.666942	11.08608	39.81619	63.84	2.999514
7.666595	11.08579	36.23661	45.353	2.712219
7.666248	11.08555	25.73067	28.994	2.833267

Longitude	Latitude	eU(ppm)	Th(ppm)	K%
7.665502	11.08485	49.85121	55.86	2.756898
7.665155	11.08461	41.46807	27.664	2.365959
7.664782	11.08424	41.05676	45.752	4.080375
7.664355	11.08392	45.57437	42.294	4.672108
7.663982	11.08357	44.98901	42.294	5.108245
7.663582	11.08328	59.14907	84.588	4.862772
7.663155	11.08288	60.85129	56.924	5.278648
7.662755	11.08259	55.80842	55.594	2.951978
7.662355	11.08219	59.67248	95.893	4.077777
7.661982	11.08187	70.76749	99.218	4.358838
7.661555	11.08157	41.4671	55.594	3.984004
7.661182	11.08123	37.64714	56.259	3.32837
7.660782	11.08091	38.02294	44.023	3.903998
7.660382	11.08056	52.34406	83.524	3.526307
7.660008	11.08024	52.52708	84.056	6.710185
7.659635	11.07989	40.31491	56.924	4.338836
7.659208	11.07955	45.21301	66.766	4.524565
7.658808	11.07925	46.297	42.693	3.949976
7.658382	11.07888	40.21267	31.388	3.485005
7.658035	11.07859	36.46227	28.994	2.790407
7.657635	11.07824	54.6737	69.027	5.293454
7.657288	11.07867	53.87741	82.593	3.454353
7.657715	11.07893	49.00849	82.194	4.129729
7.658115	11.07925	49.00849	82.194	3.369931
7.658488	11.07955	46.65134	46.417	3.585532
7.658862	11.07992	59.68994	41.496	5.272673
7.659288	11.08024	43.77488	54.929	6.750708
7.659662	11.08059	35.09877	41.762	4.381177
7.660035	11.08093	40.66876	41.363	5.566202
7.660462	11.08125	43.70415	51.604	6.6081
7.660835	11.0816	31.04398	42.028	3.95543
7.661235	11.08195	31.28554	29.26	3.894906
7.661635	11.08227	30.79891	35.644	4.85446
7.661982	11.08253	31.15774	30.59	5.851938
7.662435	11.08293	26.43603	51.604	2.417651
7.662808	11.08325	25.41048	45.22	2.341801
7.663235	11.08365	30.56594	28.728	5.415801
7.663608	11.08395	25.68794	28.728	1.948005
7.663982	11.08427	26.30959	27.132	1.895014
7.664435	11.08461	30.54477	29.659	2.168801
7.664835	11.08499	30.1077	40.299	7.823257
7.665208	11.08528	58.31132	54.929	3.35019

Longitude	Latitude	eU(ppm)	Th(ppm)	K%
7.665875	11.08587	34.40278	70.224	3.307589
7.666248	11.08619	47.36499	64.372	4.087908
7.666595	11.08648	54.73311	77.14	3.414091
7.666968	11.08677	65.91563	42.294	4.506122
7.667315	11.08712	41.58124	46.284	3.499292
7.667688	11.08741	40.83296	55.594	3.002371
7.668035	11.08771	60.67666	68.894	3.78269
7.668382	11.088	58.84322	95.893	5.880252
7.668782	11.08832	64.07682	56.658	5.195005
7.669128	11.08861	40.88544	42.56	3.673851
7.669448	11.08891	35.39565	48.013	3.516696
7.669768	11.08923	43.83849	69.293	6.546536
7.670168	11.08955	40.73832	38.304	2.552986
7.670488	11.08987	40.87335	43.092	3.141343
7.670222	11.09024	31.07188	27.93	3.689696
7.669822	11.08992	45.71427	40.432	6.87773
7.669475	11.08957	35.42891	46.55	7.471542
7.669102	11.08933	42.4544	52.934	6.458738
7.668728	11.08899	28.60908	31.122	1.678634
7.668408	11.08867	45.73652	28.728	4.419102
7.668035	11.08837	25.36287	51.604	2.33297
7.667715	11.08811	30.27101	33.117	4.654185
7.667395	11.08781	24.84961	29.127	4.003746
7.666995	11.08752	35.26589	38.703	2.748845
7.666595	11.08717	31.19403	28.994	4.046606
7.666302	11.08683	30.93501	29.659	3.899842
7.665875	11.08656	25.69438	30.59	2.118927
7.665528	11.08624	27.21261	30.324	2.637928
7.665235	11.086	31.1513	28.728	2.92756
7.664835	11.08568	50.59618	61.712	2.157891
7.664488	11.08536	30.32809	28.462	3.223427
7.664115	11.08499	26.14481	42.959	3.117704
7.663688	11.08467	63.20522	58.52	4.146614
7.663262	11.08429	44.4339	40.964	3.99881
7.662915	11.08403	50.45306	29.393	3.484226
7.662462	11.08365	54.39477	27.664	3.085494
7.662088	11.08328	44.32043	37.373	4.263246
7.661635	11.08296	35.08326	40.299	3.404999
7.661342	11.08264	44.86423	43.491	2.772743
7.660942	11.08227	40.21726	39.767	2.441289
7.660542	11.08197	35.14072	37.772	1.606161
7.660142	11.08163	35.40999	43.092	2.298162

Longitude	Latitude	eU(ppm)	Th(ppm)	K%
7.659395	11.08096	40.25052	38.304	3.064713
7.659048	11.08061	39.72907	37.639	3.113289
7.658595	11.08032	41.51461	32.053	1.709805
7.658168	11.07995	54.16619	61.313	2.946003
7.657715	11.07957	45.8334	41.629	4.435727
7.657395	11.07928	54.79301	38.038	1.865661
7.656995	11.07899	39.17512	42.693	2.445186
7.656728	11.07933	36.66246	56.658	2.780276
7.657102	11.07971	39.73902	58.653	4.153627
7.657475	11.08003	35.56911	29.659	1.590575
7.657848	11.08032	23.92844	26.733	1.981514
7.658302	11.08069	35.89632	51.737	2.242833
7.658648	11.08101	35.09643	28.994	2.238677
7.658995	11.08131	39.22049	40.698	3.00367
7.659422	11.08163	49.96526	29.393	1.794487
7.659848	11.082	51.36144	45.22	2.713518
7.660195	11.08235	44.83399	44.821	2.032427
7.660622	11.08269	40.30077	29.659	1.863583
7.660995	11.08296	51.28476	59.318	3.334344
7.661315	11.08331	38.0842	45.619	2.011906
7.661768	11.08368	34.54873	68.096	2.915611
7.662142	11.08403	25.23848	54.929	2.486747
7.662568	11.08437	30.25745	42.294	2.279199
7.662968	11.08467	41.80056	45.22	5.014212
7.663342	11.08504	46.97026	73.15	3.715932
7.663742	11.08539	54.6377	55.594	5.538668
7.664195	11.08571	49.77853	41.895	3.409155
7.664488	11.08603	44.23848	55.993	3.030945
7.667022	11.08819	31.41305	42.959	3.562933
7.667368	11.08845	54.51224	69.692	3.637744
7.667715	11.08875	40.9951	42.028	1.872675
7.668088	11.08909	46.1012	55.594	3.752818
7.668435	11.08939	49.59824	56.259	2.675073
7.668782	11.08963	49.19795	84.588	3.91283
7.669075	11.08997	59.86662	57.323	5.711148
7.669502	11.09032	51.16359	30.324	3.372529
7.669875	11.09061	41.04008	37.905	2.812227
7.669528	11.09093	55.41818	55.594	2.740533
7.669155	11.09064	47.23758	67.83	6.254826
7.668808	11.09032	45.86569	68.096	2.605458
7.668408	11.09005	45.58881	54.53	3.294861
7.668088	11.08971	41.18271	50.939	2.395831

Longitude	Latitude	eU(ppm)	Th(ppm)	K%
7.667395	11.08915	31.11032	71.288	3.395648
7.667048	11.0888	62.03957	86.184	4.831601
7.666702	11.08853	65.4851	71.953	5.172406
7.664222	11.0864	54.66365	97.356	6.424449
7.663875	11.08608	34.00746	42.56	3.244467
7.663448	11.08571	59.06692	68.894	5.428529
7.663022	11.08536	39.70829	40.698	2.485449
7.662622	11.08507	48.85893	48.013	2.31089
7.662275	11.08472	44.1178	46.284	2.405962
7.661795	11.08432	47.93406	58.653	4.255973
7.661448	11.08403	42.42611	64.904	3.066272
7.661022	11.08365	25.6895	37.24	3.320058
7.660675	11.08336	35.68637	37.373	1.85631
7.660302	11.08301	50.31813	41.762	1.76955
7.659902	11.08269	49.12185	68.628	2.822617
7.659502	11.08235	35.46082	70.889	2.918209
7.659102	11.08203	54.51663	43.757	2.943925
7.658755	11.08165	65.54091	43.757	4.647431
7.657982	11.08101	64.28404	56.126	4.774714
7.657582	11.08069	60.15589	55.328	5.124091
7.657155	11.08037	27.66372	29.792	2.189062
7.656808	11.08	24.18747	26.068	1.751627
7.656408	11.07971	23.52045	29.659	1.869558
7.656088	11.08003	31.95031	30.058	3.196672
7.656862	11.08072	25.68755	26.6	2.056325
7.657235	11.08104	26.32813	28.462	1.760718
7.657662	11.08141	24.12698	28.728	1.959435
7.658062	11.08171	28.61474	28.728	2.377908
7.658088	11.08195	49.43092	91.504	3.513838
7.658435	11.08203	42.65596	54.796	2.936392
7.658808	11.08237	36.92178	40.964	2.237118
7.659235	11.08272	35.59467	69.293	3.110691
7.659635	11.08304	43.82444	59.185	2.815084
7.660008	11.08336	24.36444	26.866	1.896313
7.660382	11.08371	24.94043	42.294	4.11778
7.660702	11.084	38.0683	42.028	4.67029
7.661155	11.08437	45.10628	50.008	5.79609
7.661528	11.08469	30.54262	51.205	2.644162
7.661982	11.08509	57.02002	62.377	3.276418
7.662355	11.08536	36.6809	40.831	2.778718
7.662728	11.08573	52.57284	84.189	4.900437
7.663102	11.08608	33.07684	38.437	1.8241

Longitude	Latitude	eU(ppm)	Th(ppm)	K%
7.663902	11.08675	57.77542	42.028	3.314862
7.666382	11.08891	52.64006	68.362	3.413831
7.666728	11.0892	39.37824	53.067	2.334009
7.667075	11.08949	47.90869	53.333	4.418583
7.667422	11.08981	35.66657	79.002	4.603791
7.667742	11.09005	28.65845	67.564	3.183684
7.668115	11.0904	42.42572	62.776	2.590132
7.668408	11.09075	60.6191	54.264	5.642831
7.668862	11.09109	33.63498	39.634	2.394533
7.669208	11.09136	41.66319	27.664	3.452275
7.668862	11.09168	41.00954	54.264	4.216489
7.668515	11.09141	33.35664	34.713	2.42986
7.668115	11.09104	52.72211	66.899	2.539219
7.667768	11.09077	49.37882	40.166	1.883844
7.667395	11.09045	47.66713	66.101	3.362139
7.667128	11.09013	40.54408	59.717	3.546049
7.666782	11.08989	43.48669	46.151	1.995801
7.666382	11.08957	46.40441	46.55	2.360764
7.666035	11.08925	47.70752	53.599	3.579038
7.663555	11.08715	57.62567	40.033	3.76113
7.663182	11.08683	48.62839	71.022	5.388526
7.662782	11.08645	60.40291	72.352	5.014732
7.662328	11.08613	61.49051	84.588	5.15734
7.662008	11.08576	39.77492	54.929	3.709957
7.661635	11.08544	61.01929	75.278	6.043901
7.661182	11.08507	50.59159	53.333	3.331487
7.660835	11.08472	63.44932	92.834	5.183836
7.660008	11.08405	61.28027	85.253	3.369672
7.659662	11.08376	59.61336	72.751	3.085234
7.659288	11.08339	47.60879	47.215	2.704946
7.658888	11.08312	64.42248	62.909	4.904074
7.658488	11.08272	59.91072	98.287	6.129362
7.658088	11.0824	45.62549	55.062	2.972239
7.657715	11.08213	63.89273	66.899	4.138561
7.657315	11.08179	60.01686	78.603	3.296419
7.656915	11.08141	46.93046	55.594	3.541373
7.656542	11.08112	56.96958	103.208	6.041303
7.656195	11.08075	59.88223	75.943	5.119415
7.655768	11.08045	46.81065	67.298	2.930677
7.655502	11.08077	64.51311	41.762	3.692553
7.655902	11.08109	49.73404	65.303	3.43643
7.656302	11.08141	55.29154	63.308	4.327147

Longitude	Latitude	eU(ppm)	Th(ppm)	K%
7.657075	11.08211	47.89728	40.964	2.444926
7.657475	11.08243	40.27443	52.269	2.36492
7.657822	11.08269	33.88834	41.363	1.809553
7.658195	11.08304	53.40717	45.353	3.047569
7.658622	11.08341	46.70968	65.303	2.885479
7.658995	11.08373	38.32996	39.102	2.042038
7.659395	11.08408	24.2541	40.299	3.196931
7.659715	11.0844	33.07323	68.628	3.035101
7.660088	11.08469	37.08607	72.352	3.605794
7.660542	11.08509	55.60852	79.401	4.304288
7.660888	11.08541	24.09449	34.447	2.437653
7.661342	11.08579	24.36483	28.994	2.249067
7.661688	11.08611	23.56894	44.688	3.78243
7.662088	11.08645	26.4731	54.264	4.603791
7.662488	11.08675	27.13719	67.963	4.632365
7.662915	11.08715	52.64747	42.294	5.466974
7.663262	11.08744	25.68462	43.89	1.995022
7.663635	11.08779	29.06703	34.58	2.240495
7.663955	11.08811	23.16348	28.196	1.398353
7.664355	11.08837	27.84528	38.969	1.354973
7.664648	11.08867	53.49488	41.496	2.859243
7.664995	11.08896	61.72455	80.731	4.105052
7.665395	11.08931	23.61693	40.432	2.968602
7.665768	11.08963	43.5741	57.323	2.867556
7.666142	11.08989	23.96747	40.033	2.171399
7.666488	11.09024	23.01567	36.841	1.679673
7.666782	11.09053	23.77918	44.023	2.693257
7.667155	11.09077	58.98146	68.362	2.898207
7.667502	11.09109	48.07142	76.209	3.395648
7.667795	11.09139	63.5339	71.953	5.400995
7.668568	11.09208	57.28899	82.726	4.710293
7.668302	11.09232	39.24136	54.796	2.485708
7.667902	11.09213	56.36929	71.687	5.465675
7.667448	11.09171	58.20595	78.869	6.258722
7.667182	11.09147	45.53584	48.279	3.215114
7.666755	11.0912	43.2383	54.929	3.506825
7.666408	11.0908	42.59362	63.973	3.137446
7.666142	11.09061	41.18691	57.19	2.76573
7.665795	11.09024	66.74723	55.062	2.00827
7.665448	11.08997	57.66937	78.869	4.73575
7.665075	11.08965	38.97659	40.698	2.512723
7.664702	11.08933	50.87549	38.703	2.361803

Longitude	Latitude	eU(ppm)	Th(ppm)	K%
7.664035	11.08875	43.0663	64.638	2.898467
7.663662	11.0884	43.88024	30.989	2.348555
7.663342	11.08816	39.13102	68.229	4.273377
7.662968	11.08779	50.04408	60.249	4.308444
7.662622	11.08749	38.6722	43.358	2.333489
7.662168	11.08712	34.606	31.255	1.719936
7.661822	11.08677	64.45828	42.028	3.911271
7.661422	11.08643	39.65736	62.244	3.322395
7.661075	11.08613	62.72874	53.732	3.712555
7.660622	11.08571	33.26523	51.604	2.760534
7.660222	11.08544	24.12093	28.994	2.180231
7.659715	11.08504	41.62671	61.446	3.509423
7.659422	11.08469	28.70283	26.999	1.230548
7.659102	11.08448	28.51415	28.861	1.497062
7.658728	11.08397	29.15854	34.846	1.621227
7.658328	11.08373	35.28511	27.132	0.887665
7.657902	11.08336	36.16549	39.9	2.846775
7.657528	11.08304	43.30103	47.88	2.931197
7.657208	11.08269	48.90966	58.653	3.615664
7.656835	11.08237	59.50175	62.643	4.655224
7.656382	11.08203	47.39455	75.943	3.236675
7.656008	11.08171	55.05525	71.554	6.481077
7.655662	11.08144	42.97196	32.319	2.785212
7.655235	11.08109	33.78932	50.008	4.976287